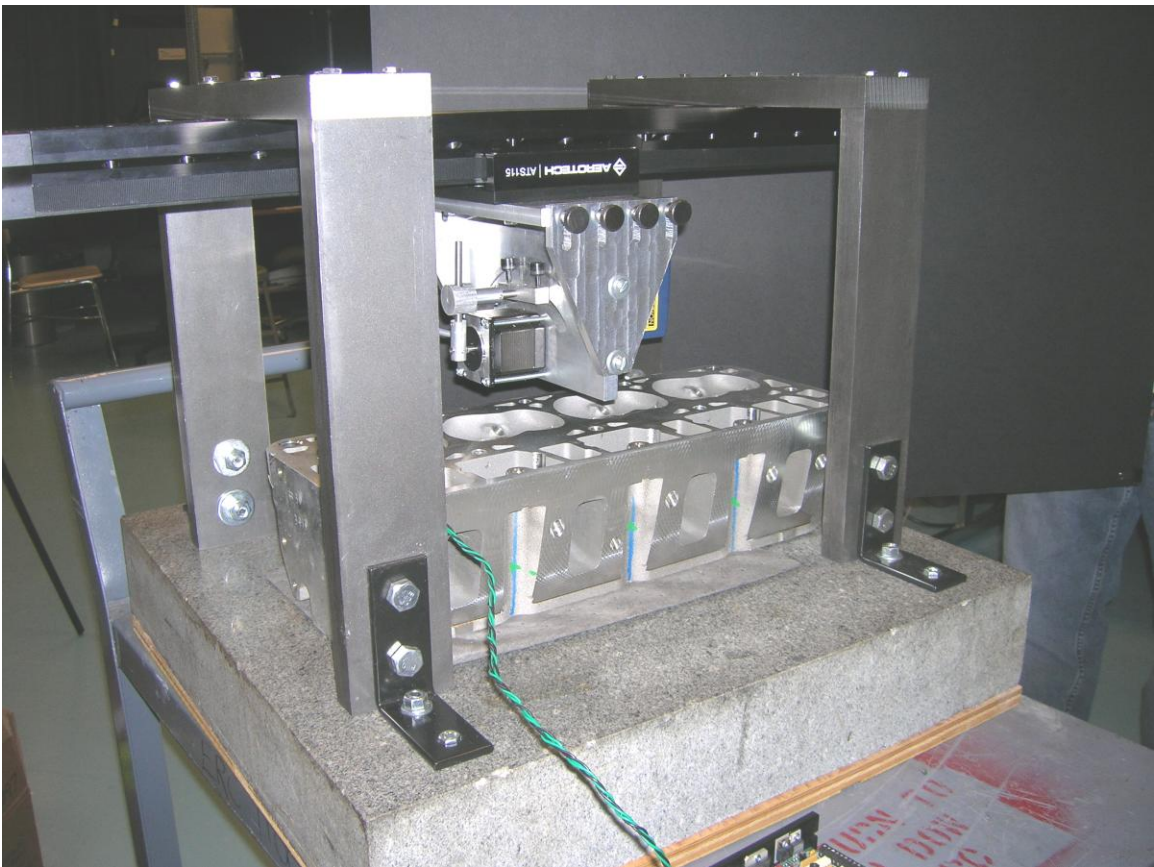


Laser sensor motion control system with application to engine valve seat metrology
Final Report

Project 5
Elizabeth Coon
Ryan Doss
Fletcher McCombie
Helen Sun



Mechanical Engineering 450, Fall 2007
Section 6: Professor Kurabayashi
December 11, 2007

Abstract

Auto-makers wish to improve the quality of newly assembled engine valve seats without sacrificing time and production levels. Currently, they use dial gauges to manually measure seat geometry. This process is time consuming and does not offer sufficient accuracy (due to human error in measurements). In response, we will use a laser sensor capable of making high accuracy measurements of seat geometry. Our main task will be to design and fabricate a mechanism that positions the sensor around the valve seats quickly and accurately. The intended outcome will be an automated, accurate, and quick way of ensuring 100% seat inspection.

Contents

Introduction	4
Information search.....	5
Customer Requirements	8
Customer identification	8
Customer requirement determination	9
Evaluation and comparison of existing methods.....	9
Engineering Specifications.....	10
Correlation of engineering specifications	10
Establishment of engineering targets.....	11
Concept Generation	11
Functional Decomposition- FAST Diagram.....	12
Concept Generation.....	12
Concept Evaluation and Selection	14
Selected Concept	24
Engineering Analysis.....	25
Positional Analysis	29
Final Design.....	49
Manufacturing and Assembly	52
Testing	59
Future Improvements	62
Conclusion	64
References	65
Bios.....	66
Appendix A: Quality Function Deployment (QFD) Diagram	68
Appendix B: Gantt Chart.....	69
Appendix C: Smart ConoProbe Laser Sensor Technical Specifications.....	70
Appendix D: Fast Diagram	73
Appendix E: Morphological Chart	74
Appendix F: Pugh Chart	76

Appendix G: Bill of Materials	77
Appendix H: Computer Aided Drawings of Selected Design Concept.....	78
Appendix I: Engineering Drawings	80
Appendix J: Matlab code for vibration analysis	88
Appendix K: Motion stage specifications	89
Appendix L: Ensemble CP 10 Code and Technical Specifications	95
Appendix M: Si Programmer Code and 3540i Driver Manual Website.....	96
Appendix N: Selected Stepper Motor Specifications	97

Introduction

Automotive engine valve seats are the surfaces that intake and exhaust valves sit against when the valves are closed during combustion. Valve seat position and orientation are critical to determining engine life, performance, efficiency, and emissions. Improper position and orientation causes leakage of heat and gases, degrading engine performance. Therefore, thorough seat inspections are required before an engine is further assembled.

Currently, valve seat inspection is a time-consuming, costly process for auto-manufacturers due to the conventional inspection device used: dial gauges. Dial gauges are manually operated and therefore time consuming to use. They are not accurate enough to ensure valve seats are of the proper geometry due to human error. Finally, though the devices are inexpensive relative to the manufacturing process, the labor costs are too high. In response, Dr. Vijay Srivatsan from the National Science Foundation Engineering Research Center for Reconfigurable Manufacturing Systems (ERC/RMS) has found that an existing non-contact laser sensor, the Smart ConoProbe (Appendix C), has the ability to measure geometry accurately and quickly at a low cost. In order to utilize the sensor's accuracy and speed of data acquisition, Dr. Srivatsan asked us to design and build a mechanism to quickly and accurately move the sensor around the valve seat. Our system provides transverse motion of the sensor along the length of the engine head and rotational motion of the sensor about the length of the engine head so that the sensor can align its laser orthogonal to the valve seat (Figure 1). In addition, our design had to compensate for external and internal disturbances such as vibrations from the manufacturing floor and friction in mechanical parts. Our resulting prototype will be a demonstrator to show to automakers.

To get an idea of how to design our mechanism around the sensor, we researched the specifications from the ConoProbe manufacturer (Appendix C). To operate correctly, the ConoProbe sensors must be located at an appropriate distance ($75 + 8.5\text{mm}$) from the engine head. To ensure precision, the sensor must make multiple passes along both rows of valve seats, which are oriented $+26^\circ$ from the vertical.

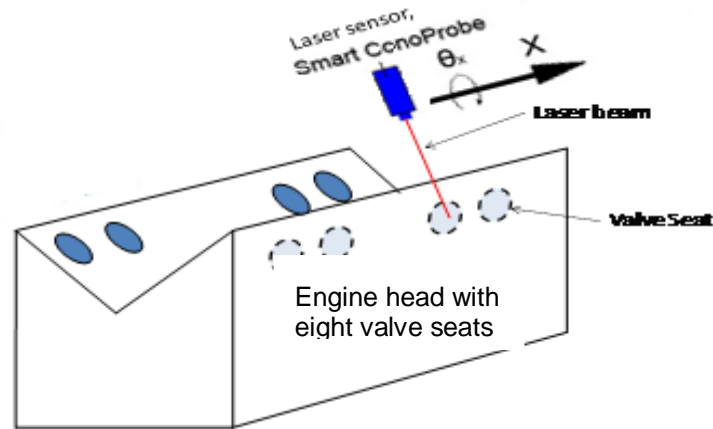


Figure 1: Isometric view of engine head and Smart ConoProbe sensor. The X-axis is the translation direction of the Conoprobe laser sensor, and θ_x is the rotation of the sensor about the X-axis.

Information search

Previous valve seat inspection techniques offer particular combinations of measurement error, measurement time, motion range, and machine price. However, none of them have the combination required for valve seat inspection: very low precision error (less than one μm), short measurement time (less than one minute), and no excessive costs and features (such as pressure regulation). The method proposed by our sponsor, moving a single non-contact sensor around the valve seats, has the promise to achieve this combination. Previous valve seat inspection methods include an air gauge mechanism, a dial gauge mechanism to measure the concentricity, and a coordinate-measuring machine (CMM). We include their benefits and drawbacks and compare them to our proposed design.

One existing measurement machine, the air gauge system, uses a nozzle that discharges a jet of air perpendicular to the measured surface to measure the distance between the nozzle and a surface [1]. An amplifier reads the back pressure and the signal processing tools converts the reading to an analog output, from which the valve seat radius and runout can be extracted. United States patent 5533384 uses this measuring technique and includes a mount (datum plane) for the nozzle and alignment and signal processing devices (Figure 1) [2].

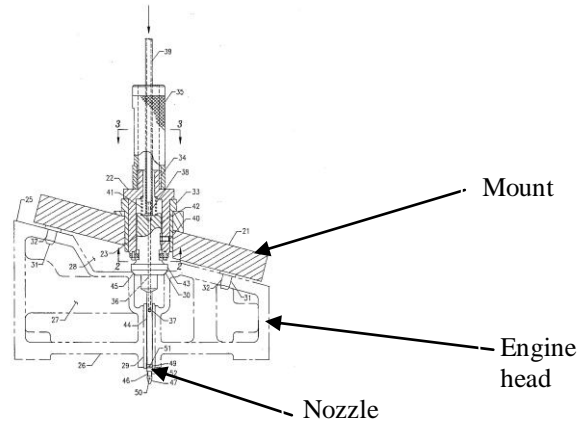


Figure 2: Air gauge measuring device mounted on the engine head. The device uses a nozzle which discharges air and measures the back pressure, which indicates the object’s distance from the nozzle.

Benefits of the air gauge system are ease of use, ease of calibration, and low device cost [3]. However, its low repeatability, caused by nozzle deflections during air discharges and pressure fluctuations inside the nozzle, is not sufficient for high precision valve applications, and its low measurement range does not span the valve seat outer diameter. Also, measurement time for 16 valves is on the magnitude of minutes which is too high to enable 100% in-line valve inspection.

Another existing measurement machine, the dial gauge system, uses a dial indicator to measure displacements from its equilibrium position [4]. A probe indicator typically consists of a spring-loaded tip which moves perpendicular to the body being measured. The needle’s linear displacement in compression is converted to the angular displacement of the dial needle. United States patent 4630377 uses this indicator to measure the seat runout [5]. It is comprised of a rotating plunger that allows the probe to translate along the valve seat axis and rotate 360° in order to measure the seat radius [Fig. 2]. This is most widely used method for in-line valve seat inspection [6].

Benefits of the dial gauge method are ease of use (manual measurements), built-in calibration with adjustable zeros, and low cost. Drawbacks are contact requirements for measurements, low repeatability (human error is introduced to measurements due to the dial readout), and long measurement time due to manual measurements.

The last existing machine, the CMM, measures in extreme detail the positions of an object’s features on an XYZ grid so that a 3D image of the object can be created [7]. A typical machine consists of many measuring probes/sensors (up to 48), a heavy granite worktable, and guiderails and spindles for sensor motion [Fig. 3]. CMMs also come with pressure and temperature maintenance capabilities. No CMM patents specifically for valve seat inspection have been obtained [8].



Figure 3.a: Left, probe indicator has a spring loaded probe with a displacement that is linear to the dial needle rotation. Right, the indicator with its mount on the engine block.

Benefits of the CMM are high repeatability, quick measurements, and high measurement ranges. Drawbacks are its large size, large weight, high relative device cost from the high number of parts and capabilities/benefits, and the requirement that the measured object must be transported to the worktable. In general, CMM's are used for image generation (such as reverse engineering CAD models of complex objects) while our design will be used only for measuring seat angle and roundness. Thus, our design will be much simpler, less costly, and more feasible for seat inspection.



Figure 3.b: Table-top coordinate measuring machine (CMM) uses a guiderail, carriage, and spindle to move the sensor around an object and measures its position.

The previous machines presented do not satisfy the current project application's requirements. For automated valve seat geometry inspection, the machine must have high precision (less than 10 μm), be non-contact, and must be quick enough to ensure 100% inspection of valves. Furthermore, it should not require engine head transport. Our proposed valve seat inspection method would fulfill all of these requirements. It uses a holographic laser sensor to measure the distance the light travels to the valve seat [9].

These measurements can be used to analyze angle and roundness of the valve seats. The laser sensor is proprietary technology and functionality details are unavailable.

The sensor was provided by the customer and has performance specifications that are suitable for the project application. It has sub-10 μm precision so that all valves are consistently evaluated. Its high data acquisition rate of 3000 Hz enables quick measurement, its measurement range of 17mm is adequate for measuring the diameter of the valve, and its cost is almost one order of magnitude below that of the CMM. Compared to the available technologies, only the sensor does not contact the engine head and maintains high accuracy.

A summary of the performance benefits and drawbacks of the previously described machines and the proposed machine sensor is shown in Table 1.

Table 1: Our proposed motion control mechanism using the Smart ConoProbe will provide the most desirable performance for valve seat inspection.

Technique	Precision (μm)	Measurement Rate (min/16 valves)	Measurement Range (mm)	Cost (\$)	Implementable In-Line
Air gauge	127	1-5	up to 0.08	15-100	No
Dial gauge	200	1-5	up to 12	20-200	No
Coordinate measuring machine	<10	<1	up to 500	80,000	No
Our motion control design using Smart ConoProbe sensor	<6	<1	up to 17	10,000	Yes

Customer Requirements

This section describes who our customers are, how we obtained their requirements, and what the engineering requirements are for our motion control design.

Customer identification

Our direct customer, Dr. Vijay Srivatsan, is the sponsor and overseer of our project, and has set the performance targets for our design. Our indirect customers are the automakers (General Motors, Daimler Chrysler, and Cummins) who will be reviewing the design prototype and concept. Though we do not have direct contact with them, their needs are

our most important requirements since they ultimately decide whether to use our motion control concept in line.

Customer requirement determination

The customer requirements for our valve seat inspection design were created based on a meeting with Dr. Srivatsan and Dr. Katz, Chief Engineer of ERC/RMS; the information search; and our knowledge of the automotive manufacturing process. Most important to Dr. Srivatsan are the system's abilities to measure valve seat geometry accurately and quickly, and to achieve 100% in-line inspection of seats. These requirements received the highest importance weights in our QFD (Appendix A).

The next three customer requirements are of moderate importance. First, our system must use only one sensor. Second, the system's product life must be long enough to offset its total capital cost. Third, the design must perform well under a variety of operating conditions, including changes in vibration and temperature.

Our four final customer requirements focus primarily on our system's ease of use. The machine must be powered by a convenient power source for demonstration purposes, preferably by a 110 Volt source. Second, to give our system flexibility to measure different kinds of seats, our design must incorporate a user interface that allows adjustments to our control settings by technical and nontechnical users. Third, the design should be easily implementable into an assembly line. Fourth, we must be conscious of cost during our design to make the proposal attractive to our automaker customers.

Following the definition of our customer's requirements, the requirements were weighted quantitatively by assigning a numerical value based on relative importance; these weights are recorded in the QFD diagram (Appendix A)

Evaluation and comparison of existing methods

The benchmark products to which we compared to our customer requirements are those that are currently in use for valve seat inspection: air gauges, dial gauges, and coordinate-measuring machines (CMMs). They are evaluated in the QFD diagram (right-most columns) against customer requirements on a scale of one to five, one meaning "does not satisfy" and five meaning "satisfies perfectly."

QFD results showed that the air and dial gauge mechanisms are not cost prohibitive, but their accuracy, measurement speed, and compensation for disturbances are insufficient for the valve seat inspection application. The CMM is accurate and quick but is costly, not easily implementable into an assembly line, and overdesigned with too many capabilities (3D images convertible to CAD files, pressure compensation, etc.) that are not used for our application.

Engineering Specifications

Once all customer requirements were identified, we defined engineering specifications that quantify them. The most important specifications (those that are the main targets of our design) are the maximum measurement errors of our electromechanical mechanism for both translational position and rotational position about the translational axis (Table 2). These errors are detrimental to the accuracy of the overall seat geometry measurements, which is the main concern of our sponsor. In addition, we must design the motion control mechanism positions the sensor as per the technical specifications of the ConoProbe Sensor (Appendix C).

Three engineering specifications influence the design of the engine head support (used to lock the block into place) during inspection, specifically, the maximum reference displacement error between the sensor control output and the base reference, the damping ratio of the fixture material, and the movement (play) of the engine head once the block has been fixed. These properties will influence the machine's accuracy of operation under a variety of conditions and the precision of the system's measurements.

Also of great importance is the time required for our system to move the sensor over all sixteen valves at least once. This will influence the inspection time. Our target is for the inspection of all sixteen valves to take less than one minute so that our design will be faster than the conventional, dial gauge measurement method. In addition, the concept needs to be capable of completing an adjustable number of passes in order to achieve acceptable seat roundness estimates for in-line inspection.

In addition, the flexibility of our controller, quantified by the step size of the sampling rate and the range of control over the translational speed, will impact the speed of our sensor movements and the ease of use of our system to users who may wish to adjust our original settings.

Finally, we will design our system to operate within a given temperature range (18~35 °C) during demonstration and future in-line use.

Correlation of engineering specifications

For each pair of customer specifications and engineering requirements, a correlation value was entered into the QFD diagrams to indicate the strength of the dependence between the specification and the requirement. Correlation values were assigned based on a scale from one to nine, one meaning weakly related, nine meaning strongly related.

Once the correlation matrix was completed, the importance of each specification was evaluated based on its weighted importance of the specifications it impacts. The specifications are shown in Table 2 below.

In addition to correlation between specifications and requirements, we also cross-correlated engineering specifications in the “roof” of the QFD diagram (Appendix A). The correlations accounted for specifications that are complimentary and competing, exposing indirect relationships between engineering specifications and customer requirements.

Establishment of engineering targets

Once the specifications were defined for our subsystem, targets for each specification were defined either directly by our sponsor or by the ConoProbe technical sheet (Appendix C). These values are listed in Table 2 below and in the QFD diagram (Appendix A). Parallel values for benchmark products are also listed in the “basement” of the QFD diagram.

Table 2: Importance Ranking of Engineering Targets

Rank (1 = most important)	Engineering Specification	Engineering Target
1	Error for translational position (x)	<1 μm
2	Error for rotational position (θ)	<1 degree
3	Reference displacement error	<1 μm
4	Cycle Time	<30 sec
5	Control of translational speed	1E-6,000 mm/min
6	Damping coefficient of fixture material	> 1
7	Number of passes sensor capable of making	1-16
8	Movement of engine head in x, y, and z directions once "fixed"	<1 μm
9	Error for translational velocity (dx/dt)	<1 mm/min
10	Sensor distance from engine head	51.5-68.5 mm
11	Step size of sensor sampling rate	1 Hz
12	Operational Temperature	18~35 °C
13	Input Voltage	110 Volts

Concept Generation

After we identified the customer requirements and engineering specifications, we created a functional analysis system technique, or FAST, diagram (Appendix D) to define and organize the functions our design needs to accomplish to meet the customer requirements. We then created concepts that served the most specific functions in the FAST diagram and listed them in a morphological chart (Appendix E) in order to illustrate our options for accomplishing each function. These concepts were then broken down into categories (e.g. mechanical and electrical) to help us identify the components that can be used in our system.

Functional Decomposition- FAST Diagram

We generated a FAST diagram for our motion control mechanism design (located in Appendix D). The diagram allows us to understand what our mechanism needs to achieve to serve its main task, which is positioning the laser sensor relative to the valve seats quickly and accurately. From the main task, we branched off basic and supporting functions, where basic functions are essential to the performance of the main task and supporting functions enhance product appeal to customers. These four basic functions are:

1. Move the sensor
2. Record the sensor position
3. Record the sensor's distance measurements
4. Secure the engine head

Moving the sensor relative to the engine head so that it scans across the valve seats is necessary to allow the sensor to record position data at the valve seat locations. Recording the sensor position is required for the post-processing algorithms our sponsor is creating to calculate the valve seat geometry from the sensor output. Recording the sensor's distance measurements is also required to gather the data about seat angle and roundness. Finally, securing the engine head is required to ensure that the valve seats are at the same reference points relative to the mechanism's base for all engine heads.

The supporting functions are focused on making the product reliable, easy to use, and aesthetically pleasing. These can be achieved through robustness of performance in varying environments, a simple user interface, conventional power plugs, methods to increase measurement precision, and quickness of measurements.

Concept Generation

Once we determined the specific functions that our design must meet to measure seat geometry, we devised high-level design concepts that perform those functions using a Morphological chart (Appendix E). In the Morphological chart, each row represents a function; columns are divided into electrical, mechanical, and other systems for ease of comparison. Groups of rows are classified into several categories, based on the higher-level functions to which they contribute. The classification groups are the following:

- Secure engine block
- Move sensor
- Record and control sensor position
- Record distance measurements
- Operate accurately in variable environment
- Easy-to-operate user interface
- Convenient to power
- Increase precision
- Decrease measurement cycle time

Representative concepts from each of these categories are described in the following paragraphs, while illustrations of the rest are also included in Appendix E with the text version of the Morphological chart. For many of these categories, one concept stood out as the clear choice for our design, in which case this function-level concept was the one chosen for all five of our final, system-level concepts.

Secure Engine Block: To secure the engine block, our most promising concept was a set of pins attached to the base. The pin is not as expensive as other concepts like the magnet, which is made of more rare material, or the clamp, which consists of a more complicated geometry. Most of the pin's cost comes from manufacturing its shape and ensuring a strong attachment to the engine block. It is accurate because it is a rigid attachment, it is easy to implement since the engine head already contains holes that the pins can use to secure it, and it is easy to procure because pins are a universally available part.

Move Sensor: To move the sensor in the linear direction, our most promising concept was a linear motion stage. The motion stage is very expensive compared to the other concepts, but provides the sub-micron accuracy that we need for our valve seat inspection application. It requires some assembly for implementation into the whole system such as screwing bolts into support structures and wiring for power and communication with a controller, but these are not complex procedures that require many steps or special skills. Motion stages are easy to buy online from companies like Aerotech and Danaher Motion. Motion of the sensor in the rotational direction did not yet have a clear choice, although one example is a stepper motor attached directly to the sensor.

Record and Control Sensor Position: In order to record and control sensor position, the optimal concept was the stand-alone controller. It is more expensive than simple brush motors but has multiple additional capabilities like speed control, multiple axis control, and built in interfaces for computers. These capabilities allow for higher accuracy in valve measurements by letting the sensor make more efficient and complex motion paths. It is much easier to implement than other concepts since it has USB ports that connect directly to the computer and to the stage. Finally, it is easy to procure online from companies like Aerotech.

Record Distance Measurements: For recording the distance measurements, the optimal concept was the laser sensor because its capabilities are suitable for valve seat inspection - it is non-contact, has a very high sampling frequency (around 3000 Hz), and has a moderate measurement range (17 mm). It is much more expensive than other concepts like the Hall Effect sensor but its capabilities override those costs. Its accuracy error is on the order of microns, compared to more than ten times higher error from Hall Effect sensors. It is easy to implement because it comes with its own software that has a user interface. The software allows you to gather data using the software or other programs like LabView. Finally, it is easy to procure online and our sponsor has provided one.

Operate Accurately in Variable Environment: The most promising concept for allowing our design to operate in a variable environment is done by accounting for

variations in vibrations, as this is the environmental change most detrimental to measurement accuracy that our product will experience (as opposed to fluctuations in temperature and air particulate levels). The best concept we devised to combat this is using a granite or cast iron mounting block to support the engine head. This is cheaper than using a fluid cushion, while at the same time providing reasonable compensation for the damping that the engine head might experience. Furthermore, this concept would be relatively easy-to-implement given its simple construction, and also easy to procure since such a block is available from our sponsor.

Easy-to-Operate User Interface: The most promising concept for an easy-to-operate user interface is a computer interface, with special attention being paid to making this interface easy to read and understand. This is a relatively low-cost solution given that LabView software is readily available in the computers that we are allowed to use. It is accurate because it uses electric signals that have little response delay, and it is easy to implement since the LabView integrates easily with data acquisition devices.

Convenient to Power: The best concept for powering our design conveniently is using a conventional three-prong cable that is compatible with a 110V AC power source. Such a connection is low-cost, given that it is so common. It is also very reliable and convenient to procure, given that 110V is easily provided from a conventional wall outlet.

Support / Integrate assembly: Support of the assembly does not have a clear best option and is explored in the system-level concepts later in this report, however one option is to position the linear stage horizontally above the engine head and then mount the rotational motion mechanism containing the sensor below it.

Follow Efficient Motion Path: The direct back and forth method (illustrated in the pictorial Morphological Chart, Appendix E) is the fastest and therefore best option, as the accuracy of all the models is the same. This method is the fastest because the linear motion can be faster and better controlled than the rotational motion, and making as many passes as possible with as few rotational movements as possible, which this method accomplishes, is best.

Concept Evaluation and Selection

Once we generated concepts for each individual function, we combined these function-level concepts into five concepts for the overall system. Once the system-level concepts were generated, we compared their ability to complete each individual function with a Pugh chart, which was used to determine one final concept that we will use for our design.

For many of the functions, one function-level concept was clearly the best option, as was described in the previous section. In these cases, all five system-level concepts contain the same function-level concept. In addition, our sponsor has recently approved the purchase of a linear motion stage with micro-precision due to the fact that the time and level of difficulty associated with building such a motion stage ourselves is too great for

this project (given our machining skills and the machines that are available to us). For this reason, all of our concepts assume the use of both the linear motion stage and the ConoProbe sensor. Because of these constraints, the concepts primarily focus on two functions: the integration and support of the linear motion stage and the control of the rotational motion of the sensor.

Finally, these five concepts were generated at different points during the design process, during which our requirements given by our sponsors were changing. Specifically, some concepts were generated at a time in which our sponsor required only rotational motion that would be manually locked into a few positions. For this reason, some concepts are able to rotate the sensor with a motor and some concepts are only able to manually rotate the sensor to discrete locations.

Of the five system-level concepts, three (Concepts # 2, 3, And 5) use the same general assembly to support the linear motion stage horizontally above the engine head (shown in Figure 4 below). The descriptions for these concepts then focus primarily on the mechanism that will be attached to the stage in order to achieve rotational motion of the sensor, and thus the individual concepts differ from the assembly concept in this fashion. In contrast, Concepts # 1 and 4 have their own method for supporting the linear motion stage.

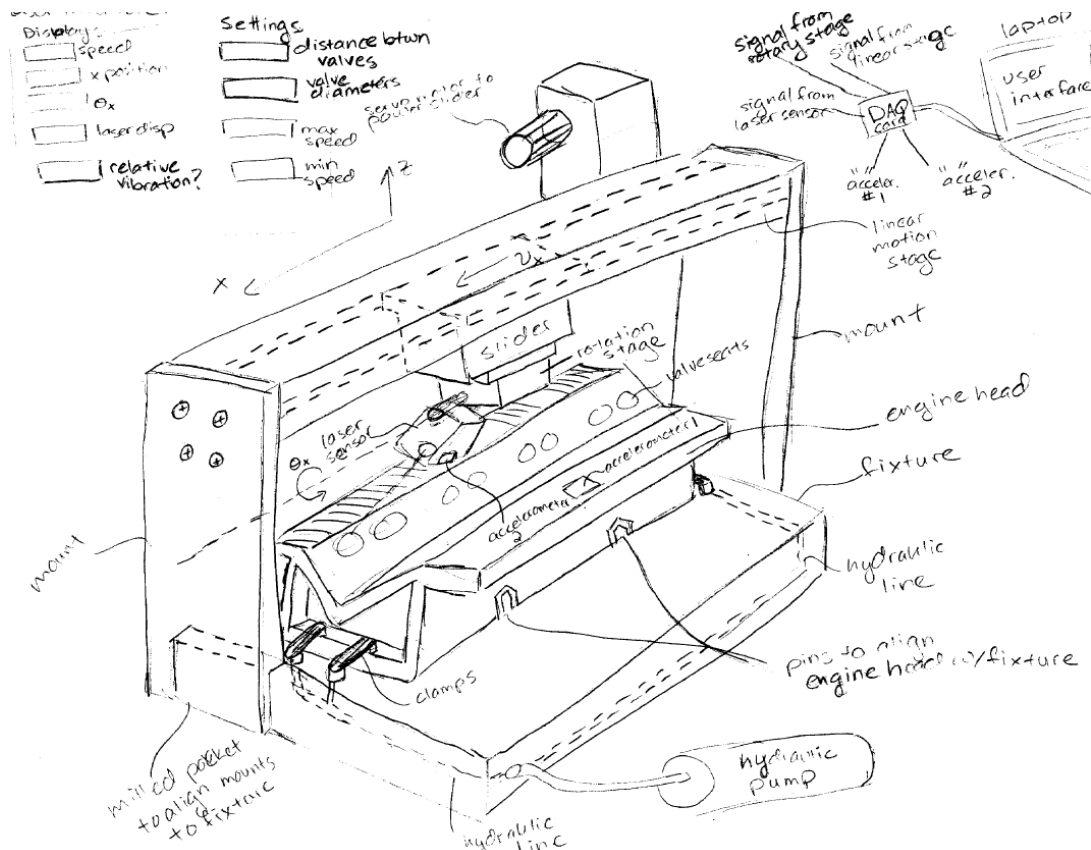


Figure 4: Concept for the assembly of the overall system, including base, engine head mount, and support of motion stage, used for concepts # 2, 3, and 5

System-level Concepts

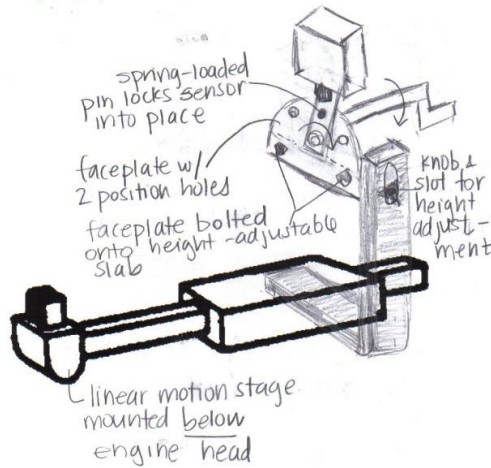


Figure 5: System-level concept # 1

Concept # 1, used as the datum concept on the Pugh Chart (Appendix F) is shown in Figure 5. This concept mounts the motion stage below the engine head, rather than above it as the assembly in Figure 4 shows. The sensor is mounted onto a linkage that contains a spring-loaded pin; the other end of the linkage is mounted onto the faceplate using a crank and a bolt. The crank is used to rotate the sensor into two predetermined positions, those of the two position holes. The sensor is unlocked from position by pushing in the spring-loaded pin and then can be rotated with the crank. The major advantages of this design are that it allows for continuous height adjustment (rather than height adjustment in intervals) and an easy-to-use rotation mechanism. The major disadvantages are that it can only provide rotational motion in discrete steps and that it is bulky, which means it requires more power to operate and is not very aesthetically pleasing.

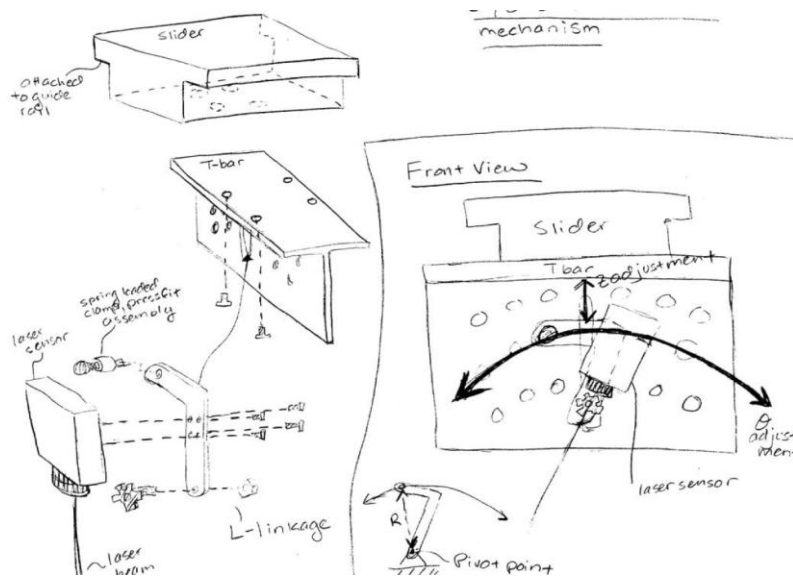


Figure 6: System-level concept # 2

Concept # 2 is shown in Figure 6. It consists of a T-bar bolted onto the motion stage slider. The T-bar has a vertical slot and three series of holes following the path of three arcs that are at different vertical positions on the bar. Attached to the bar is an L-shaped linkage that can move in the slot vertically and can rotate about the pivot point at the bottom of the linkage. This concept is easy to manufacture since there are no complicated geometries. It is simple because it only has two main parts, it is easily assembled onto the slider using just four bolts and nuts, and adjustment of the rotational position is quick and easy with the spring loaded clamp. Two drawbacks are that, like Concept #1, the rotational motion of the sensor can only be set at discrete steps and with the circular arcs, the sensor can only be positioned at pre-prescribed focal lengths.

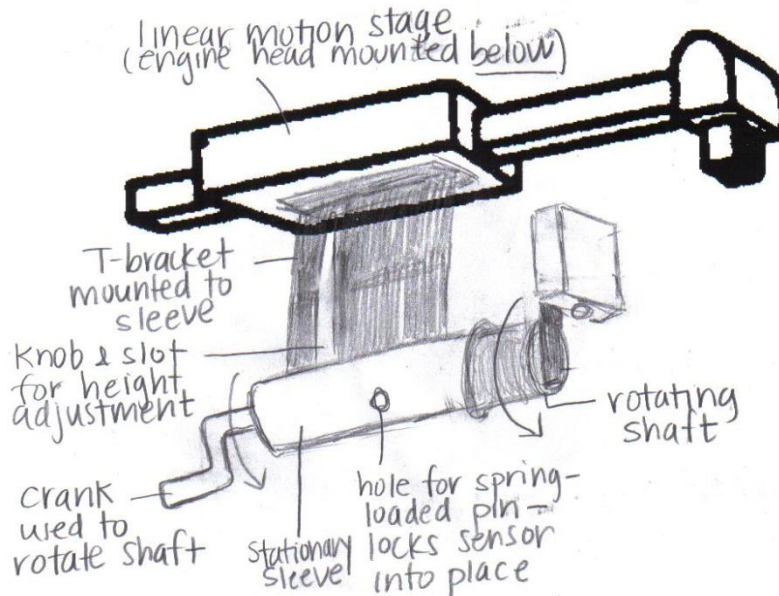


Figure 7: System-level concept # 3

Concept # 3 is shown in Figure 7 and consists of a motion stage mounted above the engine head. It also consists of a T-bar bolted onto the motion stage slider. However, this T-bar contains a slot and knob, which allows for continuous height adjustment of the rotation mechanism. Mounted onto the t-bar is a sleeve that contains two positioning holes. Inside this sleeve is a shaft that includes a spring-loaded pin. On one end of the shaft there is a crank; on the other end of the shaft, the plate to which the sensor is mounted is connected. The rotational position of the sensor can be adjusted by pushing in the spring-loaded pin and turning the crank. The main advantages of this design are that it is compact, easy-to-use, easily automated (the crank can be easily replaced with a motor), and aesthetically pleasing. A benefit of its compact design is relatively low measurement error due to vibrations. The disadvantages of this design are that the sleeve and shaft have complicated geometries that are difficult to build and assemble.

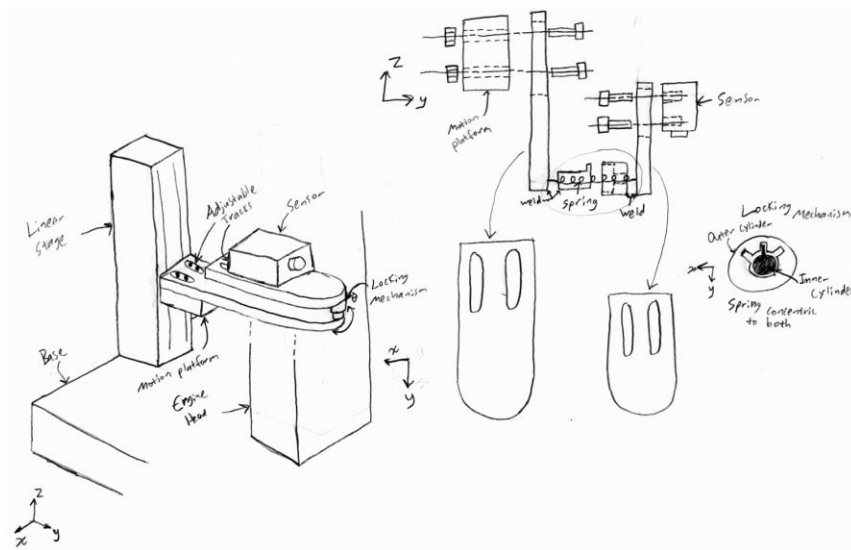


Figure 8: System-level concept # 4

Concept # 4 is shown in Figure 8, and consists of a swivel-locking mechanism. The engine head is oriented to stand up vertically. The swivel-locking mechanism consists of two plates, each with machined slots which allows one plate to be bolted down to the motion stage platform and one plate to the sensor. The plate on top, supporting the sensor, is then allowed to rotate with respect to the plate on bottom by means of a bearing. As shown in the figure, the inside of the bearing includes a locking mechanism that allows the rotation of the sensor to be locked in one of three positions. In addition, the machined slots in the plates allow both the axis of rotation and the distance of the sensor to the engine head to be adjusted. Advantages of this design are its ease of use, especially for rotating the sensor since it is not acting against the direction of gravity. In addition, it consists of few parts that are simple to make. However, the design has many drawbacks. With the sensor cantilevered out, and linear motion being in the vertical position, micro-accuracy will be difficult to attain. The large moment of inertia of the mechanism would be detrimental to its ability to resist vibrations. In addition, the locking mechanism would be difficult to assemble, and the rotational component is not easily implementable with a motor.

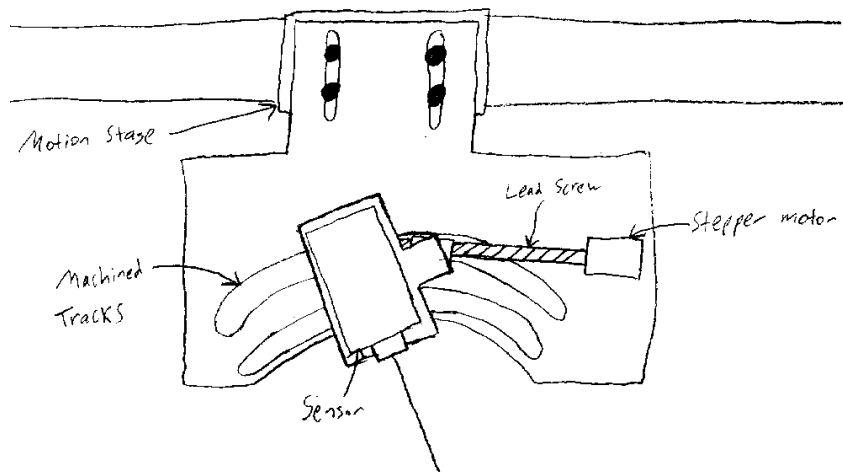


Figure 9: System-level concept # 5

Concept # 5 (shown in Figure 9) features an arch type track to guide the rotational motion of the sensor and a linear motion stage held above the engine head. By constraining the motion of the sensor with the track, it can be controlled by a stepper motor that drives a lead screw. The lead screw is threaded through an internal thread on the plate supporting the sensor. This entire mechanism is mounted on a plate that is attached to the linear motion stage; thus, the entire mechanism is positioned by the linear stage, and the angle the sensor makes with the engine head is controlled by the mechanism. The advantage of this concept is that it allows for rotational motion about a non-physical point in front of the sensor origin, the importance of which is described in the section below. The only disadvantage of this system is the relative complexity of the design in terms of the number of parts involved.

Comparison of System-Level Concepts: Once five concepts had been created, they were then compared in terms of their ability to perform the functions required for our overall design in a Pugh chart (Appendix F). These functions were weighted for importance and these weights, combined with each concept's ability to complete each function, were used to compare the system-level concepts to each other. Each design's ability to accomplish a specific function was compared to Design #1 and then scored with either a "+" if it was better at accomplishing the task than Design #1 was, a "-" if it was not as good, and an "s" if it was similar.

The most important function was the concept's ability to control the motion of the sensor. As stated earlier, one major requirement for this design is its ability to position the sensor laser orthogonal to the surface containing the valve seat, as this provides the greatest accuracy. However, due to the constraints on the distance between the sensor and the surface (which must be ~60mm) and the geometry of the engine head itself, the sensor must rotate about an axis that is not on the actual sensor body (as demonstrated in Figure 10). Thus, a concept's ability to have an axis of rotation in front of the sensor has a heavily weighted score. In addition, it was fairly important for this axis of rotation to be non-physical, that is, to have no actual structure at the pivot point as the pivot point is very close to the engine head and thus a physical pivot could interfere with the engine head during motion.

Two more important functions for our design are the ability to rotate continuously (instead of being locked into discrete positions) and the ability to easily incorporate a motor to control the rotational motion, as our sponsor currently requires both. Although our sponsors did not require these functions at the time that many of our concepts were produced, these are currently highly desirable for our indirect customers, the automakers, because the system's ability to be entirely automated is its critical advantage over the current inspection method, manual use of the dial gauge. Thus, the ability of each design to complete these functions is weighted highly.

Many of the other functions are fairly straight-forward and involve other functions required of our design having to do with the ability to focus the sensor and adjust its position apart from the two controlled degrees of freedom, the ease of manufacturing of

the design, its cost, its aesthetic properties, its ability to maintain micro-precision, and its robustness.

Once these designs were compared with the Pugh chart (Appendix 6), Design #5 was found to be the clear winner based on score. Design #5 was initially the best choice for our design because it has several stand-out features:

1. High measurement accuracy due sensor orthogonality relative to valve seat midpoints
2. Low risk of sensor interference with engine head due to non physical pivot point/rotational axis
3. Controllability using a motor
4. Adjustability for different engine heads
5. Achievement of rotation range for given engine head without adjustments
6. Simplicity of parts
7. Robustness due to structural geometry

High Measurement Accuracy Due to Sensor Orthogonality Relative to Valve Seat Midpoint: The first feature, maintaining sensor orthogonality relative to the valve seat midpoint, optimizes the accuracy of the sensor's measurements. The valve seat dimensions measured by the sensor are extracted by geometry from the sensor's focal length measurements; therefore, angles closer to 90 deg between the sensor and the measured surface requires fewer calculations to extract the measured dimensions. Because the sensor beam is rotated about the point rather than translated through the valve seat cross sections, the angle at which the beam hits each point on the valve seat changes during rotation. Therefore, maintaining orthogonality between the beam and the seat midpoint allows for angles closer to 90 degrees between the sensor and seat surfaces.

Low Risk of Sensor Interference with Engine Head: The second feature, using the arch type track, allows the sensor to not only rotate about a point that is not on the sensor body, but to rotate about a non-physical axis, that is, an axis without structure at the location of the rotational axis (Figure 10). This is important because the axis of rotation is close to the engine head and so a physical axis may interfere with the engine head itself while the sensor moves.

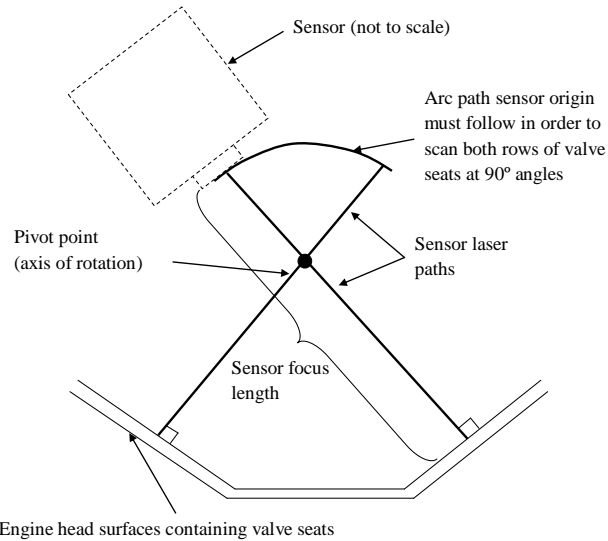


Figure 10: Schematic of non-physical pivot point.

Controllability using a Motor: The chosen design's use of a lead screw through an internal thread on the sensor support allows for easy control of the rotational motion of the sensor with a motor. A stepper motor can be used to drive the lead screw with open loop control. The same plate that contains the arch tracks provides a convenient location to mount the motor.

Adjustability to Accommodate Different Engine Heads: The chosen design offers adjustability of the sensor focal length and the vertical position of the pivot point to accommodate measurements of different engine heads. Figure 11 demonstrates how the *focal length* can be changed without changing the position of the pivot point. This can be done by allowing the sensor to be moved with respect to its support. The effect of this feature is that with an engine head that has valve seats oriented closer to the horizontal plane, the sensor will be able to be moved closer to the seat surface to keep it within its measurement range. At the same time, the pivot point location remains the same and therefore, no clearance is sacrificed between the sensor and the surface.

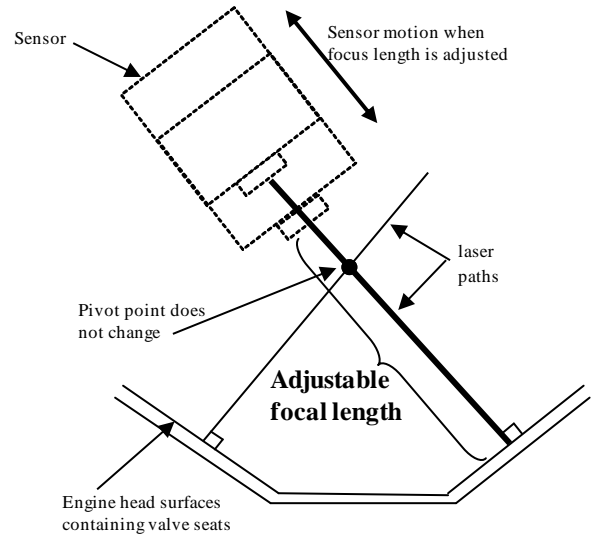


Figure 11: Schematic of adjustable focal length.

Figure 12 presents how the *pivot point* can be moved vertically. This is accomplished by moving the plate containing the entire mechanism up and down with respect to the linear stage it is mounted on. This feature's effect is that with an engine head that has more inclined valve seats, the entire plate holding the the sensor can be moved up, allowing for maximum clearance between the sensor and the surface and reducing risks of the sensor interfering with the engine head.

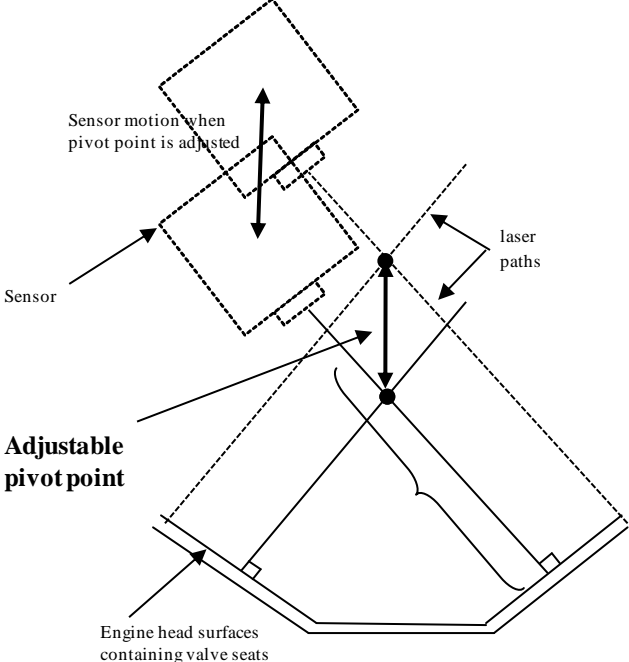


Figure 12: Schematic of adjustable pivot point.

Achievement of Rotation Range for Given Engine Head without Adjustments: The given engine head's geometry was checked to ensure that the optical path length variation during the rotational scan will not exceed the sensor's measurement range (± 8.5 mm).

This was done by calculating the maximum change in sensor focal length for the engine head given to us by the sponsor. Figure 13 shows the side view of the valve seats and their geometry.

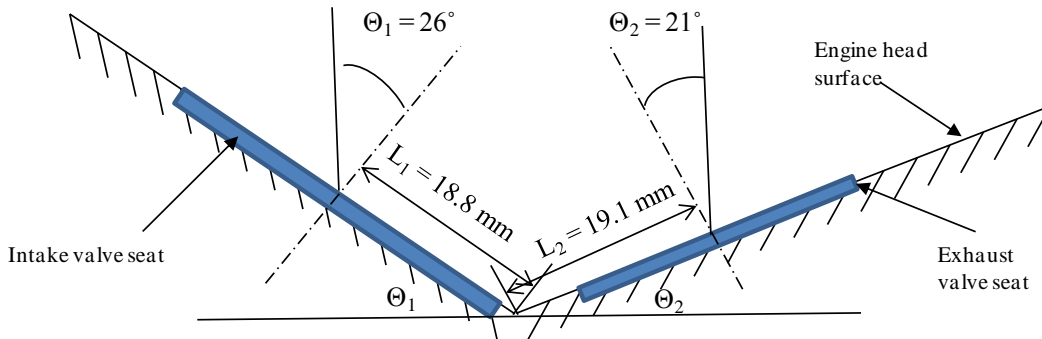


Figure 13: Schematic of engine head and valve seat geometry.

In our calculations, we assume that the sensor path will travel from one valve seat midpoint to the other. We calculated, using the variables shown in Figure 14, a conservative estimate of the change in sensor focal length. We did this by using the expression for total vertical distance change from the midpoint of the seats to the intersection line of the seat planes, $L_1 \sin(\theta_1)$ and $L_2 \sin(\theta_2)$. The calculated results are 8.2 mm and 6.8 mm, within the sensor's measurement range of ± 8.5 mm. In reality, the actual change in sensor focal length are these values subtracted by a factor, $R_b(1-\cos(\alpha_1))$, shown in Figure 14. This factor comes from the fact that a constant radius laser beam makes an arc as it is rotated.

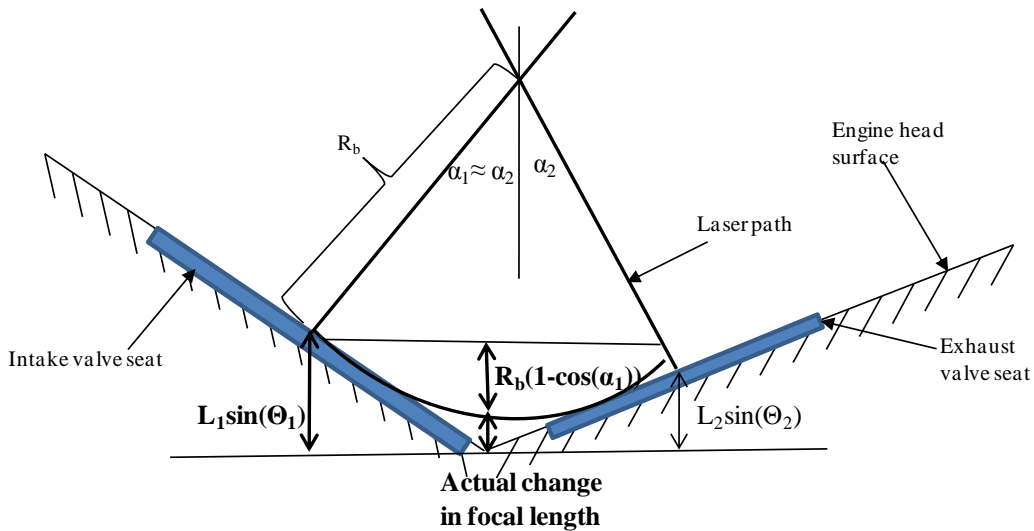


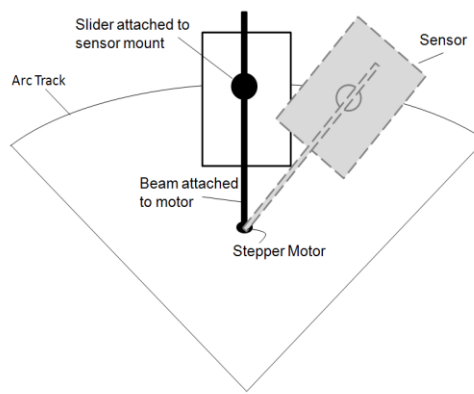
Figure 14: Schematic of adjustable pivot point.

We have proved that the total sensor focal length change is less than its measurement range. As a result, our design will be able to rotate through our desired points (the midpoints of the valve seats) without requiring adjustments of the focal length or pivot point, making the seat inspection procedure much simpler and easier to make automated.

Simplicity of Parts: The chosen design utilizes one part (the plate containing the tracks and the motor) for many functions and thus assembly will not be difficult.

Robustness from Structural Geometry: Finally, with the chosen design, the linear stage operates in a horizontal direction so that it does not compete with gravity, which helps assure its fine precision. Because this concept is the only one that satisfies all of the most important functions well and in a simple manner, it has been chosen for our final concept. Most importantly, it enables the sensor to move accurately in an automated method, making it distinctly appealing to our customers, the automakers.

Change in mechanism design: Since the original selection for our final concept, we have modified the mechanism that controls the sensor position along the arch track. In place of a lead screw driving an internal threaded bearing attached to the sensor mount, the motor now rotates a beam that applies force on a slider attached to the sensor mount. This design allows the motor to be placed below the track, which decreases the width of the plate. This is important because when creating the final design, it became apparent that there was a great need to reduce the width of the plate for structural reasons and the height of the plate could be increased to accommodate the new motor position without much consequence. This new mechanism design is shown below.



Selected Concept

In order to provide more clarity to our engineering analysis and final designs, we will briefly describe the final concept in greater detail. Our selected concept, the arch shaped track allowing rotation of the sensor about a non-physical pivot point, has four major parts, shown in Figure 15:

1. The sensor mount/fine tuning adjustment
2. The arched track and plate with new mechanism described above
3. The plate mount
4. The motion stage supports

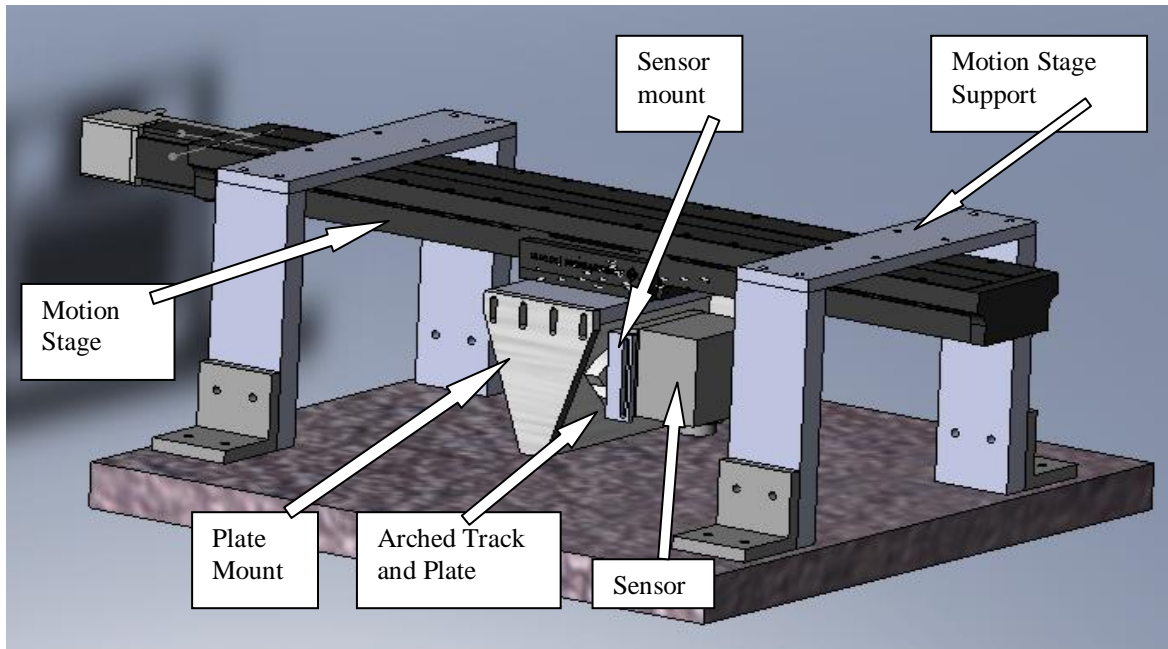


Figure 15: Drawing of assembled design including major components

The sensor mount/fine tuning adjustment consists of a U-shaped block with slots on the sides. The sensor is bolted to the mount along the slots and can slide up and down with respect to the mount.

The arched track and plate are connected as one rigid part. The plate is rectangular and the arched track is an extruded arc. The sensor-mount slides along the arched track to allow for rotation of the sensor. The motion of the sensor along the track is controlled by the mechanism described above.

The plate support consists of two parallelogram plates and a horizontal plate. The three plates are welded to each other. The horizontal plate is bolted onto the motion stage slider. The parallelogram plates contain side slots on which the plate with the arched track is bolted. The arched track plate can slide vertically with respect to the plate support.

The motion stage support consists of two large, U-shaped bars that extend over the motion stage. They are connected to the granite block via four L-shaped brackets.

Engineering Analysis

Once our final concept had been selected, we completed a detailed design of our system. We identified design constraints and determined variables that are set through qualitative, technical reasoning, and variables that are determined through quantitative engineering analyses. Our design considers the following factors:

1. Spacing constraints from the ConoProbe sensor, engine head, and purchased component geometries and specifications
2. Structural soundness (resistance to fatigue, yielding, vibrations)
3. Motor transmission effectiveness/efficiency

The table below lists the design variables, the type of analysis used to define them, and the values determined for each one through analysis. We include descriptions of the qualitative reasoning behind determining some of our mechanism’s dimensions in the “Final Design” section, where they are included with the description of the components. Next, we describe how the design variables were identified using a qualitative and quantitative analysis.

Table 3: Variables to be determined by analysis

Variable	Determined by	Value
Mechanism material	Qualitative analysis	Aluminum 6061-T6511
Structural support material	Qualitative analysis	Carbon steel
Base material	Qualitative analysis	Granite
Motion stage selection	Qualitative analysis	Aerotech ATS 115
Small mechanical parts	Qualitative analysis	Mcmaster shafts, bearing, track roller
Motor	Motor torque analysis	Sure Step Motor 23055
Roller/peg location on sensor mount	Position analysis	15 mm from sensor top and bottom, 23.5 mm from sensor right and left edge
Track arc angle	Position analysis	88.4°
Track width	Position analysis	55 mm
Motor mounting position	Position analysis	15 mm below track’s bottom surface
Mechanism plate length	Position analysis	224 mm
Mechanism plate width	Position analysis	124 mm
Mechanism plate thickness	Vibration analysis	25 mm
Motion stage support C channel length	Structural analysis	300 mm
Motion stage support C channel width	Structural analysis	80 mm
Motion stage support C channel thickness	Structural analysis	13 mm
Motion stage support vertical post height	Structural analysis	338 mm
Motion stage support cross section dimension	Structural analysis	25×75 mm

Qualitative Analyses

The qualitative analyses include material selection, motion stage selection, track roller selection, and ball bearing selection.

Material Selection

Aluminum 6061-T6511 has been identified as the material of choice for all machined parts for the system. This choice has been made for four main reasons. First, this material is widely available in the shop we will use for prototype fabrication in a stock size that will accommodate all pieces we need to machine (1 inch by 6 inch, or 25.4 mm by 152.4 mm). Second, aluminum is easy to machine and some of the structure supporting the rotational motion of the sensor is somewhat complex. Third, aluminum has a high strength to weight ratio, and thus we can reduce the weight of the structure supported by the motion stage to ensure that we do not exceed the stage's load limits. Finally, this type of Aluminum is weldable, which is necessary for our design.

Granite was chosen as the material for the engine head base because of its ability to attenuate external vibrations and because our sponsor requested that we use it.

Medium carbon steel was selected as the material to make the motion stage support. Medium carbon steel was chosen for its high strength (yield and compressive strength around 70 ksi), its low cost (around \$0.3/lb), and its high availability in the shop and in stores [CES EduPack 2007].

Motion Stage Selection

A purchased motion stage provides linear translation along a platform at the necessary speeds and with micro-precision unattainable from our own manufacturing skills. Thus, at the request of our sponsor, we selected and purchased a custom stage. Our purchased linear motion stage is an Aerotech, Inc. model ATS115 with 600 mm travel. This model meets all required engineering specifications which include repeatability, travel, speed, load, and cost-effectiveness. Most importantly this linear motion stage is repeatable to 1 micron which is of primary concern of our sponsor. The travel of 600 mm is required to scan a variety of engine heads which will have a maximum length of 500 mm. The ATS115 is capable of moving a load of 40 kg at 250 mm/s. In comparison, we will be using the motion stage to move a load of approximately 20 kg at 100 mm/s. The motion stage is also low cost with high performance, making this model more attractive to our sponsor which has purchased the motion stage for this project. Overall, the ATS115 meets all engineering specifications requested from our sponsor and set by our design. The manufacturer specifications of the ATS115 can be found in Appendix K.

Track Roller Selection

The track rollers were selected by making a conservative estimate of the maximum static and dynamic radial load each could experience. The maximum static load the rollers should experience is the weight of the sensor divided by two (only the top two rollers support sensor weight), or 0.4185 pounds. A conservative estimate for the dynamic load is 5 pounds. A safety factor of two was employed, giving a minimum dynamic load capacity of 10 pounds; it was later proven in the torque analysis that this load is 0.8516 pounds.

All track rollers available through McMaster Carr meet this load capacity and are relatively inexpensive. Thus, the smallest size available was selected, given the desirability of developing a compact mechanism, and the small average radius of curvature about which the rollers must run (4.016"). A track roller can be seen below in Figure 16.

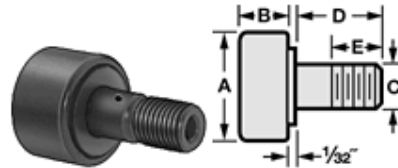


Figure 16: Photo and schematic drawing of track roller

Table 4: Key track roller dimensions

A (Roller Diameter)	1/2"
B (Roller Width)	3/8"
C (Stud Diameter)	3/16"
D (Stud Length)	5/8"
Thread Size	10-32
Thread Length	1/4"
Max RPM @ No Load	11,500
Radial Load Capacity, Static	790 lbs.
Radial Load Capacity, Dynamic	680 lbs.
Additional	Hex head (good for blind-hole installation, and those requiring greater tightening torque) Crowned (slightly curved surface that compensates for minor misalignment between the track and roller) Item 3659K11 \$19.33 each

Linear Bearing Selection

A linear bearing runs along the shaft that the motor spins, and is connected through a pin to the sensor. A self-aligning bearing was selected, given that as the shaft is rotated, it will tend to be misaligned with the bearing. The maximum horizontal load the linear bearing could experience is that exerted when the sensor is at either edge of the arc: 2.57 pounds (see torque analysis). Given the desirability of a compact mechanism, the linear bearing with the smallest outer diameter (1/2") was selected. This bearing can support horizontal load of 939 pounds, much less than any horizontal load we would expect during the operation of our mechanism.

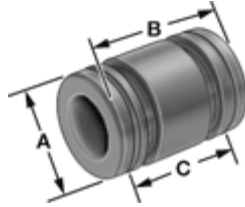


Figure 17: Dimensioned linear bearing

Table 5: Linear bearing dimensions

A (Outer Diameter)	1/2"
B (Overall Length)	3/4"
C (Distance between External Ring Slots)	0.437"
Inner Diameter	1/4"
Static Horizontal Load Capacity	939 lbs.
Additional	Self-lubricating 6061-T6 aluminum shell 0.002" ceramic coating for added corrosion resistance Item 9533T1 \$11.90 each

Quantitative Analyses

The quantitative analyses include positional analysis, arc geometry, arc and track analysis, torque analysis, vibrations analysis, and structural analysis.

Positional Analysis

The positional analysis was used to identify key variables required to allow our mechanism to be realizable and at the same time, to position the sensor quickly and accurately around the given engine head. We started off by determining the geometry of the arcs that the laser beam origin and the laser sensor center must make about the pivot point (axis of rotation) in order to hit the desired beam positions and to be within the sensor's measurement range for focal length. During the process, the locations of the pegs that connect the sensor to the arched track were set. Then, the track dimensions were determined as well as the position of the motor using the concept of an effective transmission angle. Finally, the dimensions of the plate that the track is rigidly connected to were set, allowing us to calculate the clearance that our mechanism is able to maintain between the sensor and the engine head.

Arc Geometry

The geometry of the arcs that the sensor must pass through and that the laser beam end must hit was determined based on:

1. The valve seat orientations
2. The sensor standoff length of 60 mm and measurement range of ± 8.5 mm

First, our goal is to have the laser beam be perpendicular to the valve seat plane when it reaches the valve seat midpoint. This is shown in Figure 18.

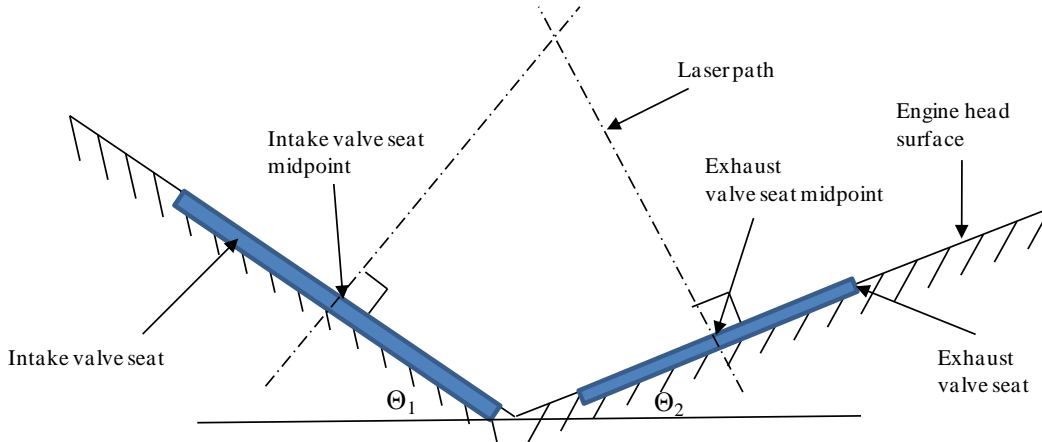


Figure 18: Laser hits both the intake and exhaust valve seat midpoints at 90 deg from the valve seat plane.

To find the radius of the arc below the pivot point that meets this goal, we used an assembly drawing of the engine head given to us by the sponsor (not shown for proprietary reasons) and drew lines that intersected the valve seat midpoints at 90° and intersected each other at a relative angle, θ , shown in Figure 19. From the assembly drawing, we obtained the horizontal length between the lines at the engine head surface, 27.604 mm [see Figure 19], and extracted the angles 64 and 69 deg from the valve seat inclination angles θ_1 and θ_2 . The angle θ is 47 deg since the angles in a triangle add up to 180 deg. We then used the law of sines to get x_1 and x_2 :

$$\frac{\sin(69)}{x_1} = \frac{\sin(64)}{x_2} = \frac{\sin(47)}{27.604} \quad (1)$$

We found that $x_1=35.2$ mm and $x_2=33.9$ mm. To get the full radius of the lower arc, we add e_1 and e_2 to x_1 and x_2 , respectively, took their average, and got that R_b , the lower arc radius centered at the pivot point and ending at the valve seat surfaces, is 45.96 mm. Since the sensor standoff length is 60 mm, we want the total distance between the sensor lens and measured surface to be 60 mm. Thus, the top arc radius centered at the pivot point and ending at the sensor optical lens, R_t , is $60 - R_b = 14.04$ mm. Figure 20 shows this geometry.

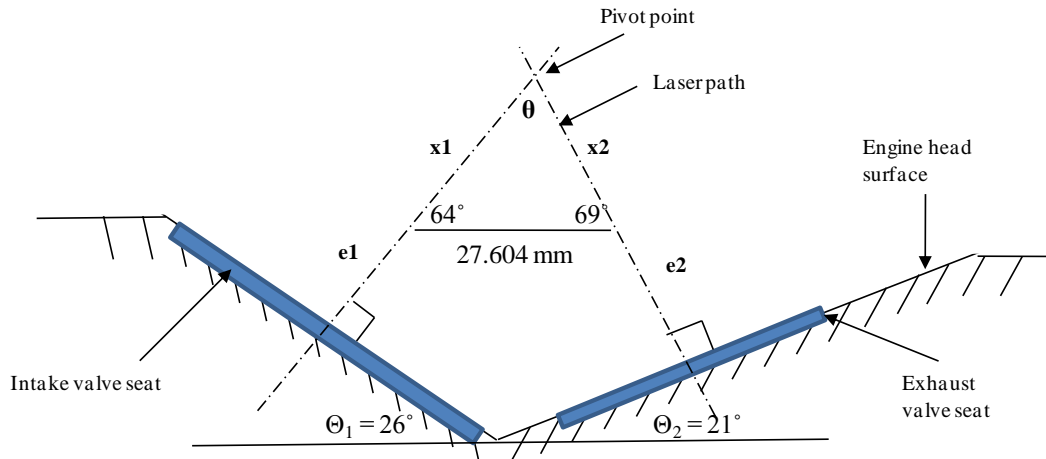


Figure 19: Schematic of variables used to determine the lower arc radius

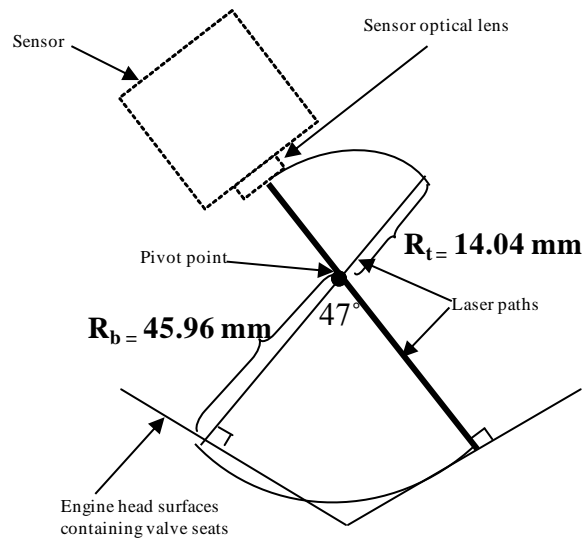


Figure 20: Schematic of the radii of the arcs centered at the pivot point and ending at the valve seat surfaces and the sensor optical lens

Peg Locations and Track Dimensions

Now that we have the arc radius R_t , we are ready to determine the locations of the pegs on the sensor. The pegs are connected to rollers that sit on the arch track. To set the peg locations, we looked at the length and width of the sensor, 85 mm and 94 mm. We decided to use three pegs, two sitting on the top edge of the track and one sitting on the bottom edge as shown below in Figure 21.

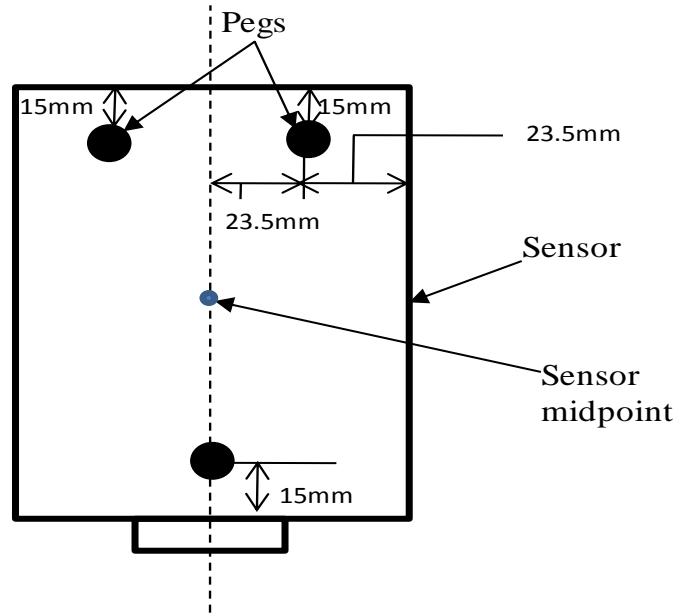


Figure 21: Peg positions relative to the sensor

To decide on the peg geometry, we looked at the benefits and tradeoffs of the number and position of the pegs. Having many pegs improves the stability of the sensor motion (since there are more contact points between the rollers and the track), but requires precision manufacturing to locate them along the same arcs as the track. Having only a few (two) pegs is easy to make, but is not as reliable since only two rollers take all of the force applied by the motor. Since the motor will be providing a force at the midpoint along the sensor length, that force gets transmitted to the pegs via moments, or the distance between the pegs and the point of force application multiplied by the force at each peg. From the moment balance, the more pegs there are, the less load each peg receives from the motor. Thus, our choice of three pegs provides a middle point between tradeoffs of reliability and ease of manufacturing. The locations of the pegs on the sensor were chosen to be far from the midpoint of the sensor so that the moment arm of each peg is sufficiently large that the force each peg sees is minimized, but not too far from the sensor midpoint that the track would need to increase in length significantly.

From the positions of the pegs, we can get the dimensions of the arch track, specifically the track chord length and thickness. The track thickness is the vertical distance between the top and bottom pegs, which is 55 mm (calculated from the sensor height, 85 mm, minus the two 15 mm offsets of the pegs). Finding the track chord length is more complicated. Figure 22 shows the known dimensions of the track, sensor, and laser path used to calculate the track length (the arc lengths at the top and bottom surfaces of the track). From these dimensions, a triangle can be drawn to determine the chord length of the track's top arc.

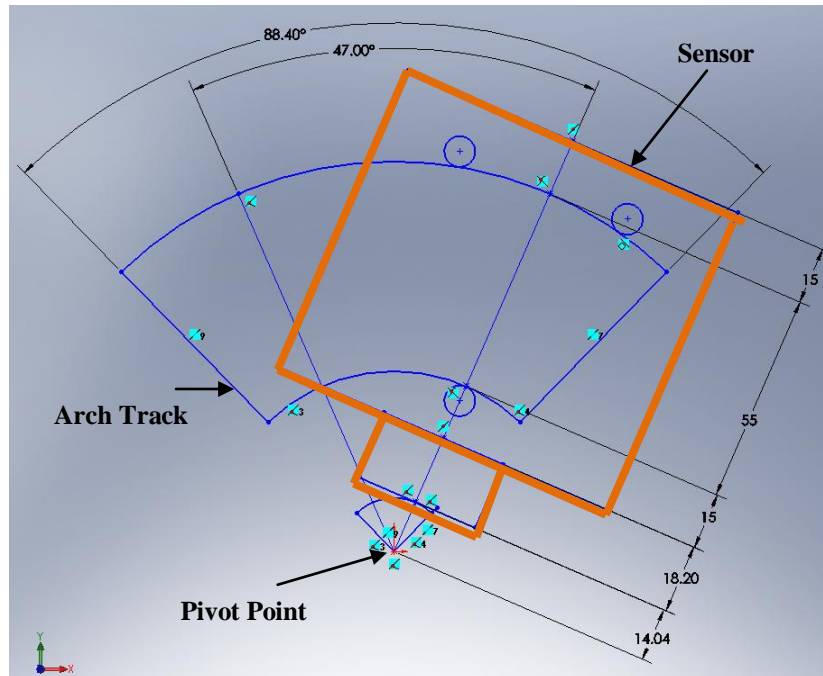


Figure 22: Dimensions of track and sensor based on peg location and calculated arc geometry.

The top arc chord length is equal to the chord length of the arc passing through the sensor midpoint and spanning 47 deg plus twice the additional chord lengths need to accommodate the top pegs. The chord length of the arc passing through the sensor midpoint is determined from Figure 22, where a triangle such as that in Figure 23 is shown and the length is found to be 81.3 mm using the law of sines (see Eq. 1).

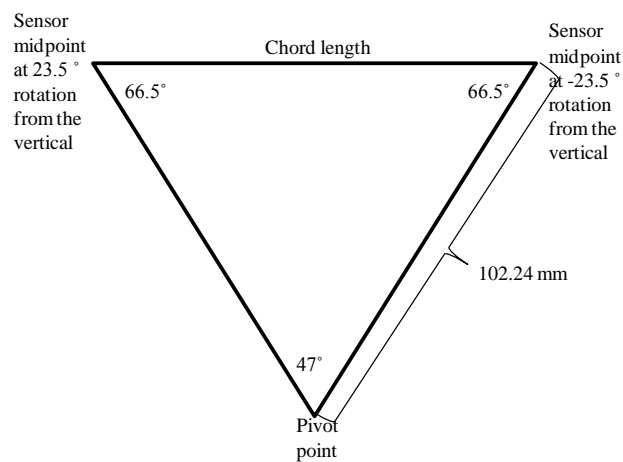


Figure 23: Triangle whose top length is the chord length of the arc passing through the sensor midpoint

Next, we need to determine the horizontal distance between the sensor midpoint and the right top peg when the sensor is tilted at its maximum of 23.5 deg (when the laser is orthogonal to the valve seat midpoint), shown in Figure 24. This horizontal distance, x , is equal to $23.5/\cos(23.5)$ which turns out to be 25.63 mm.

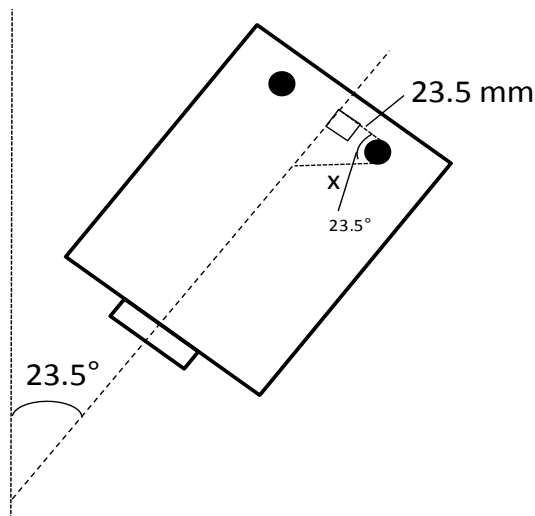


Figure 24: schematic showing the extra horizontal distance that the top pegs add to the top track arc's chord length

In addition, another 10 mm is added to the top arc's chord length to ensure that the pegs will not slide off of the track. Given the 81.3 mm chord length from the sensor midpoints, the 2×25.63 mm and 10 mm additional length to accommodate the pegs, a final chord length of 142.56 mm is found. The purpose of finding the track chord length is to determine the dimensions of the plate on which the track is mounted.

Dimensions of Plate with Arched Track

The width of the plate with the arched track was found using the top track arc's chord length and the sensor's range of motion allowed for focal length adjustment, and the height was found using both the sensor dimensions, motor dimensions, and range of motion coming from the sensor's fine tuning mechanism. Both dimensions were made to accommodate spacing constraints and to minimize the inertia of the plate.

We defined the plate width to be the top track arc chord length plus the extra horizontal distance that the sensor sticks out of the track. Figure 25 shows the geometry of the sensor when it is tilted a maximum angle of 23.5 deg from the vertical. Knowing that the pegs are located 15 mm below the sensor's top edge and that the sensor can be extended along the 23.5 deg axis 10mm due to the fine adjustment mechanism, the total inclined distance d in Figure 25 is 15 mm. Then, to get w , we simply added the distance of the peg from the right sensor edge, 23.5 mm, and the thickness of the fine adjustment mechanism, 9 mm, to get w equal to 32.5 mm.

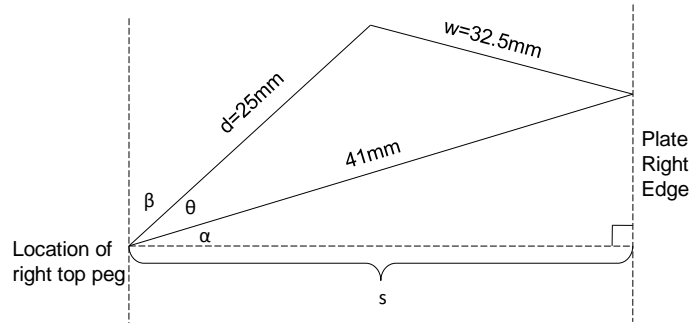


Figure 25: Geometry of sensor with maximum tilt of 23.5°

Then, using basic trigonometry, the following equations were used to obtain the total plate width:

$$\beta = \frac{88.4}{2} = 44.2^\circ$$

$$\theta = \tan^{-1}\left(\frac{32.5}{25}\right) = 52.43^\circ$$

$$\alpha = 90 - \beta - \theta = -6.63^\circ$$

$$s = 41 \cos \alpha = 40.7 \text{ mm}$$

$$\text{total_plate_width} = \text{chord}L + 2 * s = 142.56 + 2 * 40.7 = 224.0 \text{ mm}$$

Where chord L is the top track chord length that we calculated from the previous section.

To determine the plate height, we did a force/position analysis to determine the relationship between the transmission angle of the motor force and the distance between the motor shaft and the center of the track. The angle β is defined as the angle between the force perpendicular to the motor shaft and the component of that force tangent to the center-of-track-arc. The ideal β value is zero, where all of the force from the motor is used to move the sensor along the arc. Steps taken to obtain the relationship were:

1. Find the chord length of the arc going through the center of the track. Figure 26 and the equations below show that $AL=96.86\text{mm}$.

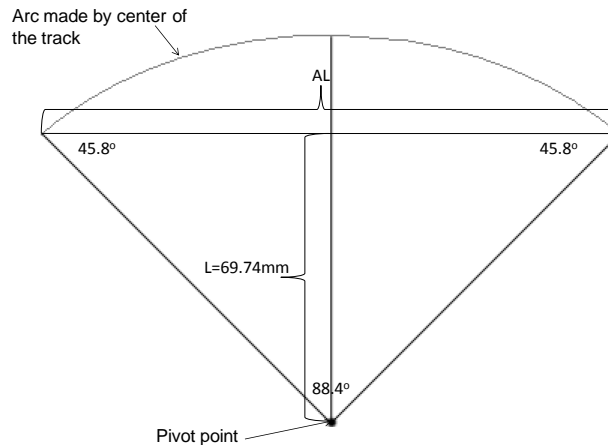


Figure 26: Geometry of center-of-track arc about the pivot point

$$\frac{\sin(88.4)}{AL} = \frac{\sin(45.8)}{69.74}$$

$$AL = 96.86 \text{ mm}$$

2. Find the angles that the force perpendicular to the motor shaft make with the horizontal and vertical and the vector tangent to the center-of-track-arc. Figure 27 and equations below show that the angles add up to 90 degs.

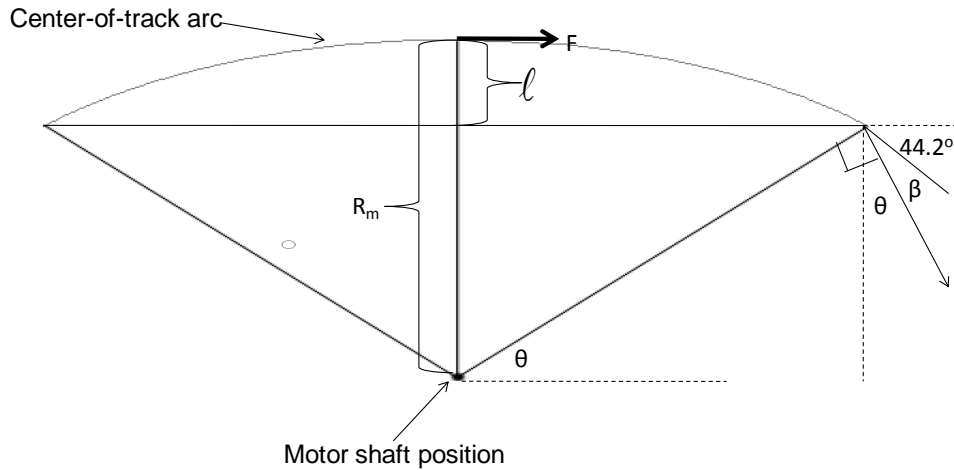


Figure 27: Geometry of center-of-track arc about the motor shaft

$$\ell = L(1 - \cos(44.2)) = 19.7 \text{ mm}$$

$$90 = \theta + \beta + 44.2$$

$$\beta = 90 - \theta - 44.2$$

$$\beta = 45.8 - \tan^{-1}\left(\frac{R_m - \ell}{AL/2}\right)$$

$$\beta = 45.8 - \tan^{-1}\left(\frac{R_m - 19.7}{48.43}\right)$$

The relationship between transmission angle β and R_m is nonlinear, as shown by the last equation. Plotting efficiency $(1-\beta/90)*100$ against the distance between the motor shaft and the bottom-of-track arc, $R_m - (\text{track width})/2$, Figure 28 is generated below. Efficiency is defined as the percentage of motor force that is being used to rotate the sensor.

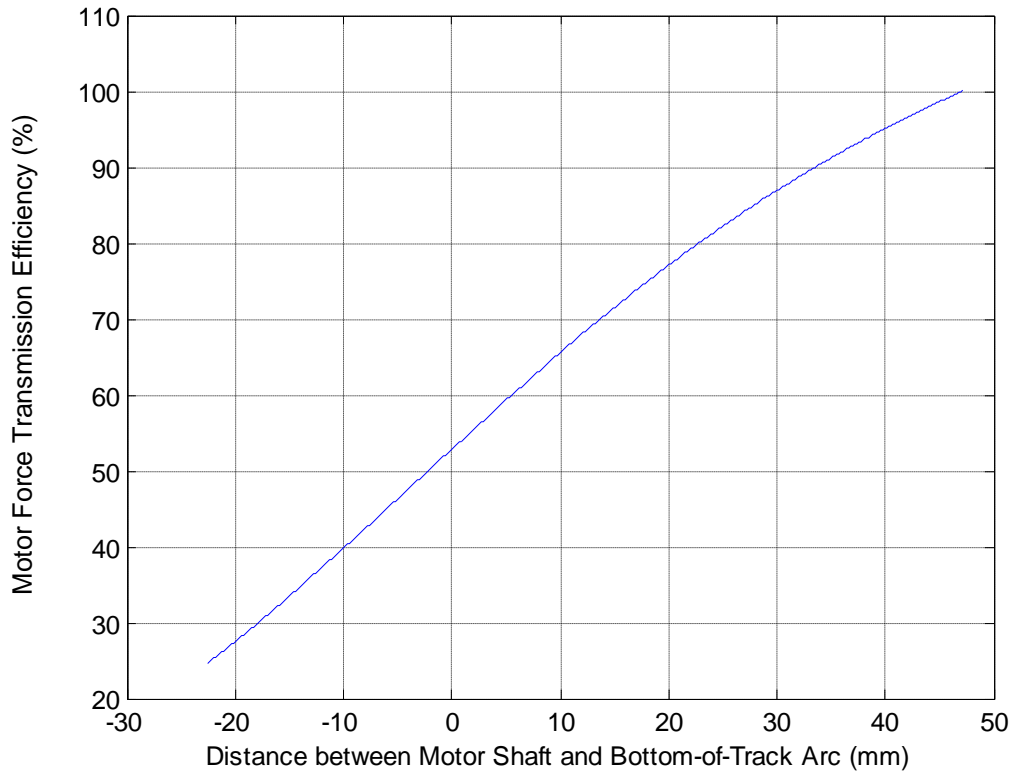


Figure 28: Plot shows relationship between the distance of the motor from the track’s bottom surface and the force efficiency. Positive distances relate to the motor shaft positioned below the track arc.

Figure 28 shows that if the motor shaft is placed at the same vertical position as the bottom-of-track arc, the efficiency is still greater than 50%. That is, more than 50% of the force applied by the motor is used to rotate the sensor while the rest is transmitted to the bearings and is useless. We chose the motor shaft to be located 10 mm below the bottom-of-track arc because it maintains about 65% force efficiency while not being too far below the arc that it interferes with the engine head.

Using our selected motor’s dimensions and our chosen motor position, the height of the plate with the arc track was determined to be 123.58 mm. Figure 29 shows the dimensions. The space above the track, 25mm was set based on the amount that the sensor stuck out of the track and the its adjustable vertical range from the fine tuning mechanism.

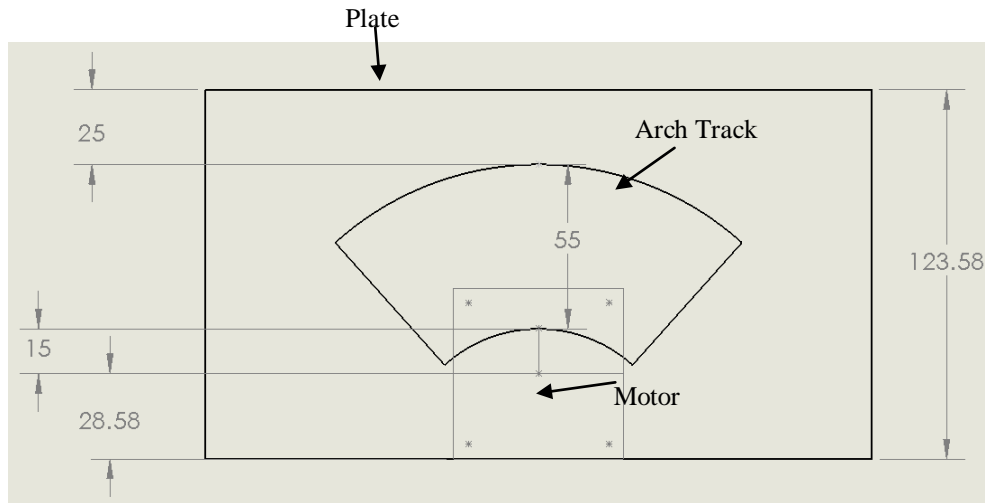


Figure 29: Height dimensions of plate with arch track

Once the plate height was set, we checked that it does not interfere with the engine head. Using the fact that the distance from the sensor optical lens to the engine surface is 60 mm, and that the lens is located 33.2 mm below the bottom-of-the-track arc, the clearance between the plate and the engine was found to be 34.3 mm. This clearance provides ample room for the plate to pass obstructions from the engine head.

Resolution of rotational motion: In order to determine the resolution angle for control of the rotational motion of the sensor, we first derived an equation relating the angle the motor has turned from the horizontal (θ_{motor}) with the angle the sensor makes with the horizontal (θ_{sensor}) by using the geometry of our mechanism. This equation was found to be (with all angles in degrees):

$$37.24 * \sin(\theta_{sensor} + 90) = 74.74 * \sin(270 - \theta_{sensor} - \theta_{motor})$$

Numerically differentiating this equation about a value for a sensor angle of 26 degrees (the largest angle needed to inspect valve seats) and multiplying by the minimum angle of rotation controllable by the stepper motor yields a value of 0.3 degrees/pulse, which is the resolution for the control of our sensor rotation.

Motor Torque Analysis

Following the completion of the position analysis, we used the resulting geometry of the sensor motion to calculate the torque needed by the stepper motor to control the sensor motion. To do this, we consider the geometry as shown in Figure 30, as the greatest amount of torque will be needed when the sensor mount is positioned at one of the extreme ends of the arc.

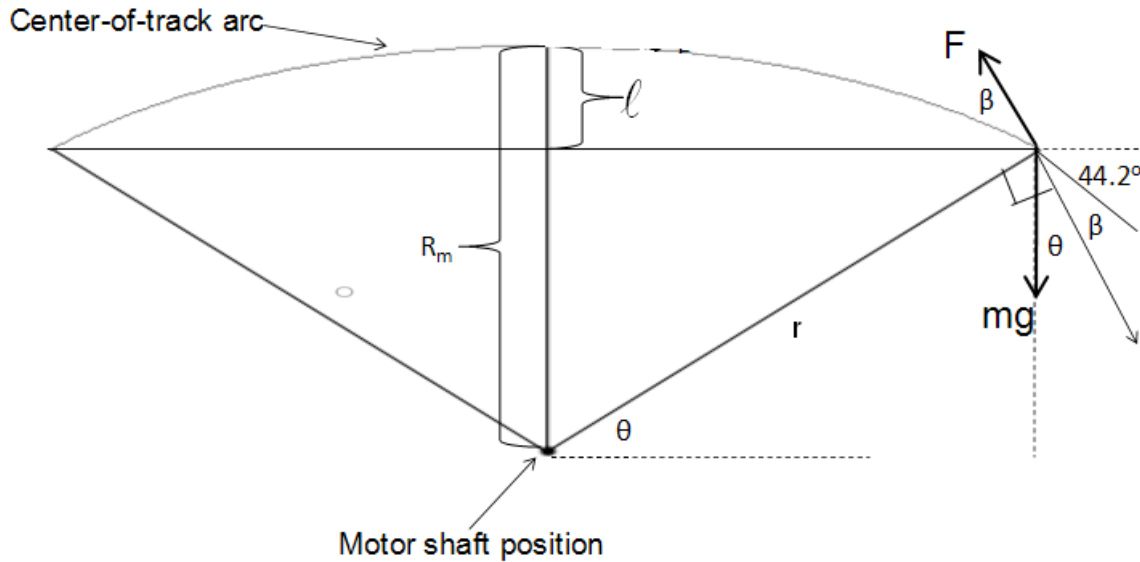


Figure 30: Geometry of the motor torque analysis

As shown in Figure 30, there are two forces acting on the sensor mount: namely, gravity (mg) and the force exerted by the motor (F). The torque T applied by the motor will be equal to the product of the moment arm along the beam r and the resulting force F , or $T = F \times r$. Assuming that both the force F and gravity act at nearly the same point, the static force balance on the motor yields the following equation.

$$\frac{T}{r} \cos \beta = mg \cos(\beta + \theta)$$

Using values of $r = 51.6$ mm, $\beta = 25.6$ deg, and $\theta = 20.2$ deg from the positional analysis and a conservative mass m of 1.5 kg, the maximum torque T required is found to be 0.59 Nm, or 83.6 oz-in. This translates to a maximum force F of 11.4 N, which will be transmitted to the rollers connecting the sensor mount and the arc track. Using these results, we checked our purchased motor and bearing ratings to ensure that the maximum torque and loads they can handle are larger than our values. The motor's maximum torque is 166 oz-in, which gives us a factor of safety of 2. The bearing's maximum radial load is 3024 N, which gives us a factor of safety of 796. Thus, our assumptions in selecting purchased components are valid and the components will not fail during operation.

Vibration Analysis

Because of the high level of precision required for the positioning of the sensor, any time-varying deflections of the structure due to vibrations must be kept well under the total tolerance of one micron in the x-direction (transverse motion of the linear stage). For this reason, all of the parts have been designed as rigidly as possible and all mechanisms that allow motion are clamped down during operation. This ensures the primary cause of deflection is the elasticity of the material used for all parts. Because micro-precision is

not needed in the other two directions, vibrations have not been considered in the other two directions.

The part that will cause almost all of the deflection is the plate supporting the mechanism, as it must be both relatively large and supported only at two ends to allow both the mechanism's motion and vertical adjustment of the plate. Although the length, width, and thickness of the of the plate and the material used to construct it will all affect its vibration characteristics, we have limited the choice of material to Aluminum 6061-T6511 (as described above) and we have limited two of the three dimensions of the plate (the length and width) as being the smallest dimensions allowable by the position analysis. This is to both limit the amount of structure that is hanging away from the motion stage and make the design more aesthetically pleasing. Thus, the major design variable to be determined from a vibration analysis is the necessary plate thickness.

Vibrations causing deflection of the sensor relative to the motion stage may be introduced into the system three ways. The first is from the surrounding environment external to the system. For this reason, we have included a thick granite base that should be capable of dampening any vibrations from the environment (which should be small) to negligible levels. The remaining two sources of vibrations are possible harmonic excitation due to a rotating imbalance in the motor driving the motion stage and possible sudden decelerations of the motion stage that will occur should the motion of the linear stage not be perfectly smooth. Vibrations occurring due to non-smooth motion may arise due to a sudden "shock" deceleration or a persistent driving harmonic excitation due to forces such as friction.

Assumptions for vibration analysis: For the following analysis, the entire deflection in the x-direction of the sensor relative to the motion stage is assumed to be caused by the deflection of the plate supporting the mechanism. That is, the support structure mounting the plate to the stage is assumed to be rigid due to its design. Furthermore, the motion of the sensor is assumed to perfectly match the motion of the plate in the x-direction. This means that the sensor will not move relative to the support it is bolted to, and the support will not move relative to the plate it moves on. In order to ensure this, the sensor support will be clamped to the plate during transverse motion of the stage, during which micro-precision is needed. The validity of this assumption is supported by the fact that in the x-direction alone, all displacement of the structure between the sensor and the motion stage must come from compression or extension of very rigid structure of short length with the exception of the deflection of the plate, which will deflect due to bending moment. Thus, because the compression of a rigid structure of small scale is negligible compared to the deflection of a plate in the out of plane direction, the focus of this analysis will be on the plate itself.

Furthermore, this plate is assumed to be thin, as its thickness is approximately one order of magnitude less than the other two dimensions, and the plate is assumed to behave as an elastic structure with small deflections. The boundary conditions assumed for the plate are shown in Figure 31 below. If we were to introduce a coordinate system u , y , and z , where u is the out of plane deflection of the plate, y is the distance coordinate in the y -

axis, and z is the distance coordinate in the z -axis, then sides “a” would be considered free (such that $\frac{\partial u}{\partial z} = 0$ along each side “a”) and sides “b” would be considered clamped (such that $u = 0$ and $\frac{\partial u}{\partial y} = 0$ along each side “b”). Side “b” is considered clamped as it is welded to a support (Appendix I.4) in such a way that there should be almost no displacement and no rotation at the edge, and the support is then bolted down in such a way that it should not move relative to the motion stage.

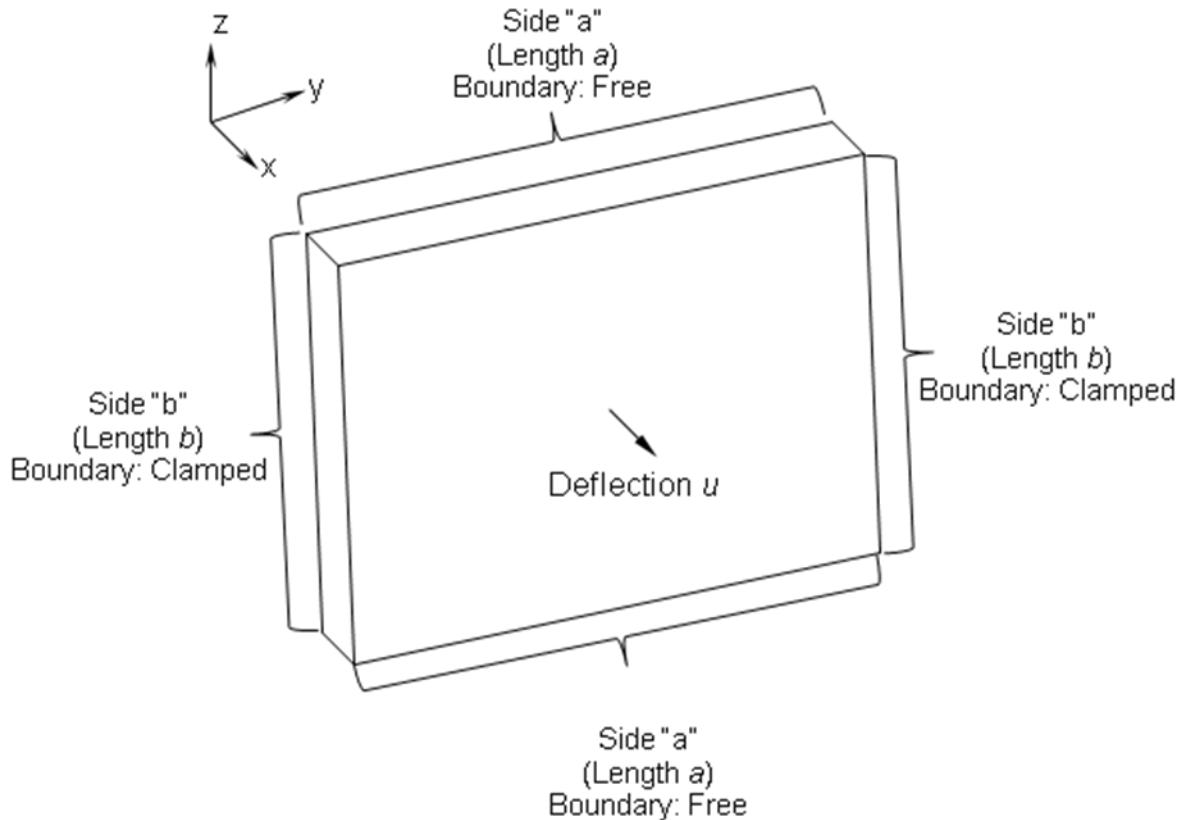


Figure 31: Boundary conditions for plate during vibration analysis

Vibrations due to harmonic excitation from motor: When a rotating mass has a nonzero product of inertia (i.e. if the mass is not perfectly distributed about the axis of rotation) harmonic excitation of the supporting structure may result. The response of the structure is a displacement varying sinusoidally with time that is proportional to the severity of the rotating imbalance. Figure 32 from *Engineering Vibration* by Daniel J. Inman show the response displacement normalized by the strength of the rotating imbalance (characterized by the ratio of the structure mass to the mass and eccentricity of the rotating imbalance) plotted against the frequency ratio, or the ratio of the driving frequency (the frequency of the motor driving the imbalance) to the natural frequency of the system. Regardless of the damping ratio characterizing the system, the normalized magnitude of the response appears to approach zero as the frequency ratio approaches zero. Because the rotating imbalance of the motor should be small considering both its

size relative to the structure and the quality of the motion stage, ensuring a very high natural frequency for our plate should ensure a negligible response to the harmonic excitation from the motor.

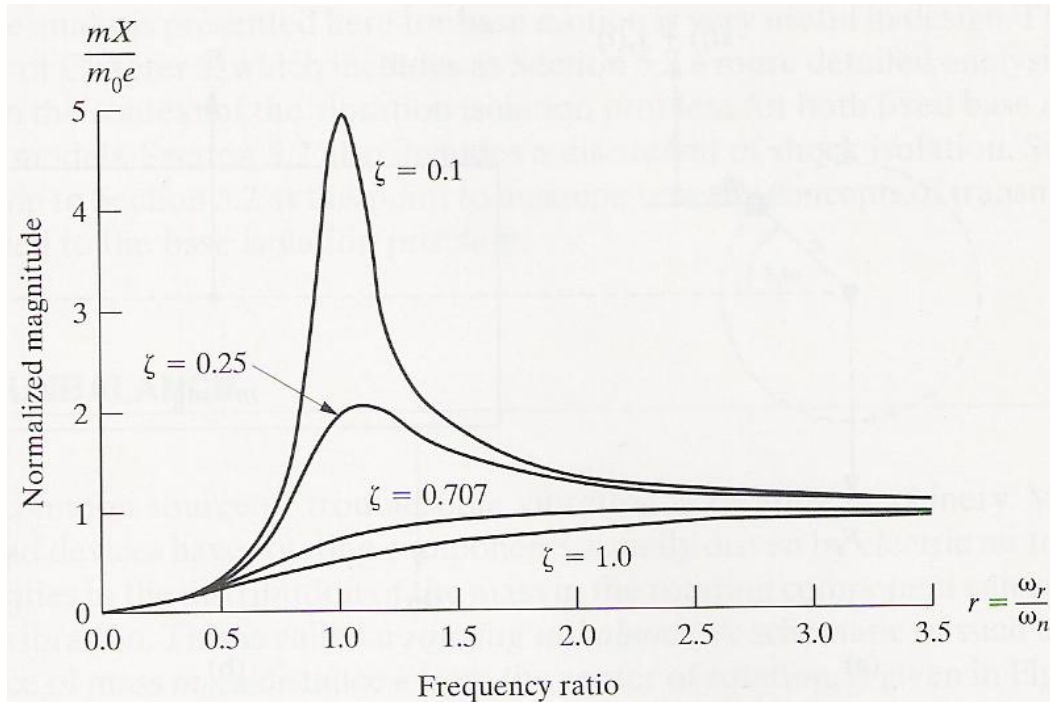


Figure 32: Normalized magnitude of the response to harmonic excitation approaches zero as the ratio of the driving frequency to the structure’s natural frequency approaches zero (taken from *Engineering Vibration, 2nd Ed.* by Daniel J. Inman)

The natural frequency (ω_n) of a plate in rad/s with the boundary conditions assumed above for out of plane vibrations is given by equation below (from [12]).

$$\omega_n = \frac{\lambda^2}{a^2} \sqrt{\frac{Eh^3}{12\gamma(1-\nu^2)}}$$

Here, a is the length of side “a”, E is Young’s modulus for the material, h is the thickness of the plate, γ is the density of the material per unit thickness, ν is Poisson’s ratio for the material, and λ is a vibration parameter dependent on the ratio of the lengths of sides “a” and “b” and the boundary conditions (from [12]). For this equation, all material constants are based on Aluminum 6061-T6511 [13], and all parameters depending on the geometry and boundary conditions are based on the geometry and assumptions that have already been listed. Thus, the only parameter that needs to be determined is the plate thickness h . Figure 33 shows the resulting damping ratio of the plate as a function of its thickness. The damping ratio is based on a driving frequency of 10 Hz (63 rad/s), as given the pitch of the screw driving the motion stage and the maximum transverse speed required for our design, this is the maximum driving frequency that will be encountered.

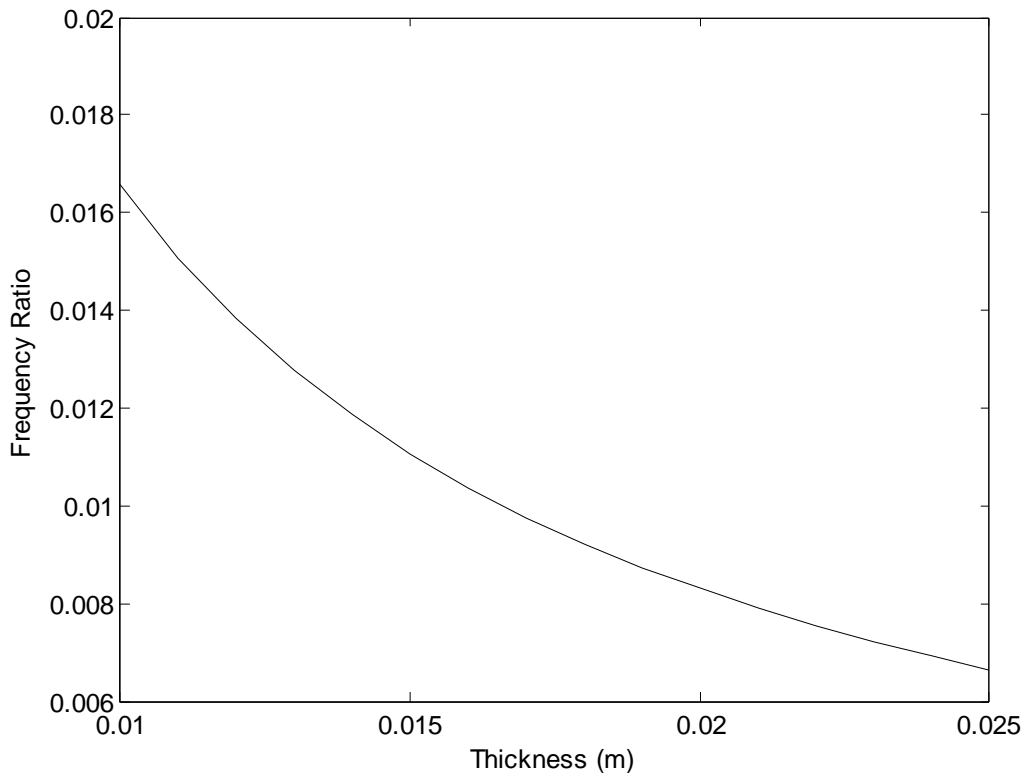


Figure 33: Frequency ratio decreases with increase in plate thickness

As shown above, the frequency ratio is very close to zero and continues to decrease as the plate thickness increases. Although the plate thickness cannot exceed 25mm due to the thickness of the stock that will be used to construct it, choosing a thickness of 25 mm will provide a frequency ratio of ~0.007, which ensures negligible response to harmonic excitation.

Deflection due to non-smooth motion of linear stage: If the motion stage maintains a constant velocity, the motion of the sensor should exactly match the motion of the linear stage. However, if the sensor experiences an acceleration or deceleration relative to the motion stage, then the plate could deflect such that the actual position of the sensor will not match the location of the motion stage. Such deflection can be modeled by determining the equivalent force acting on a plate due to the accelerating masses of the plate, sensor, mount, and external track, and then modeling the plate as an Euler-Bernoulli beam to determine the resulting maximum deflection.

The mass of the plate, when subjected to an acceleration (or when the ends of the plate are subjected to a relative deceleration) will create an equivalent force that can be modeled as a distributed force over the length (a) of the plate. The total mass of everything mounted on the plate, conservatively estimated at 2 kg from the density of the material, the geometry of mount and track, and the mass of the sensor, is then modeled as a point force acting at the middle of the plate, which is the worst case scenario for deflection. This model is shown in Figure 34 below.

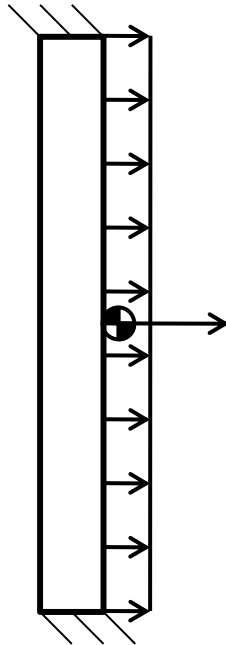


Figure 34: Deflection of plate modeled as Euler-Bernoulli beam under distributed load from plate inertia and point force from inertia of objects mounted on plate

This deflection can be calculated by superposition of the deflection due to the distributed load and the deflection of the concentrated load. By assuming an acceleration of 1 g for our initial analysis, the deflection u can be calculated by equation below, taken from the superposition of two equations from the databook for course ME 382 at the University of Michigan.

$$u = \frac{mga^3}{192EI} + \frac{pbhga^4}{384EI} \quad (x)$$

In this equation, m is the mass of all objects mounted on the plate, g is the acceleration due to gravity, I is the moment of inertia of the plate about the y-axis, and all other parameters are the same as for the equation for natural frequency. This 1 g deflection, as a function of the plate thickness, is shown in Figure 35 below.

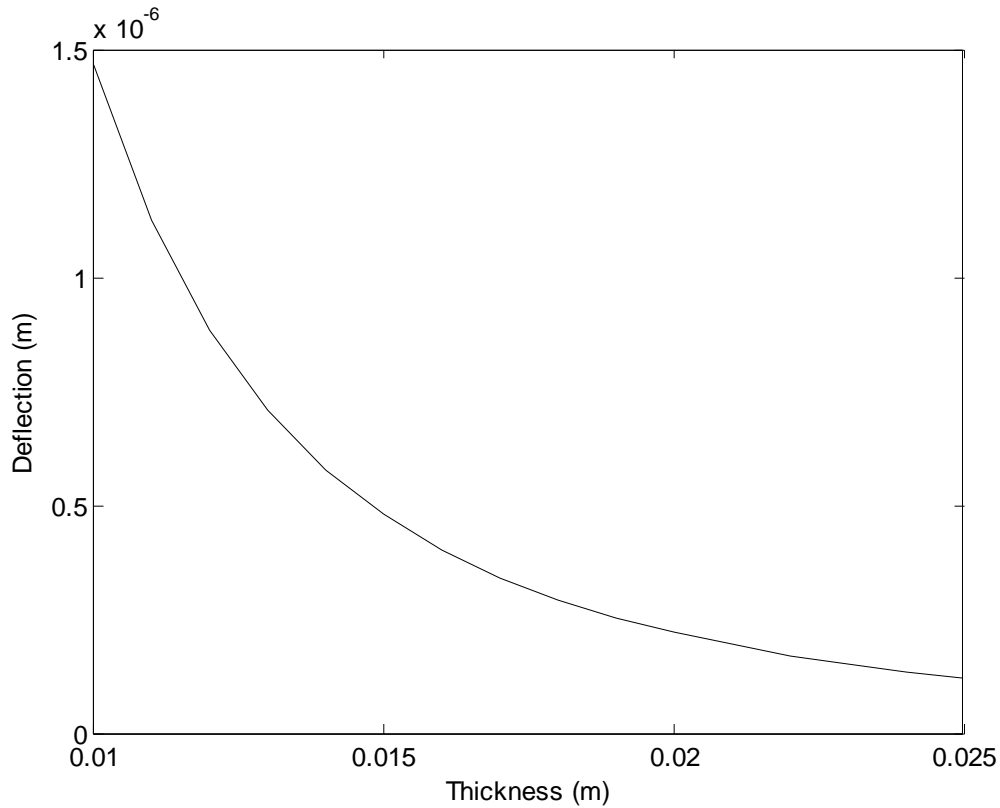


Figure 35: Deflection of plate under 1 g load decreases with increasing plate thickness

As shown above, the plate deflection crosses the 1 micron threshold at a plate thickness of 11.5 mm and decreases all the way to 0.12 microns at a plate thickness of 25 mm. Because an increase in plate thickness improves the deflection characteristics of the plate under both harmonic excitation and rapid deceleration, the maximum plate thickness allowed by the stock material (25 mm) has been chosen for our design. Once this thickness had been chosen, we calculated deflection of the plate as a function of the deceleration of the plate supports (in g's), the results for which are shown in Figure 36 below.

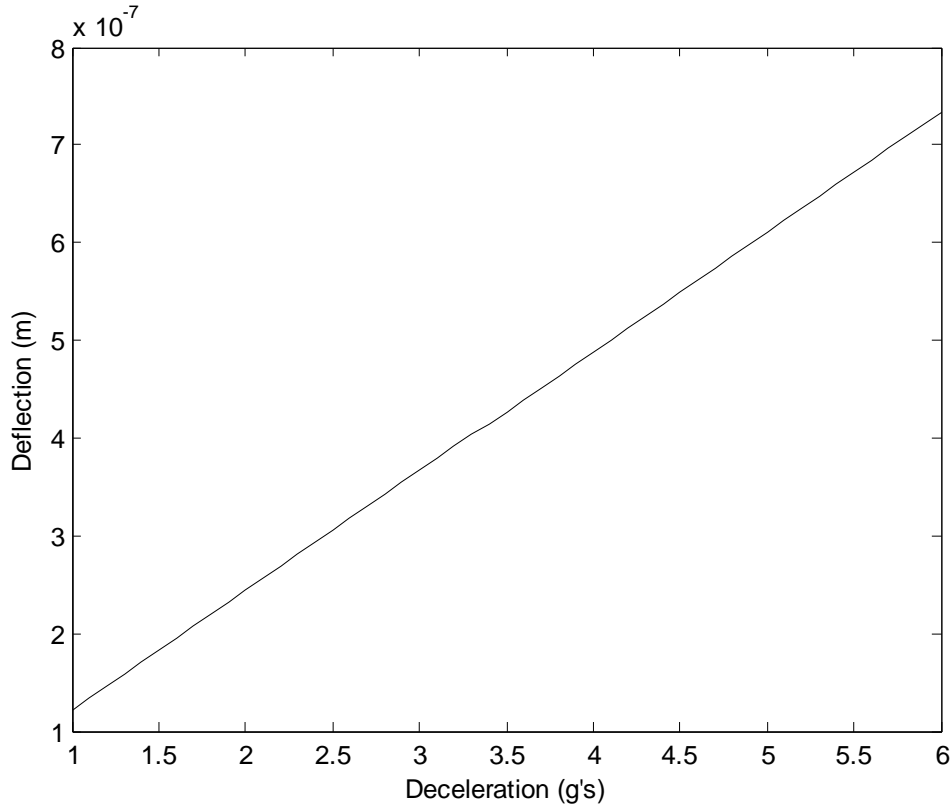


Figure 36: Plate deflection stays within sub-micron range for a large range of motion stage decelerations.

As shown above, the maximum deflection of the plate should stay within 0.5 microns for all motion stage decelerations up to 4 g's, which is well beyond any loading the stage should experience during normal operation.

Therefore, a plate thickness of 25 mm ensures that the plate will be almost entirely unaffected by harmonic excitation from a potential rotating imbalance of the motor driving the stage, or any harmonic excitation of a reasonable driving frequency, and that the plate will deflect half a micron or less for all loads on the motion stage that may arise from non-smooth motion of up to 4 g's.

Finally, to consider vibration response due to harmonic excitation during unsmooth motion, we will look at the case where the plate thickness has been set at 25 mm. From the natural frequency equation above, the natural frequency for this system (converted to Hertz) in the x-direction should be 1500 Hz. The resonant frequency, as a function of the damping ratio ζ and natural frequency for the system, is given by equation below (from [11]).

$$f_r = f_n \sqrt{1 - \zeta^2}$$

Similarly, the normalized magnitude of the harmonic response $\frac{xk}{F}$ of a one dimensional response is given by equation below (from [11]).

$$\frac{Xk}{F} = \frac{1}{2\zeta\sqrt{1-\zeta^2}}$$

In this equation, X is the displacement response, k is the stiffness of the system, and F is the magnitude of the force driving the harmonic excitation. By taking the stiffness of this case to be the inverse of the slope from Figure 36 and setting the threshold displacement response at 0.5 microns, we can solve for the loading (F) in g's as a function of the damping ratio. Plotting the resulting loading against the resonant frequency needed to drive that response for a range of damping ratios from 0 to .707 yields Figure 37. A range of damping ratios is used for this plot because the actual damping ratio for the system is not known.

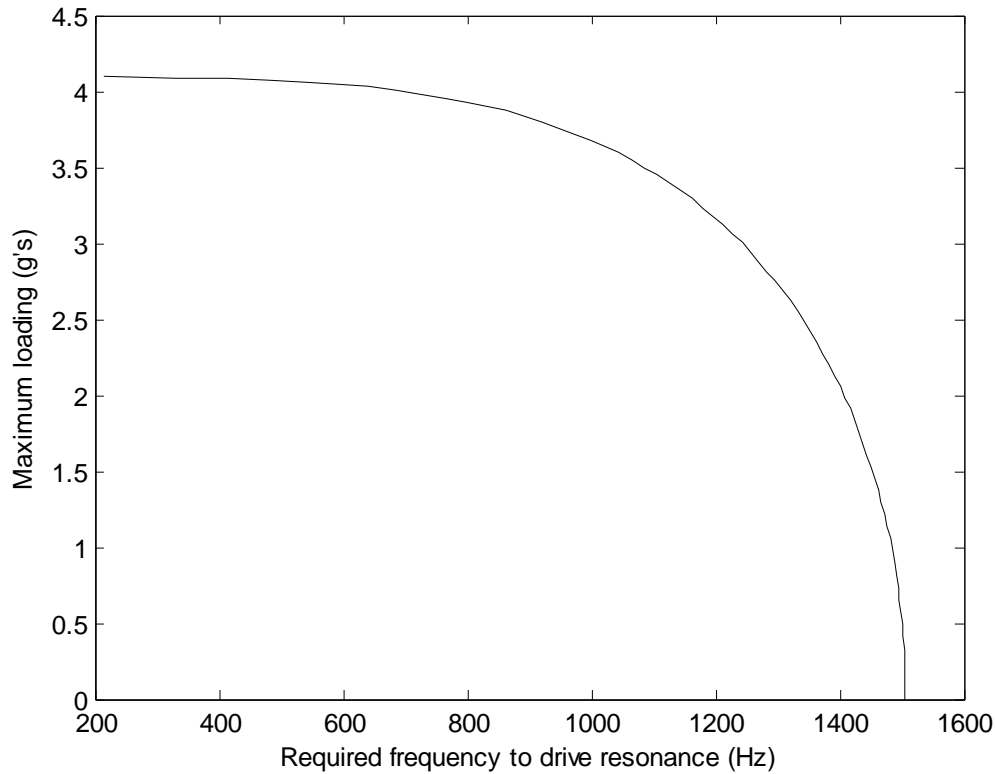


Figure 37: Threshold magnitude of driving loading as a function of required driving frequency for threshold displacement of 0.5 microns

This figure shows the magnitude of the loading driving the harmonic excitation that would be required to exceed a 0.5 micron response against the driving frequency required to force the resonant response in the system for the range of damping ratios listed above. This shows that in order for the plate to deflect 0.5 microns in a worst case scenario, the driving harmonic excitation must either have a very high magnitude or a very high frequency. For example, if a driving frequency of 1000 Hz was somehow achieved, the magnitude of the driving loading would still have to be at least 3.7 g's for the displacement response of the plate to be half a micron. Because the driving harmonic excitation should not come close to approaching these combinations of frequencies and

magnitudes, this structure should suffice for the required precision of the sensor displacement.

Motion stage support structural analysis

The support structure consists of a granite block, four 6061 aluminum vertical posts, and two T6061 aluminum top supports. The granite block is 65 x 65 x 4.5 cm and is used to isolate the inspection device from external vibrations. Four vertical posts rest on the granite block. On each set of two vertical posts sits one top support (see Figure 15, p. 24). The posts and the top support were chosen to minimize deflections of the structural support under the load of the linear stage. The motion stage is 10 kg, the sensor is 0.5 kg, and aluminum mounted materials including the arc motion plate are 5 kg. Thus, a total of 15.5 kg must be supported by the four vertical posts and top support.

First a stress analysis was done on the vertical posts to confirm that a dimension of 2.5cm x 7.5cm could be used for the top support. This dimension was chosen based on available raw materials and confirmed by a stress analysis for 6061 aluminum beam under the fixed-free condition. The vertical support with the loading force is shown in Figure 38 with an area of 19 cm², modulus of 70 GPa, and resulting strain of 10⁻⁶. Following this analysis the dimensions of the top support were set based on the criteria for mounting the motion stage. The motion stage has bolt holes located 50 mm apart along the length of the engine head and at 100 mm apart in the traverse direction. This set minimum requirements of the top support to be 5 cm x 13 cm (w x L). The final dimensions of the top support will be 8cm x 30cm (w x L) based on a deflection analysis illustrated by Figure 39. We also have a thickness (t) to the top support of at least 13 mm to support holes for 0.25 inch bolts. This allows ample room for bolting the vertical posts, top support, and motion stage together. The results of this analysis provided a second moment of inertia (*I*) of 156 mm³ and a max deflection at the center of the top support of 0.01 mm. This deflection is minor when compared to our measurement range of 8.5 cm therefore the aforementioned dimensions will provide a solid support structure for our prototype. We expect to see our results of deflection minimization for both initial demonstration purposes and recurring operation.

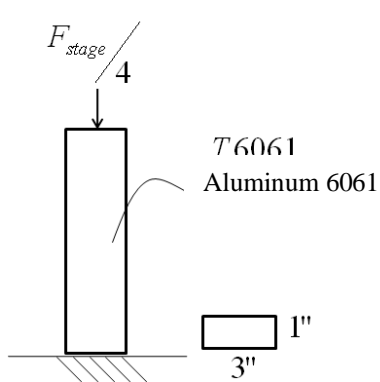


Figure 38: Fixed-Free diagram with force on vertical support

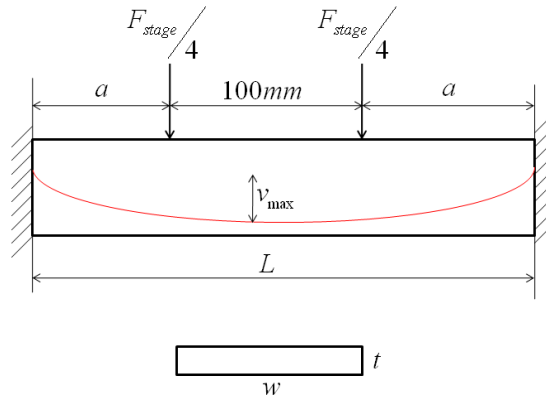


Figure 39: Fixed-Fixed diagram with force on top support, max deflection shown at center of beam

An assembly analysis provided a confirmation that the previously chosen dimensions would allow for assembly of the granite, four vertical posts, top support, and the linear motion stage. The vertical posts will be connected to the granite block by bolted L brackets. The top of the vertical posts are connected to a top support by two bolts on each post. These top supports support the linear motion stage, which will have in total 8 connection bolts between the top support and motion stage. We will be purchasing the granite block and raw materials for the vertical posts and top support. We will then mill holes to fit the aforementioned connection bolts.

This support structure is created for the ATS 115 Linear motion stage from Aerotech, Inc. It is unlikely that the motion stage can be easily replaced with a different model. However, the diverse operations of our system are allowed by adjustability in the sensor system attached to the slide of the motion stage.

It should be noted that the support structure was changed during the manufacturing process to be made of 1018 mild steel. This steel will provide greater rigidity while adding minimal cost. For the structure the rigidity is most important, while added weight is not of concern as it does not appear in our engineering goals. Dimensions are kept constant and the only change on the above variables is the modulus of elasticity value has increased from 70 GPa to 210 GPa. This factor of three between moduli of elasticity lowers the stress in the structure by a factor of three and decreases the maximum deflection of the top support. Thus, by selecting mild steel we have improved the support system while not addition significant cost.

Final Design

The final design consists of four major components that allow the sensor to rotate and translate about the valve seats and that support the motion stage on which our mechanism is mounted. Figure 15 shows a complete assembly of the design, including the four parts that we designed: the fine tuning mechanism, arch track and plate, plate support, and the motion stage support. Each part is described in detail below from the laser sensor to its connections to the motion stage, granite base, and finally the engine head that the sensor is measuring.

Sensor mount / fine tuning mechanism

The laser sensor is oriented so that the optical lens faces downwards and is connected with bolts to the sensor mount assembly. The mechanism allows for adjustment of the distance between the sensor and the surface of the engine head for focusing purposes (see Figure 40) and allows for mounting rollers into the plate. This part consists of the sensor plate (Appendix I.1), onto which the sensor is mounted that slides within the sensor mount bracket (Appendix I.2). Once the position of the sensor has been adjusted, the plate can be locked down relative to the bracket by tightening bolts that are fed through slots machined into the bracket and threaded into the plate containing the sensor mounts. These two parts were designed such that they are as small as possible while still being large enough to easily hold the sensor, thick enough to thread screws into, and rigid enough to ensure negligible displacement of the sensor at any time. The mechanism has

three track rollers screwed into it and is attached to the arched track and plate through the rollers. The bottom roller is adjustable with a set screw such that the rollers can be clamped down tighter on the external track to allow less play and ensure smoother motion.

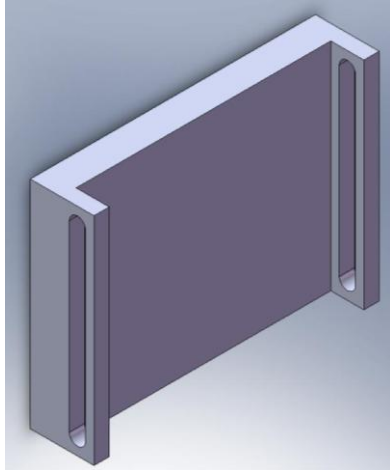


Figure 40: Sensor Mount Bracket

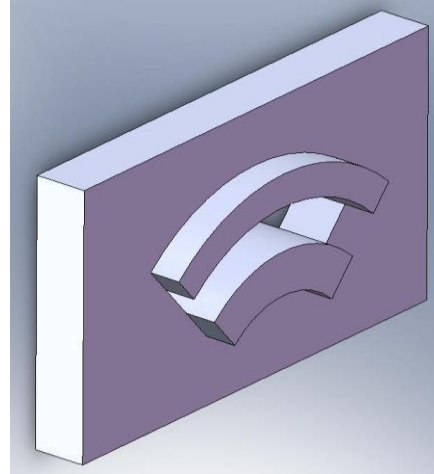


Figure 41: Arched Track

Arched track and plate

The arched track (Appendix I.3) enables the rotation of the sensor about a non-physical pivot point. It consists of an extruded track with a constant radius arc, along which the sensor mount will move (see Figure 41). The track width and radius were determined with the positional analysis in the previous section. Its thickness was determined from the thickness of the track rollers (9.5 mm).

Plate support and motion stage attachment

The plate support (shown below in Figure 42) is designed to attach the arched track and plate to the moving platform of the linear motion stage. This support has been designed such that the plate can be moved up and down relative to the engine head in order to adjust the pivot point/axis of rotation of the mechanism (see Figure 12). This support has also been designed such that the arch plate is fixed on two edges to minimize vibrations (as described in the vibration analysis section). This fixture is achieved by bolting each side of the plate to triangular support pieces (see Appendix K.4). These triangular supports, in turn, are bolted down to the motion stage attachment (see Appendix K.5), which is bolted down to the motion stage. By bolting or welding everything down and providing considerable rigid support in the x-direction by use of the triangular support, the motion of the sides of the arch plate should have only negligible deflections (much less than a micron) compared to the position of the motion stage, which will validate the assumptions made for the vibration analysis.

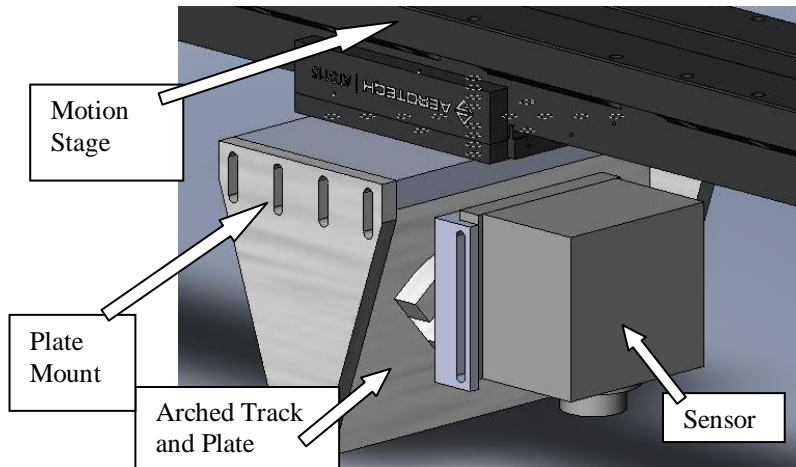


Figure 42: Arched track mounted to plate supports and linear motion stage.

Motion Stage Supports

The motion stage supports position and support the motion stage above the engine head. It consists of two U-shaped supports consisting of a top support (Appendix I.6) and side supports (Appendix I.7) that extend over the top of the stage, onto which the stage is bolted using predefined holes on the stage. The width of each beam is greater than the width of the motion stage, allowing for increased stability in the transverse direction (along the engine head width). This stability is essential because the sensor is usually rotated off-center from the middle of the motion stage, creating a moment about the x-axis. Each beam is attached to the granite block base using L-brackets (Appendix I.8) and bolts.

The granite base is a rectangular block on which all system parts are mounted. The engine head is mounted upon 8 vertical pins that protrude through the granite base. The motion stage supports are bolted onto the base so that the length of the motion stage is positioned directly along the length of the engine head.

Addition of Motor and Transmission

A stepper motor is used to drive the sensor's rotation. The transmission from the sensor to the motor uses a shaft that is screwed onto the sensor mount (see Figure 43). From the sensor mount, the shaft runs through the thickness of the arc plate in the middle of the arc track. The side of the shaft shown in Figure 43 rotates within a cylindrical sleeve that sits within a housing that contains a linear bearing that is directed perpendicular to the sleeve. The bearing rides along a second shaft which is rigidly connected to the rotating motor shaft. This is done using set screws through the second shaft. The rotary stepper motor is mounted on the back of the arc plate at the vertical centerline of the arc track. The motion of the motor and thus, the sensor is controlled using a controller from Applied Motion Products and the Si Programmer. The Si Programmer contains simple motor commands. Useful commands that were used on our motor for demonstration purposes are included in the Appendix.

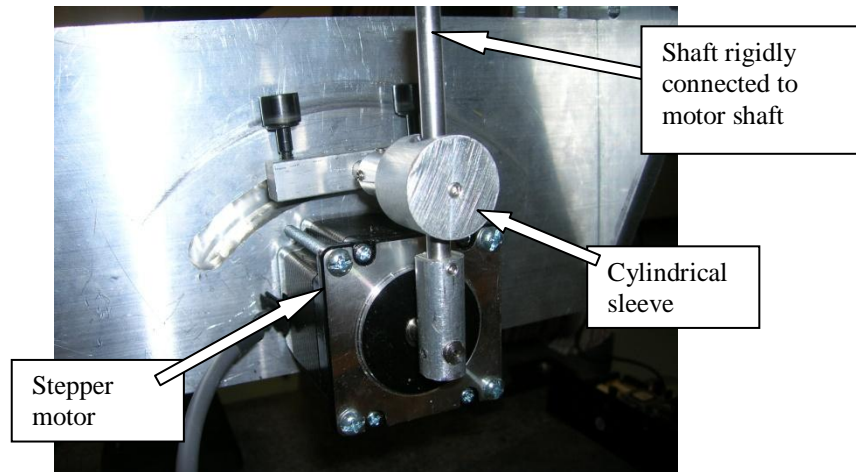


Figure 43: Prototype transmission

Finally, the roller mechanism also contains a pair of rollers on the back side of the arch plate that are rigidly connected to the shaft running through the plate such that these rollers can be used to hold the sensor mount tight against the plate. These back side rollers prevent the rollers on the track from binding up. They act to support the moment caused by the motor shaft and thus allows smooth motion and control of the sensor mechanism via the stepper motor.

In summary, our final design allows a user to scan all 16 valve seats by controlling the motion of the sensor both along the engine head length and width. The device can accommodate a variety of engine head sizes, given its open geometry and the ability to adjust both the focal point and fine-tune focus of the sensor. In addition, it maintains a clearance between the sensor and the engine head that allows for non-contact measurements to be taken. All of the sensor's motion is controllable due to the use of a motor and linear stage, allowing for adjustability of speeds and positions. Finally, our design is justified using sound engineering analysis and reasoning, ensuring a high level of reliability. Our design's combination of adjustability to accommodate different engine heads, controllability of sensor motion, high reliability, and micro-precision and accuracy, and most importantly, its ability to be automated and quick at measuring valve seat geometry, makes it a viable and desirable concept for our potential customers, the auto manufacturers.

Manufacturing and Assembly

The following describes the steps we took to fabricate our prototype. Our product is not intended for mass production, thus the manufacturing details below are suitable for small scale fabrication. Note that the engine dimensions made for this mechanism are confidential and thus, are not included in the report.

Sensor mount

The first piece of the sensor mount, the sensor plate, was machined by hand on a milling machine out of 1/2 inch by 6 inch Aluminum 6061-T6511 stock using a 3/4" end mill. Following milling, the two holes were drilled and countersunk also using the mill.

The second piece of the sensor mount, the sensor mount bracket, was machined out of 1 inch by 6 inch Aluminum 6061-T6 stock by use of a CNC mill in the ERC with the help of Steve Erskine. The slots in this piece were then milled out with a 1/4" end mill in the student machine shop. Finally, the body holes on the back of the bracket into which the top two rollers are threaded were drilled and tapped with a 6-32 tap. However, for the bottom roller, a slot 10 mm long was milled to allow the position of the roller to be adjustable in order to "tighten" the rollers on the outside track. A countersunk slot was machined on each side in order to allow a pair of machine nuts to hold the roller tight to the sensor mount bracket. In addition, a 1/4" hole was drilled 3/8" deep into the backside of the sensor mount bracket for the shaft that will ultimately control the bracket's movement to be placed. Finally, a set screw was added through the bottom of the plate such that it could be tightened onto the shaft of the bottom roller, thus allowing the bottom roller to easily be tightened onto the external track.

Once both parts were made, the sensor was fastened to the sensor plate using two M4 fasteners, the sensor plate was fastened into the sensor bracket using four 1/4" -20 thumb fasteners (for easy adjustment), and the bearings were threaded into the sensor mount. Finally, once the arch plate had been made, the roller bearings on the sensor mount assembly were slid onto the external tracks and the shaft was fed through the slot in the plate into the hole in the back of the sensor mount. When it was determined that the shaft did not fit tight enough, the end of the shaft was drilled and threaded with a 4-40 tap and a screw was fed from the front side of the sensor mount bracket through a smaller hole in the bracket and into the shaft, which was then tightened.

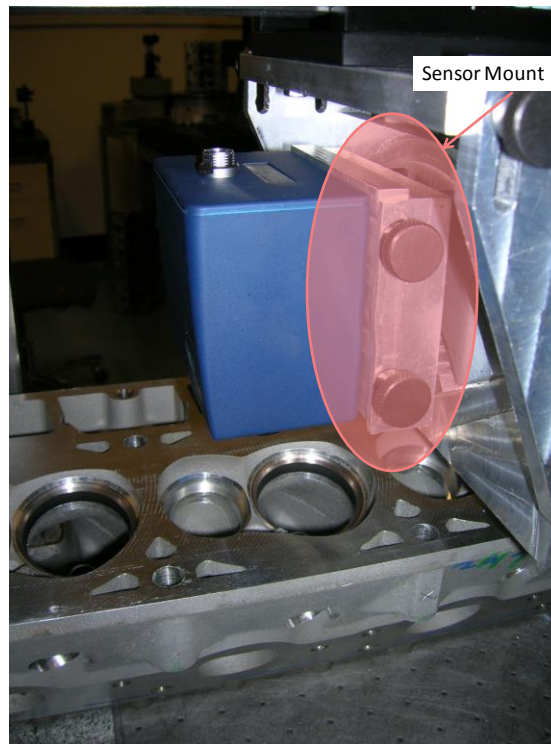


Figure 44: Prototype Sensor Mount

Arc plate and support assembly

The arc plate, made out of 1 inch thick Aluminum 6061-T6511 stock, was first squared into the dimensions of the plate shown in the engineering drawings using a mill. Then, four holes for the motor mount were drilled through the plate. Following this, a reference point (a small hole) was drilled into the point on the plate where the motor shaft is located. This point was used to center the plate on a rotary table around the pivot point (since the length from the pivot point to the reference point is 32.34 mm). Once the plate was secured on the table, the track was milled out using a 1/2" end mill. At this point, the ends of the arc were not cut off yet. Cutting the arc ends was left as the last step to since it left room at either end of the arc to make adjustments in machining the grooves. Then, a T-slot cutter was used to cut the grooves along which the track rollers would rest. The depth of the grooves was made slightly less than the depth of the rollers to allow for a tight fit between the top and bottom rollers. Finally, the arc ends were cut with 1/2" end mill by first zeroing the angle on the rotary table along the vertical midpoint axis of the plate. Then, after rotating the plate 25° and -25°, the end mill was used to cut off the arc ends.

Following the completion of the arc plate, the two triangular supports were milled out of 1/2 inch by 6 inch Aluminum 6061-T6511 stock. The slots were milled using a 1/4" end mill, and the two body holes used to fasten the supports to the arc plate were drilled. After drilling and tapping the corresponding holes in the arc plate with a 1/4-20 tap, the supports were then fastened to the arc plate.

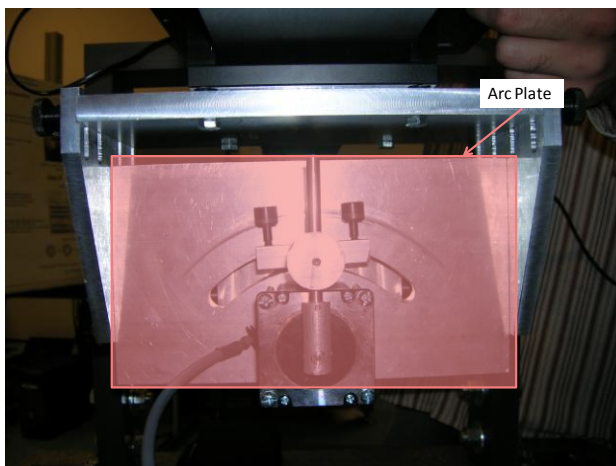


Figure 45: Prototype Arc Plate

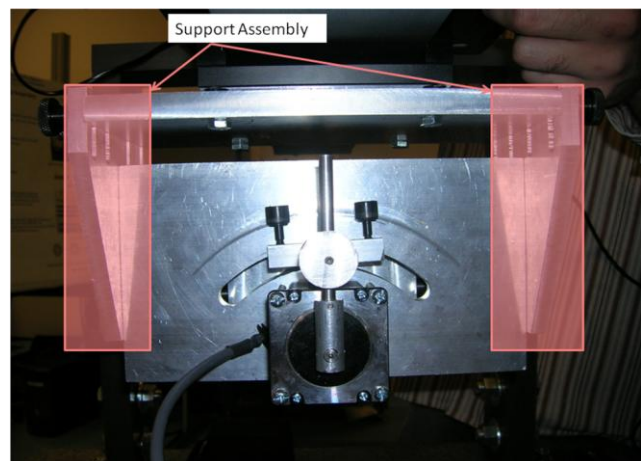


Figure 46: Prototype Support Assembly

Motion stage attachment

The motion stage attachment was milled out of 1/2 inch by 6 inch Aluminum 6061-T6511 stock; the four attachment holes for the motion stage and the 8 attachment holes for the arc plate supports were also drilled and tapped using the mill. Then, the arc plate support assembly was bolted to the motion stage attachment using 8 thumb fasteners and the attachment was bolted to the motion stage using 4 M6 bolts.

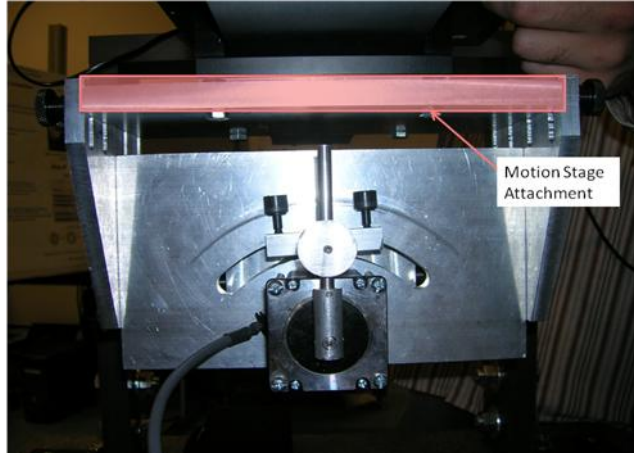


Figure 47: Prototype Motion Stage Attachment

Top support: The top supports were made out of 15” pieces of 1” by 3” steel stock by simply drilling the necessary attachment holes into it using a mill.

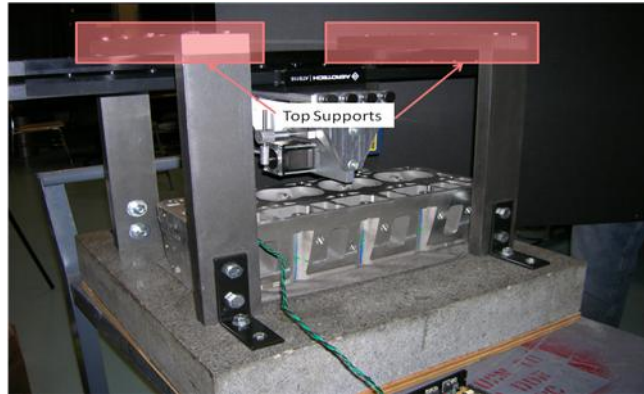


Figure 48: Prototype Top Supports

Vertical supports: The vertical supports were made out of 15” pieces of 1” by 3” steel by simply drilling, and if needed, tapping, the necessary attachment holes.

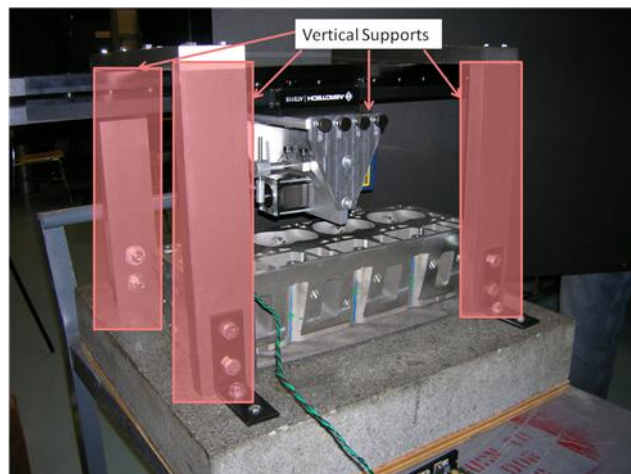


Figure 49: Prototype Vertical Supports

Structure Assembly: First, attachment holes were drilled into the granite block with a $\frac{1}{2}$ " masonry bit and $\frac{1}{2}$ " anchors were placed into the holes at a depth of 3". Then, the purchased L-brackets were fastened to the granite using the anchors and the four vertical supports were fastened to the four L-brackets using $\frac{1}{2}$ " bolts and machine nuts. Next, the top supports were fastened to the vertical supports by use for two $\frac{1}{4}$ " bolts for each vertical support. Finally, the motion stage, with everything attached to it, was bolted to the top supports by use of 4 $\frac{1}{4}$ " bolts for each top support for a total of 8 $\frac{1}{4}$ " bolts supporting the motion stage.

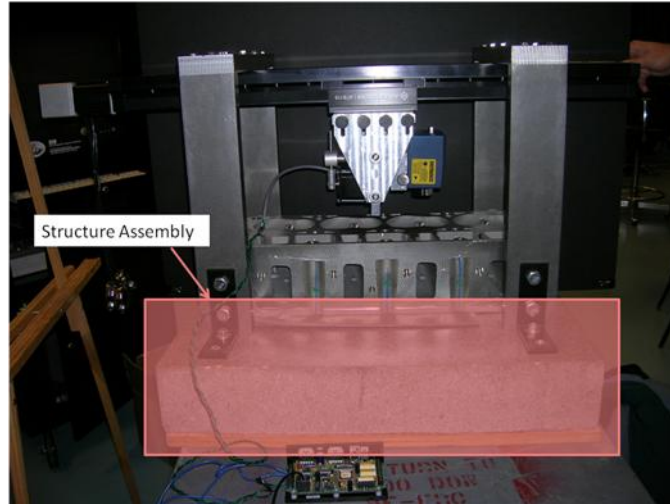


Figure 50: Prototype Structure Assembly

Mechanism transmission: In order to fasten a shaft perpendicular to the motor shaft, a small adaptor was made out of $\frac{3}{8}$ " round aluminum stock. First, a $\frac{1}{4}$ " hole was reamed into the cylinder both into one end and through a side perpendicular to it. The motor shaft was then inserted into the side hole, and a piece of $\frac{1}{4}$ " steel stock, sanded down, was inserted into the end hole to compose the shaft. This piece was then tightened down to both the motor shaft using three 6-32 set screws and the steel shaft using one 6-32 set screw.

Next, a small piece containing both the linear bearing through which the first shaft is fed through and a sleeve bearing in which the second shaft (attached to the sensor bracket) rotates was made out of $\frac{3}{4}$ " round aluminum stock. To start, a $\frac{1}{2}$ " hole was drilled through the side of the stock and the linear bearing was forced into this hole and tightened down with a set screw. A $\frac{3}{8}$ " hole was reamed into the end of the stock and a $\frac{1}{4}$ " sleeve bearing was placed into it and tightened down with four set screws. Finally, material was removed from the piece with a lathe in the area around the sleeve so that this part would not hit the motor body during motion.

Once this part had been made, the shaft coming from the sensor mount was slid into the sleeve bearing in this piece, and the shaft coming from the motor was fed through the linear bearing, thus completing the mechanism.

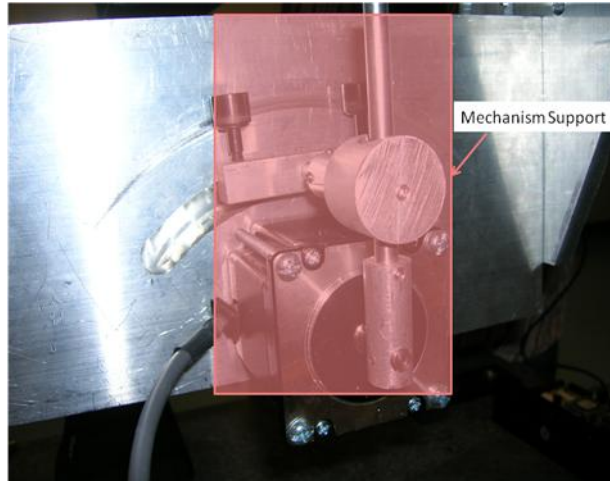


Figure 51: Prototype Mechanism Support

Electronics assembly: Following the completion of the mechanism, the stepper motor from the rotational mechanism was connected to an external driver from Applied Motion Products using 24 gauge copper wires (Appendix N). The external driver connected to the PC via an adapter cable and was programmed for standalone operation via Si Programmer control software. Commands used to drive the motor on the prototype are included in Appendix M. The selected motor from Sure Steps runs on 32 VDC, 4A maximum. However, for the prototype rotational mechanism, a 110V input (19V, 1A output) portable power supply was bought and powered the stepper motor through the external driver. This portable power supply was sufficient for demonstration purposes. The linear stage was bought with custom wiring and was connected to an Aerotech, Ensemble CP10 controller. The stage and controller were conveniently powered by a conventional 110 VAC wall socket, and the controller was connected to the PC via a USB cord. The Ensemble runs with proprietary Ensemble IDE software and drives the linear stage to move at speeds up to 250 mm/s and through a variety of movement patterns such as ramps in velocity, steps, and others. Commands used to drive the stage on the prototype are included in the Appendix L.

Testing Plan

The fabricated prototype will be tested to confirm that it meets all engineering specifications set forth earlier in this report. These engineering specifications are listed below by rank.

Table 6: Importance Ranking of Engineering Targets

Rank (1 = most important)	Engineering Specification	Engineering Target
1	Error for translational position (x)	<1 μm
2	Error for rotational position (θ)	<1 degree
3	Reference displacement error	<1 μm
4	Cycle Time	<30 sec
5	Control of translational speed	1E-6,000 mm/min
6	Damping coefficient of fixture material	> 1
7	Number of passes sensor capable of making	1-16
8	Movement of engine head in x, y, and z directions once "fixed"	<1 μm
9	Error for translational velocity (dx/dt)	<1 mm/min
10	Sensor distance from engine head	51.5-68.5 mm
11	Step size of sensor sampling rate	1 Hz
12	Operational Temperature	18~35 $^{\circ}\text{C}$
13	Input Voltage	110 Volts

The team's prototype fabrication included the manufacturing of the support structure, motion stage mounts, and rotational motion mounts. The software to calibrate sensor measurements will be completed at a later phase of the project. Thus, the system can be calibrated to meet certain engineering specifications but we will not be performing these calibrations. The engineering specifications that will be met at a later date (and are outside the scope of our project tasks) are (1) error for translational position, (2) error for rotational position, (3) reference displacement error, (4) cycle time, or (11) step size of sensor sampling rate. The fundamental metric for the success of our prototype will be its ability to make two passes along the length of the engine head, scanning all 16 valve seats. A visual inspection of the sensor's motion range while running will be sufficient to determine whether or not our prototype meets this metric. A similar test will be used to determine the number of passes the sensor is capable of making (7). Also important is the rotational mechanism's ability to achieve the desired rotation positions for the specific engine head, to locate the sensor between 51.5 and 68.5 mm away from the engine head surface, and to maintain a reasonable clearance between the mechanism's plate bottom and the engine head top surface. These determine whether the sensor will be perpendicular to the valve seats at their midpoints, whether it will be able to take accurate measurements, and gives an idea of the types of obstructions that the mechanism will be able to clear.

The control of translational speed to travel (5) will be conducted through our controller and will allow for adjustment of a step size of 1 mm/s from 0 mm/s to 250 mm/s. This specification will be tested by setting the speed of the linear motion stage with our controller and measuring travel distance per unit time.

The movement of the engine head in the x, y, and z directions once "fixed" (8) will be tested by marking the original position of the engine head, running the sensor mechanism, and measuring the movement) of the engine head.

The sensor distance range from the engine head (10) will be measured by adjusting the sensor to its maximum and minimum focal length positions. These positions are determined by the location of the sensor on the arc plate, and the position of the arc plate in its holster. Manual measurements with calipers are sufficient to give approximate dimensions of sensor distance range, clearance, and rotation, though in the future, more exact techniques need to be employed.

We will not test the operational temperature of the mechanism, given that resources are not available to test the sensor in a climate-controlled environment. However, given the thermal expansion coefficients of our material choices (primarily aluminum and steel) and the operating range of the sensor (18-35° C) we expect the device to be operable in the desired range of 18-35° C.

Finally, we designed electrical components of mechanism to operate off of two conventional, 110V inputs (13). This can be observed by confirming proper operation with 110V inputs.

Testing

Testing was conducted after fabrication and allowed for engineering specifications to be evaluated. Although the only way to truly test the performance of our system would be to use it to make actual measurements with the sensor and compare them to previous measurements, this was not possible for two reasons. First, the motion stage must be calibrated before it can be used to make measurements; because calibration is a multi-week process for which the stage must be sent away, we finished our prototype prior to motion stage calibration in order to have a prototype for the design expo, and thus it has not been calibrated yet. Secondly, there was insufficient time to learn how to operate the sensor and use it due to the late arrival of the motion stage and thus the late date of final assembly of our prototype.

Once the stage is calibrated in the future, testing can be conducted to determine the position and velocity errors for translational and rotational motion as well as the proper cycle time for the measurement process (as the motion can be programmed to almost any speed and thus knowledge of the fastest speeds that still provide accurate measurements are needed). Without this possibility however, we have conducted some simple testing to at least ensure our prototype can provide the motion needed for these measurements to take place.

Repeated translational motion

We found the prototype capable of making multiple passes along the entire length of the engine head and capable of operating at the desired translation speed of 100 mm/s (this “desired” number requires actual measurements for refinement). We also noted the sensor distance can be properly adjusted to meet the appropriate measurement range. The engine head does not move on the granite block during operation. Also the entire operation is powered conveniently by an 110V power source.

Linear motion control

As mentioned in the testing plan, the fundamental metric of success for our prototype is its ability to pass along the entire length of the engine head. The linear motion stage has a 600 mm travel capable of carrying the inspection sensor well past all engine heads tested. The longest tested engine head has a length of 500 mm, with which we conducted a visual inspection to confirm that with the engine head placed on the granite block our prototype has the capability of scanning the entire length of the engine head. We also noted that the prototype can make these passes in any quantity; making multiple passes is easily programmed into the controller. Each pass can be coded by the Ensemble IDE software included in the controller package from Aerotech, Inc. This software also lets us control the translational speed metric, whereas we desire a translational speed of 100 mm/s. The controller allows 1 mm/s steps with speeds between 0 and 250 mm/s.

Mechanism metrics

To ensure the sensor hits our desired positions and to gauge how well the mechanism clears the engine head, manual measurements were taken using calipers. The sensor was found to be able to move along the track to our desired ± 26 deg smoothly and thus, meet our rotation requirements. Also, at the maximum rotation position, the sensor distance from a variety of engine head valve seat surfaces were tested to be between 55 to 75 mm, both of which have 20 mm adjustability. Thus, with the given adjustments for our system we can reach the desired measurement range of 51.5 to 68.5 mm. Finally, the clearance between the mechanism plate's bottom surface and the flat surface of the engine head was found to be approximately 33 mm when the course adjustment was positioned at the bottom of its vertical range and when the fine adjustment was positioned in the middle of the vertical slot (see Fig. 52 and 53). Compared to the designed clearance of 34 mm at this same position, our design is pretty spot on – the one mm discrepancy can be attributed to our machining errors in the arch track, sensor mount, and motion stage attachment. The maximum clearance we can obtain is actually roughly 43 mm, when the fine adjustment is shifted downwards to its limit of 10 mm along the slot (see Fig. 52). The 43 mm clearance provides more than ample room to clear engine head obstructions, and was verified through manual measurements using calipers. We note that because our measurements were rough measurements, more precise measurements should be obtained in the future.

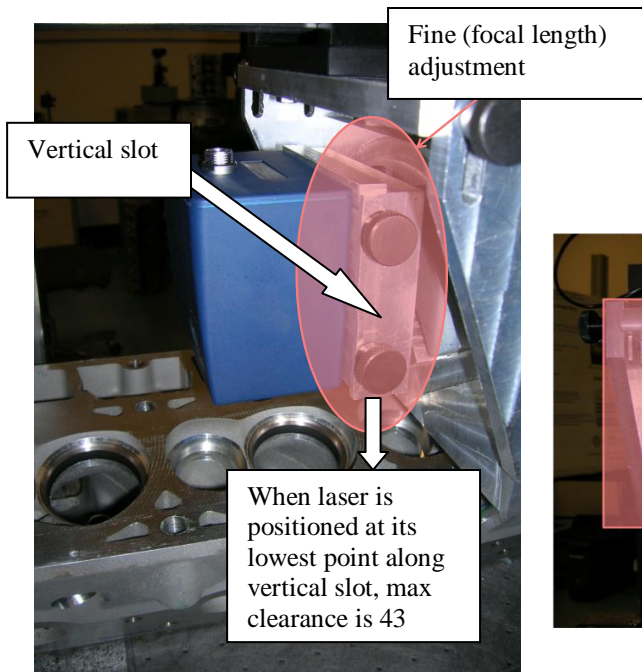


Figure 52: Prototype Support Assembly

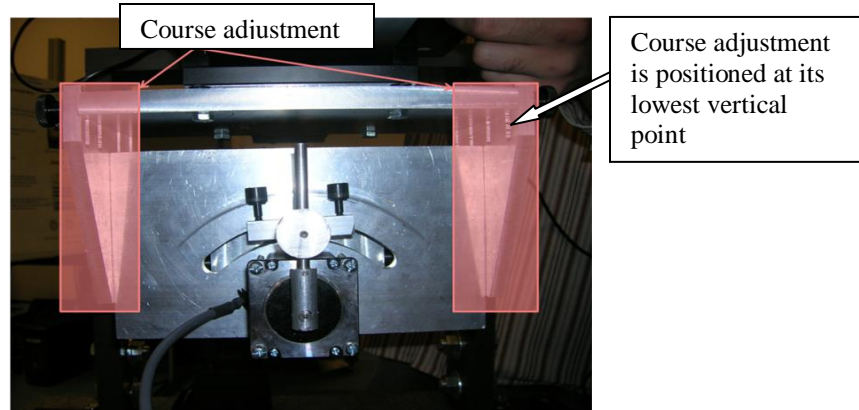


Figure 53: Prototype Sensor Mount

Engine head stability

Another visual inspection was conducted to view the engine head movement during prototype operation. The engine head was stable throughout operation and there was no noticeable play. However, we would like to have a better mechanism to place the engine head precisely on the granite block. This can be done in the future, once a specific demonstrator engine head is decided upon and further validation can be conducted to ensure no motion of the engine head.

Power supply

The entire prototype operation is fully functional with two conventional power inputs of 110V. The linear stage and controller had a custom 110 V plug, while the motor and driver were assembled with an AC adapter of 15 VDC, 1 A. However, the motor controller actually requires a 32 VDC source to provide the motor with all of the power required to achieve its maximum torque. Although the 15VDC source was able to supply enough power to the motor to provide rotational motion over very small angles, the full 32VDC source was required to provide the full motion.

Motor life

One aspect of the prototype that failed testing however was the lifetime testing of the motor. Although the motor ran continuously the entire time at the expo without problems, and the motor was able to provide the necessary torque to move the sensor to both extreme positions numerous times, the motor failed during additional testing after the design expo. Although the reason for failure is not immediately known, it is known that the motor was very inexpensive and possibly of low quality. This issue is addressed further in future improvements.

Manufacturing Changes

We made several changes during the manufacturing process to refine our design and manufacture a fully operational prototype. These engineering change notices (ECN) were carried out efficiently. The changes include design changes in the granite, structure, bolt interfaces, triangular supports, and rotational arc motion device.

Stud anchors are used to attach the angle (L) brackets to the granite. These were originally ½” bolts, however after finding that the 3” depth of only four bolts were sufficient for carrying the load of the structure, we used 3/8” diameter for the remaining four bolts. This allowed for faster manufacturing time while not sacrificing the rigidity needed for the structure to granite interface.

The structure was originally planned to be made with 6061 aluminum, however, evaluating the raw material needed for the structure we found that 1018 mild steel was only 3 cents more expensive per pound. We decided to create the structure out of the mild steel because we were able to order our parts direct from a material supplier. This prevented additional manufacturing time for the mild steel while at the same time allowing us to create a more rigid structure with a small investment.

We also wanted to preserve the finish and operation of the ATS 115 motion stage. To do this we included rubber washers at the mounting points for the linear stage to the aluminum and mild steel. This will minimize vibrations while protecting the finish on the linear motion stage.

The structure that hangs from the motion stage slider was originally going to be supported by two triangular attachments that were to be welded to the arc track. However, after some load analysis we found it sufficient to place two bolts per triangular attachment to the arc track. These bolts maintained our operation goals for the prototype while allowing for a simpler manufacturing process.

Future Improvements

Due to the tight time schedule, the availability of machine shop time and lab time, and the limited resources associated with the project, improvements to our prototype in the form of additions and redesigns that would be beneficial, but were unable to be completed, are discussed here.

One necessary addition to the prototype is the integration of a 32 V power supply to power the stepper motor. Because we were originally under the impression that the controller supplied by Aerotech, Inc. could drive the stepper motor we had chosen, we had to quickly find a different power supply for the motor. The current prototype power supply for the stepper motor is a 15V power supply from Radio Shack, which has been modified so that it can be wired to the stepper motor controller. Although this power supply can provide enough input power for the stepper motor to control the motion of the sensor mount and sensor over small angles, the 32 V source for which the stepper motor is designed for will provide the torque for which we designed the system and allow the

full motion required. A 30 VDC source has been used to verify that the mechanism will work with this power; however, it is a lab source and is not practical for system integration.

A second improvement is the addition of an adjustable mechanism capable of locking down different engine heads to the granite base. This will ensure no movement of the engine head during measurements and allow for correct positioning for the engine head. In order to position the engine head, pins could be mounted in the base that could align with existing holes in the engine head. Clamps, similar to ones used by many other machines in the ERC lab, could then be used to clamp down the head, although clamps may be unnecessary if it is found that the engine head does not move when placed on the granite base.

A third improvement to our design would be the addition of a clamping mechanism to ensure no relative movement between the sensor mount and the arch plate during linear motion when micro-precision is necessary for measurements. Currently, if the rollers on the backside of the plate are tightened against the plate, the sensor will be held with no play; however, this requires that the beam supporting these rollers be moved so that the rollers are over tightened against the back of the plate and then loosened slightly whenever rotational motion is desired, where as a clamp would prevent this constant adjustment.

A fourth improvement that could be made to the system would be a redesign of the roller installation on the sensor mount. Currently, a pair of rollers on the back of the arch plate hold the rollers attached to the sensor mount tight to the plate, allowing smoother motion and less play, but on the front side of the plate, it is the ends of the rollers, which do not roll, that are held tight to the plate. This could be improved by the addition of rollers on the front side of the arch plate, similar to the ones that currently exist on the backside, that could “sandwich” the plate and allow even smoother motion of the mechanism. If done correctly, this could also effectively eliminate the play between the plate and the sensor mount, which would eliminate the need for the clamp described above and allow for micro precision of the linear sensor movement as well as the ability to simultaneously rotate the sensor.

A fifth improvement to the system would be replacement of the stepper motor. As previously mentioned, the motor, despite its ability to provide the necessary torque, failed after extensive use. This problem may be fixed by replacing the motor with one of a higher quality. Because the motor used was a standard size (NEMA 23) with standard mounting provisions, any motor of this size may be used as a replacement, allowing for an upgrade during replacement.

Finally, in order to improve the aesthetics of the prototype the steel structure can be painted and all of the aluminum parts can be sanded (if necessary) and anodized.

Conclusion

After determining the customer requirements and engineering specifications for our design, we listed and organized these functions in a FAST diagram and then generated function-level concepts to complete these functions in a Morphological chart. These function-level concepts were then combined to create five system-level concepts to complete the overall function of our system: precise motion control of the ConoProbe sensor in order to allow precise measurement of engine valve seats. These system-level concepts were then compared with a Pugh chart, and one concept was chosen for our design due to its unmatched ability to control the rotational motion of the sensor accurately, to eliminate any interference with the engine head, and to enable the valve seat inspection technique to be completely automated.

We then defined this concept in more detail by performing a number of engineering analyses, including position analysis, motor torque analysis, vibration analysis, and structural analysis, in order to develop detailed design parameters. The results of these analyses were translated into detailed CAD models, a bill of materials, and a manufacturing plan. With the detailed design of our final concept, we built and tested the system in order to deliver a complete prototype by the design expo on December 4th. The prototype can now be found in the Metrology Lab of the ERC (1100 Dow).

In summary, our final design allows a user to scan all 16 valve seats by controlling the motion of the sensor both along the engine head length and width. The device can accommodate a variety of engine head sizes, given its open geometry and the ability to adjust both the focal point and fine-tune focus of the sensor. In addition, it maintains a clearance between the sensor and the engine head that allows for non-contact measurements to be taken. All of the sensor's motion is controllable due to the use of a motor and linear stage, allowing for adjustability of speeds and positions. Finally, our design is justified using sound engineering analysis and reasoning, ensuring a high level of reliability. Our design's combination of adjustability to accommodate different engine heads, controllability of sensor motion, high reliability, and micro-precision and accuracy, and most importantly, its ability to be automated and quick at measuring valve seat geometry, makes it a viable and desirable concept for our potential customers, the auto manufacturers.

References

1. "Putting Air Gages to Work ." Edmunds Gages. 26 Sept. 2007
<<http://www.edmundsgages.com/metworldart04.htm>>
2. "Apparatus for inspecting an engine valve seat." Patent Storm. 26 Sept. 2007
<www.patentstorm.us/patents/5533384-claims.html>
3. "Accutire ABS Coated Air Gauge." MSN Shopping. 26 Sept. 2007
<<http://shopping.msn.com/prices/shp/?itemId=845526187>>
4. "Probe Indicator." Wikipedia. 26 Sept. 2007
<http://en.wikipedia.org/wiki/Dial_gauge#Probe_indicator>
5. "Valve seat runout gage." Free Patents Online. 26 Sept. 2007
<<http://www.freepatentsonline.com/4630377.html>>
6. Quoting Dr. Vijay Srivatsan from ERC-RMS.
7. "ABSOLUTE Digimatic Indicator ID-C Series 543-Standard Type." Mitutoyo U.S.A. 26 Sept. 2007
<<http://www.mitutoyo.com/TerminalMerchandisingGroup.aspx?group=1198>>
8. "Crysta-Apex C Series 191-Standard CNC CMM." Mitutoyo U.S.A. 26 Sept. 2007
<<http://www.mitutoyo.com/TerminalMerchandisingGroup.aspx?group=1013>>
9. "Digital holography." Wikipedia. 26 Sept. 2007
<http://en.wikipedia.org/wiki/Digital_holography>
10. "Linear actuator, integrated position control." Danaher Motion. 11 Oct. 2007.
http://www.danahermotion.com/documents/index.php?product_cat_id=464
11. *Engineering Vibration, 2nd ed.*, Daniel J. Inman.
12. *Formulas for Natural Frequency and Mode Shapes*, Robert D. Blevins.
13. *Mechanical Behavior of Materials*, Norman Dowling

Bios



Ryan Doss

Ryan was raised in west Michigan until graduation from Grandville High School in 2004, after which he headed for Ann Arbor. For the past two summers, Ryan has worked for The Boeing Company where he worked in 777 payloads and structures engineering and 787 & 747-8 dynamic loads analysis in 2006 and 2007, respectively. Ryan is currently conducting research in the area of dynamics with application to biomechanics to measure knee kinematics with inertial sensors for the study of non-contact ACL failure mechanisms. Following graduation, Ryan will likely head to graduate school, after which he will either continue his career in the aerospace industry in the fields of dynamics or stability and control or continue to conduct research in academia. Outside of academics, Ryan serves in the Campus Crusade for Christ ministry at U of M as a community group leader and co-leader of the praise band and runs marathons and other races of unreasonable distance.



Fletcher McCombie

Fletcher was born on the northwest side of Chicago in the suburb of Barrington. He grew up in the same area, moving from to Hoffman Estates and eventually to South Barrington. Throughout secondary education he had deep interest in math and science through calculus and physics. The University of Michigan was an easy choice for higher education, as it offers the best engineering program in the Midwest. Academic studies at Michigan have led to pursuits in dynamics and controls. After graduation Fletcher hopes to be active in and out of work, pursuing industry achievements, community involvement, and a continual pursuit of better health for himself and his fellow citizens. Fletcher's extracurriculars include music, film, website development, land reclamation, health activism, and of course his continual pursuit of knowledge.



Helen Sun

Helen is from Charlottesville, VA where she graduated from Albemarle High School. She decided to go to the University of Michigan – Ann Arbor because of her interest in automotive systems. She declared her major in Mechanical Engineering during her third semester in college and has really been motivated to pursue continued education in Controls Systems Design and Design Methodology based on her classes, teachers, and industry experiences. Her industry experiences include a Toyota Engineering Design Co-op and a General Motors Drive Quality internship. Her research experiences include the bowel actuator packaging project and a shape memory alloy creep stabilization project which led to a conference paper at SPIE. Her research was conducted at the Smart Materials and Structures Design Lab at the University of Michigan. She plans on getting a PhD and either doing research or teaching in the future.

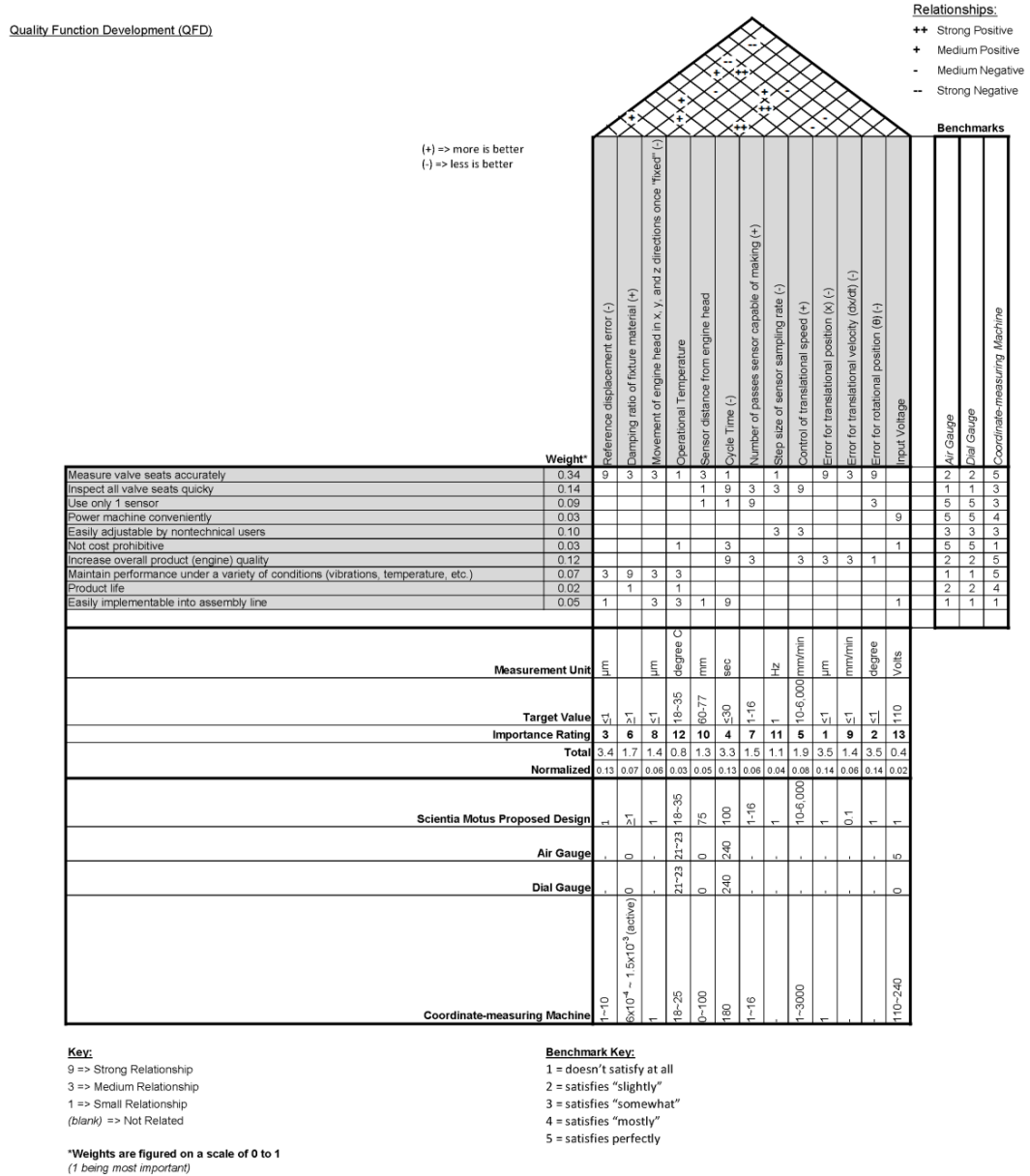


Liz Coon

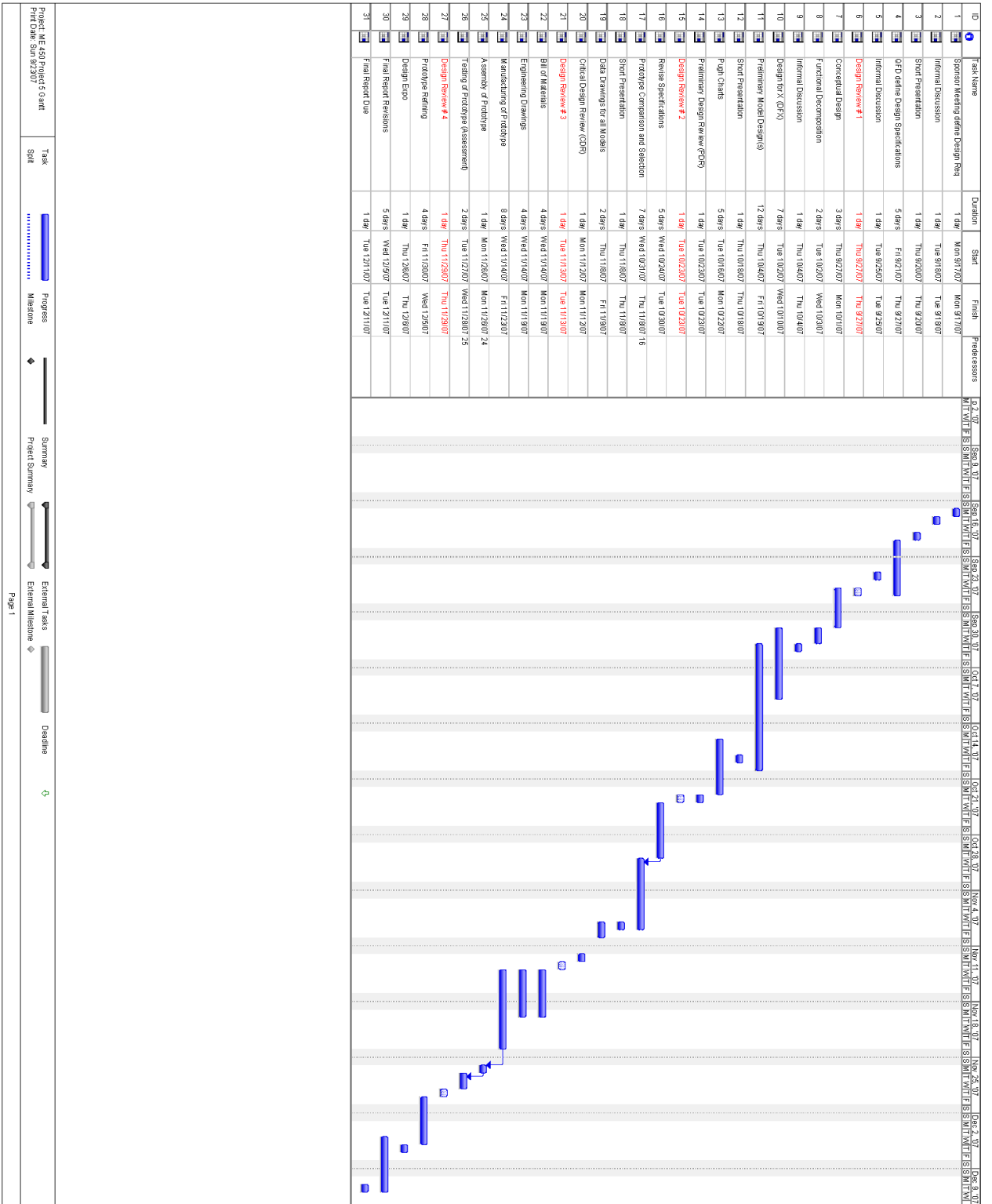
Liz is from East Lansing, MI, and graduated from East Lansing High School in 2004. She decided to pursue a bachelor's degree in mechanical engineering because of her interest in physics, mathematics, and the workings of mechanical systems. During her college career she has worked in a number of labs, which has included research on electroplating nickel-titanium shape memory thin films in the Materials Science Department at Michigan State University; jurkat cancer cell electrical properties research at a Nuclear Engineering lab at the University of Michigan; and nuclear reactor operation and experimentation experience at the Universidad Nacional de Córdoba in Argentina. Liz also has an interest in supply chain and operations, and did an internship investigating make-to-order cardiovascular products this summer at Cordis, a Johnson & Johnson company, in Miami Lakes, Florida. After she graduates with her bachelor's degree in May 2008, she plans on pursuing an industrial and operations engineering master's degree at the University of Michigan.

Appendix A: Quality Function Deployment (QFD) Diagram

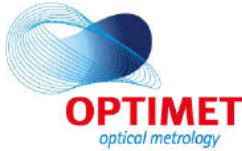
The following diagram depicts our customer requirements, engineering specifications, and the relationships between the two that have contributed to the importance of each specification.



Appendix B: Gantt Chart



Appendix C: Smart ConoProbe Laser Sensor Technical Specifications



Smart ConoProbe

Description

The Smart ConoProbe (**Smart**) is a non-contact optical sensor for distance and 3-D measurements based on the unique conoscopic holography technology. The Smart ConoProbe measures the distance to a single point at a rate of up to 3,000 Hz with up to sub-micron precision.

Features

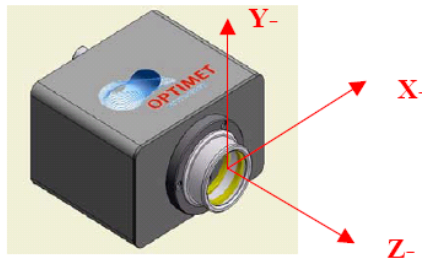
The Smart offers a variety of objective lenses allowing various standoffs and working ranges in the same sensor. The Smart is a "system on chip" platform and all data processing, including pre-programmed functions are in the sensor head. Operation modes are either external or internal trigger. Software integration is possible by using ActiveX interface (in GUI or GUI-less mode) or by using DLL files. Multiple sensors operation in parallel is possible using standard Ethernet LAN communication.

Technical Specifications

Configuration	Standard					High Definition	
	25	50	75	100	200	25	50
Objective Focal Length (mm) (*)							
Precision ⁽¹⁾ (μm)	<1	<3	<6	<12	<60	<1	<2
Reproducibility 2σ ⁽²⁾ (μm)	<0.3	<0.8	<1.5	<3.0	<15	<0.3	<0.5
Standard deviation ⁽³⁾ (μm)	<0.6	<1.5	<3.5	<6	<30		
Measurements Range (mm)	1.8	7.5	17	34	120	0.6	1.8
Standoff ⁽⁴⁾ (mm)	18.5	40	60	90	175	15	45
Laser Spot Size ⁽⁵⁾ (μm)	20	40	65	100	200	8	20
Angle coverage ⁽⁶⁾	170°						
Data Handling							
Maximum Measurement Rate (Hz)	3000						
Interface							
Communication	Ethernet 10/100 UDP						
Control Discrete Signals	ROG – output External Trigger – input Analog Signal - Ranging +/- 5Vdc						
General							
Weight (g)	380						
Dimensions (mm)	62X85X94						
Operating temperature ⁽⁸⁾	18 to 35°C						
Supply Voltage	12V- 0.5 Amp DC						
Light source	Visible red laser Diode – Wavelength 655 nm						
Laser class	FDA Class II - IEC class 2						

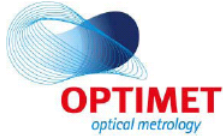
NOTES:

- Extended lenses for focal lengths from 50 to 200 and other objectives for different focal lengths are available upon request.
- **Glossary**
 - a) **Measurements Range** - Range over which distance measurements meets measurements specifications.
 - b) **Relative Distance Measurement** - Distance measurement between two points in the Measurement Range (in contrast to Absolute Distance Measurement).
 - c) **ROG** - Read Out Gate – Internal measurements synchronization pulse, used when Smart is the master.
 - d) **External Trigger** - External start of measurements, used when Smart is the slave.
 - e) **Analog Signal** – Conversion of Z measurement to an analog representation (Optional)
 - f) **Smart ConoProbe** - Axis definitions:

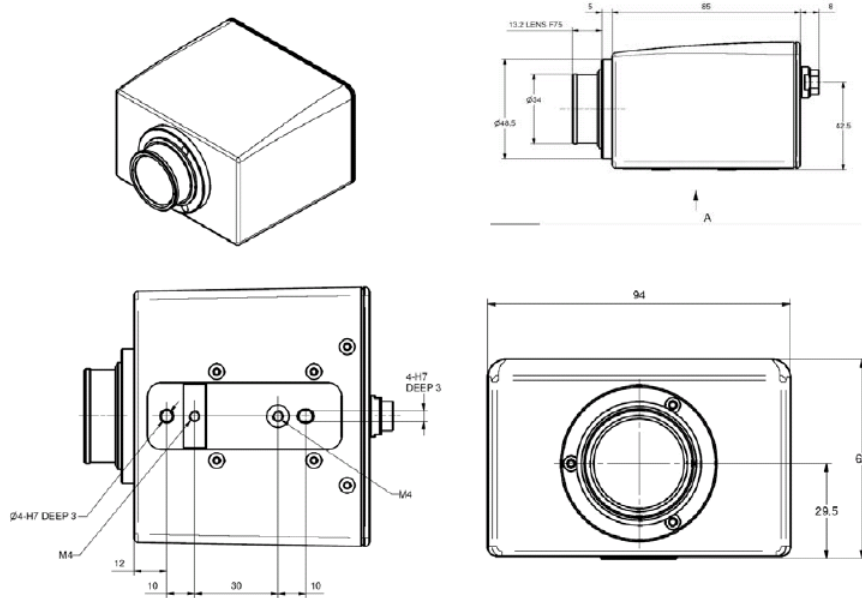


- (1) Specifications are defined under the following parameters and conditions:
 1. Measured object - Diffusive surface of certified Johansson blocks.
 2. Relative distance measurements covering 50% of the measurement range.
 3. Averaging over 200 measured points.
 4. Sampling step of $\frac{1}{2}$ of the spot size.
 5. Measurements done along Y axis.
 6. Environmental temperature and Laser Power same as in the calibration.

Different measurement parameters such as reflective surface (fine-machined-N6 surfaces) or smaller sampling steps may affect precision.
- (2) **Reproducibility**: The Standard Deviation of 5 relative measurements of parallel profiles scans with offset -normal to scan direction (parallel to X axis) Measurement parameters same as (1).
- (3) **Standard deviation** - Standard deviation of the random error (Measurement Uncertainty) of absolute distance measurements at the middle of the measurement range. Measurement parameters same as (1).
- (4) **Standoff** - The distance from the tip of the objective lens housing to the center of the measurement range. The tolerance of the standoff distance may deviate up to 10% of the stated value.
- (5) **Laser beam spot size** - the effective spot width in the Y-Axis measured at the center of the measurement range at FWHM points. The Lateral resolution can be estimated as half of the spot size.
- (6) **Angle coverage** - Measurable points up to $\pm 85^\circ$ from normal incidence angle. For angles up to 60° , the angle estimation (by indirect measurement) is within a tolerance of 0.05° . For angles exceeding 60° the angle estimation (by indirect measurement) is within a tolerance of 0.25° (assuming minimum of 50 measurable points). Measured in Y direction.
- (7) Calibration is done at 22-24°C. Temperature dependence of relative distance measurement is less than $0.025\%/^\circ\text{C}$.

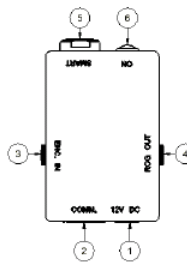


(8) Dimensions:



(9) Communication Box:

- 1). POWER INLET-12V
- 2). COMMUNICATION ETHERNET
- 3). ENCODER INPUT
- 4). ROG OUTPUT
- 5). ODU CONNECTION
- 6). POWER INDICATOR

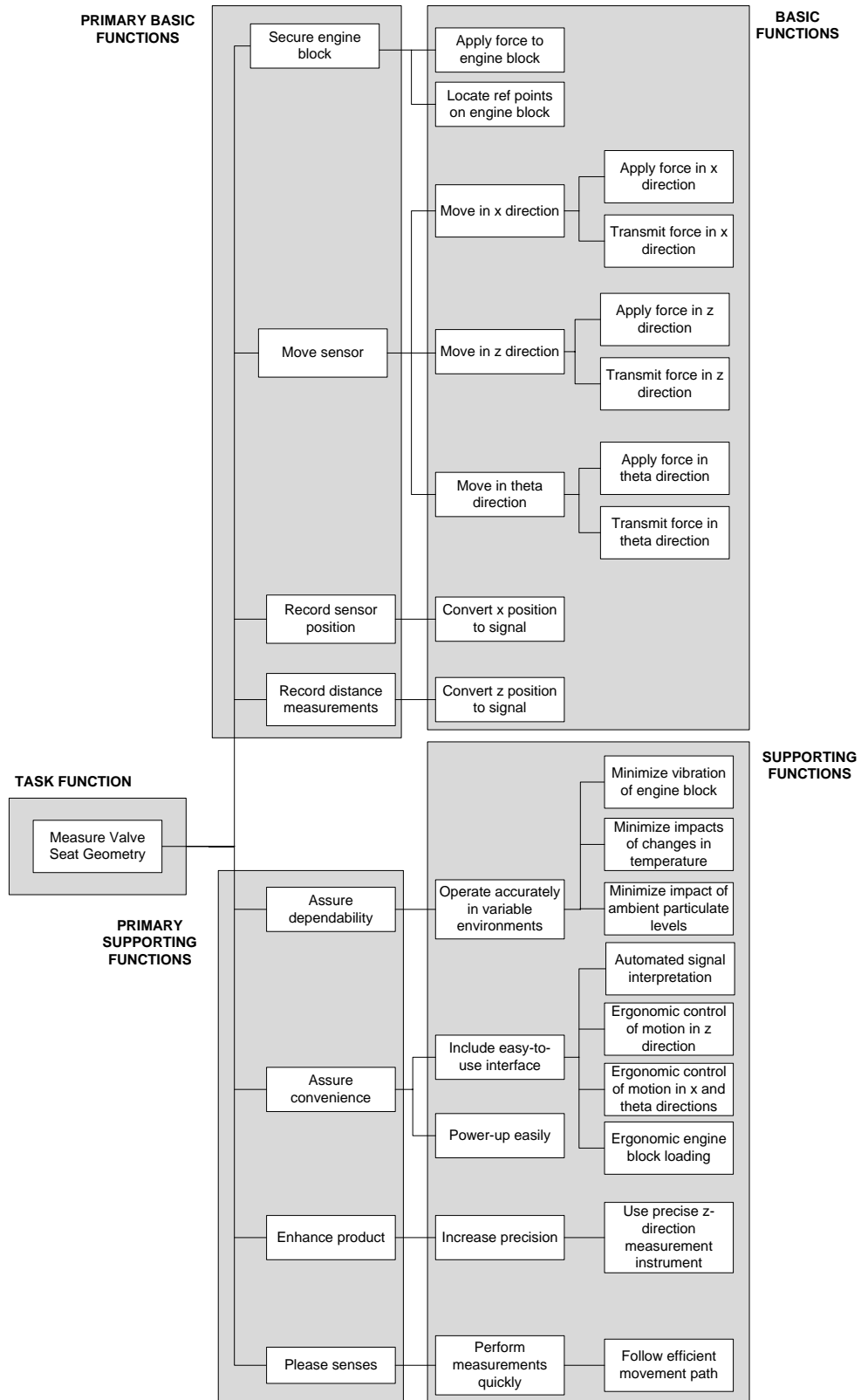


Home Office:
 Optimet, Optical Metrology Ltd.
 6 Hartom St, P.O.B 45021,
 Jerusalem 91450, Israel
 Tel: +972-2-5484444
 Fax: +972-2-5865387
 Email: mktg@optimet.com
 http://www.optimet.com

USA Office:
 Optimet, Optical Metrology Inc.
 260A Fordham Rd.,
 Wilmington, MA 01887, USA
 Tel: +(978) 657-6303
 Fax: +(978) 657-6054
 Email: sales@optimet.com
 http://www.optimet.com

Japan Office:
 Ophir Japan Ltd.
 3-43 Kishiki-cho, Omiya Ku,
 Saitama-shi,
 Saitama 330-0843, Japan
 Tel: +81-48-646-4150
 Fax: +81-48-646-4155
 Email: info@ophirjapan.co.jp
 http://www.ophirjapan.co.jp

Appendix D: Fast Diagram



Appendix E: Morphological Chart

Text format

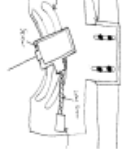
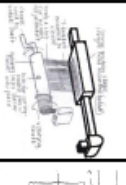
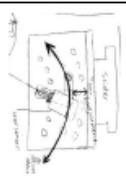
Function	Concept Type											
	Electrical Concepts			Mechanical Concepts					Other Concepts			
Secure engine block	Apply force to engine block				Clamp	Magnets	Security bar					
	Locate reference points on engine block									Pins		
Move sensor	Apply force in x direction	AC motor	Stepper motor	Servo motor	Linear motion control stage							
	Transmit force in x direction				Power screw	Linear motion stage, magnetic guide rails	Linear motion stage, air guide rails	Rotating belt	Rack & pinion	Pneumatic system	Hydraulic system	
	Apply force in z direction				Hand pump	Hand lift	Crank handle	Foot pump		Hydraulic system		
	Transmit force in z direction				Power screw	Solid bar and lock screw	Punched bar and lock screw					
Record sensor position	Apply & transmit torque	Torque motor	Stepper motor	Servo motor	Rotary motion control stage							
	Convert x position to signal				Hall effect sensor	Linear encoder	Linear variable differential transformer	Linear spring & force transducer		Ultrasound	Infrared sensor	GPS
Record distance measurements	Convert z position to signal									Smart ConoProbe		
	Minimize vibration of engine block				Fluid cushion					Granite base	Cast iron base	
Operate accurately in variable environment	Minimize impact of change in temperature				Cooling/heating module					Insulate parts		
	Minimize impact of change in ambient particulate levels				Air purification system	Isolating walls around module						
	Automated signal interpretation	LabView	C++									
Easy-to-operate user interface	Ergonomic motion control in x and y directions			Touchscreen	Joystick	Knobs	Wii-type controller	Keyboard		Speech recognition		
	Ergonomic motion control in z direction				Hand pump	Hand lift	Crank handle	Foot pump		Hydraulic system		
	Ergonomic engine block loading				Horizontal conveyor belt loading	Vertically loading robotic arm	Manual horizontal loading	Manual vertical loading				
Convenient to power	Use conventional power	110 V compatible, 3-prong system										
Increase Precision	Use precise z-direction measurement instrument									Smart ConoProbe		
Decrease measurement cycle time	Follow efficient movement path				Long pass-small tilt system	Short pass-long tilt system	Pass-tilt-lift system					

Picture format

Concept Type	Electrical Concepts	Mechanical Concepts	Other Concepts
Function			
Secure engine block		clomp magnet SSR PTNS	Suction
Move sensor	AC motor Stepper motor	Linear motion stage	
Record and control sensor position	controller Labview or C++	linear encoder spring load cell	inductive transducer potentiometer
Record distance measurements	Hall effect sensor	linear variable differential transformer	laser sensor
Operate accurately in variable environment		granite or cast iron engine head mounting block	heating/cooling system insulation
Easy to operate user interface	input output easy to read, understand computer interface	hand crank knobs joystick	assembly manual speech recognition
Use conventional power	3 prong, 110V plug in	single package for many wires	
Support/integrate assembly	pin joint sensor motor	linear motion rotation actuator (motor) linear motion rotation actuator	
Decrease measurement cycle time	easy to reach motion system user path	rotation actuator mounted on linear actuator laser path value axis	linear actuator mounted on rotation actuator

Appendix F: Pugh Chart

As stated in our morphological chart	Function	Weight	Concept 1	Concept 2	Concept 3	Concept 4	Concept 5	
Move sensor	Rotate sensor Nonphysical pivot point	0.09 0.18	5 5	5 5	5 5	5 5	5 5	
Easy to operate user interface	Easy to adjust	0.09	5	5	5	5	5	
	Easy to make	0.05	5	5	5	5	5	
	Easy to assemble	0.05	5	5	5	5	5	
Easy to manufacture	# parts	0.05	5	+	+	+	-	
	Ease of adding motor	0.18	5	-	-	5	+	
Cost	Cost	0.05	5	+	5	+	5	
	Appeal to senses	0.01	5	5	-	+	+	
Increase precision	Maintain measurement precision	0.14	5	+	-	+	5	
Operate accurately in variable environment	Robust	0.13	5	+	-	5	5	
		11.00	Total +	+3	+3	+5	+6	
			Total -	0-1	-3	-1	-2	
			Total	0-2	0	+4	+5	
			Weighted total	0	0.17	-0.10	0.28	0.55



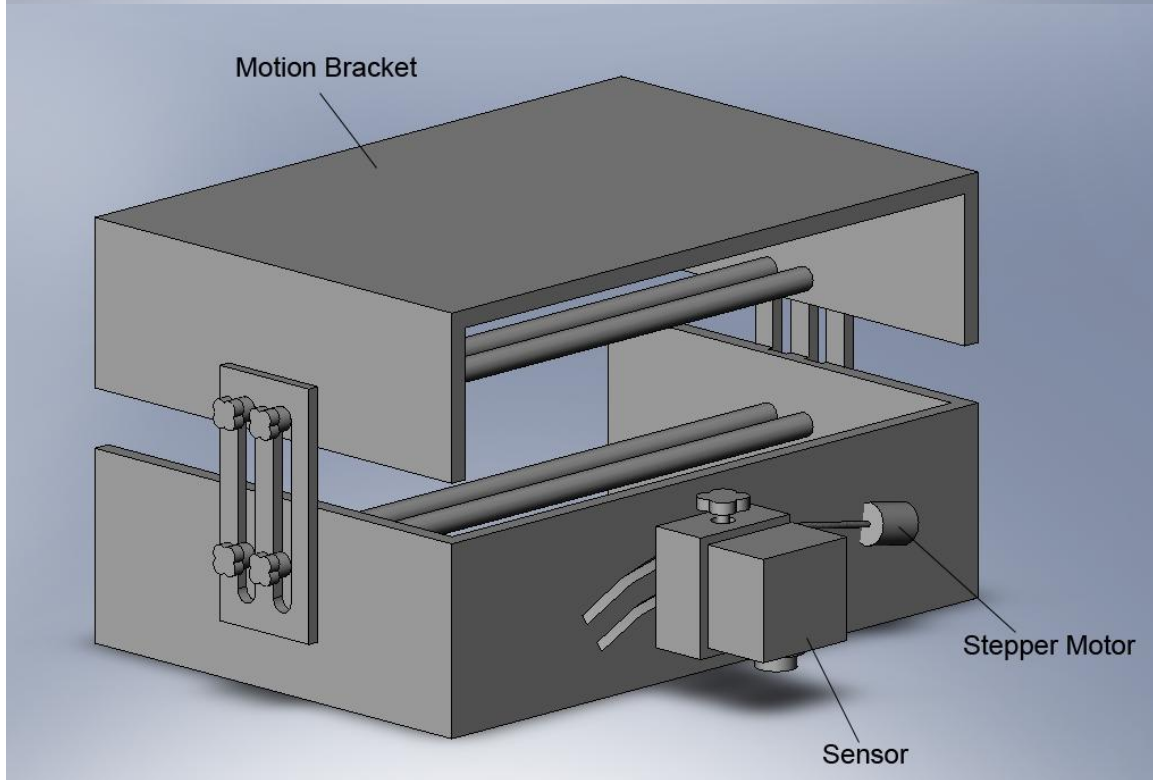
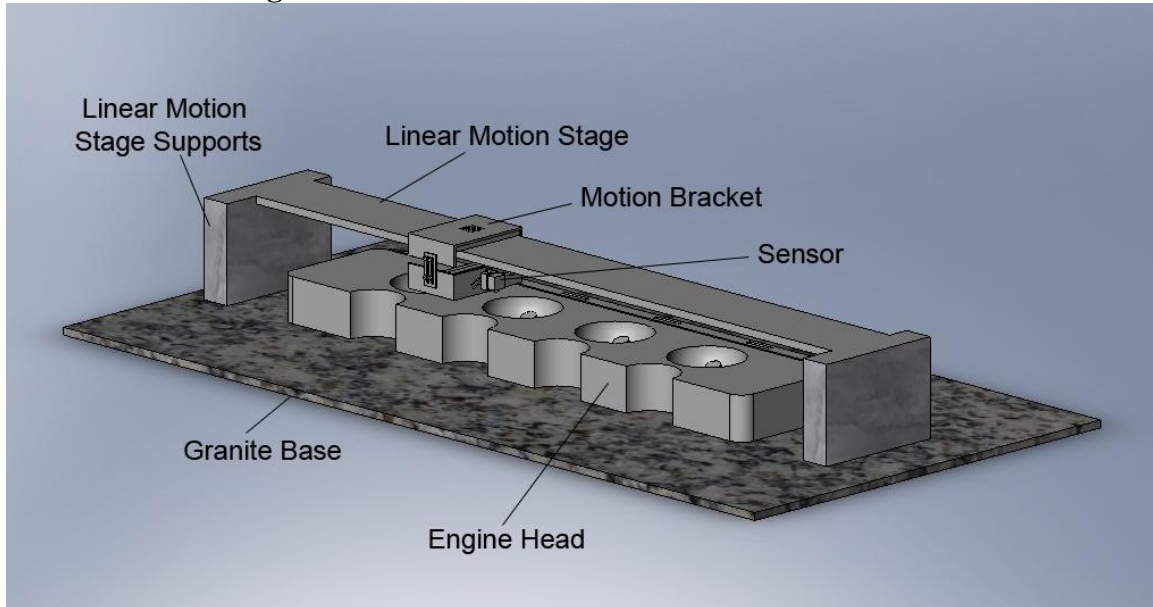
Appendix G: Bill of Materials

Quantity	Part Description	Purchased From	Part Number	Price (each)
7 pieces (various lengths)	1"x6" Aluminum 6061-T6511 Stock	University of Michigan	N/A	\$0.00
1	Granite Block 45mm x 650 mm x 650mm	University of Michigan	N/A	\$0.00
1	Linear Motion Stage 600 mm long	University of Michigan via Aerotech, Inc.	ATS115-600	\$0.00
1	NEMA 23 Step Motor	Sure Step Stepping Systems	STP-MTR- 23055	\$30.00
1	Smart ConoProbe non-contact optical sensor	University of Michigan via Optimet	N/A	\$0.00
5	Track Rollers 1/2" diameter, 3/8" width roller	McMaster-Carr*	3659K11	\$19.33
34	1"x1/4"-20 Screws	University of Michigan	N/A	\$0.00
1	10 ct. 1"x1/4"-20 hex bolts 300 stainless steel	McMaster-Carr*	92245A537	\$6.07
1	10"x1/4" Linear Motion Shaft w/machinable ends	McMaster-Carr*	1144K11	\$19.76
1	1/4" Self-Aligning Bearing, closed	McMaster-Carr*	9533T1	\$11.90
1	12" x 1/2" ID – 1" OD Aluminum Tube	McMaster-Carr*	9056K281	\$8.03
2	.25"x1/4"-20 Set Screws	University of Michigan	N/A	\$0.00
6	1018 Mild Steel Stock 1"x 3"x15"	University of Michigan	N/A	\$0.00
4	1/2" Washers	Carpenter Brothers	N/A	\$0.13
8	1/2" Wedge Stud Anchors	McMaster-Carr*	97799A300	\$5.95
4	2" Steel Corner Brackets, zinc plated	McMaster-Carr*	1556A44	\$5.67
1	Linear Motion Stage Controller	University of Michigan via Aerotech, Inc.	Ensemble CP10	\$0.00
12	Round Knob with knurled rim (style #1)	McMaster-Carr*	6079K13	\$3.31
1	1/4" Sleeve Bearing	Carpenter Brothers	N/A	\$4.79
4	1/2" Nuts	Carpenter Brothers	N/A	\$0.17
1	18-8 SS Round Head Phillips Machine Screw 4"x1/4"-20	McMaster-Carr*	91773A572	\$9.23
TOTAL				\$297.63

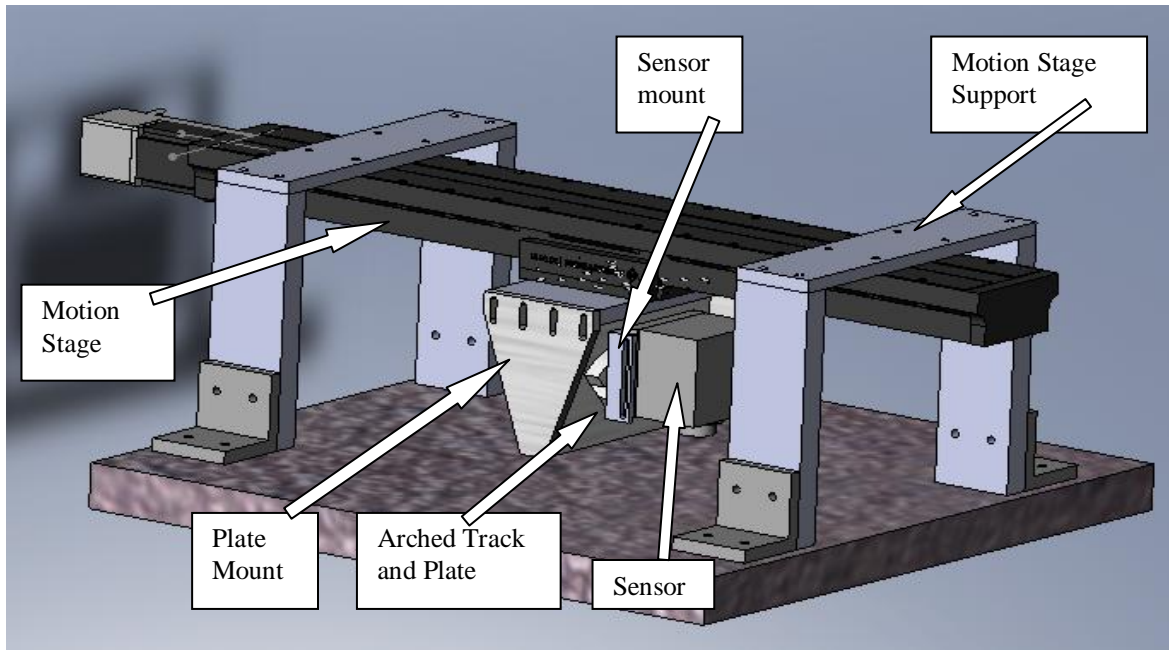
*<http://www.mcmaster.com>

Appendix H: Computer Aided Drawings of Selected Design Concept

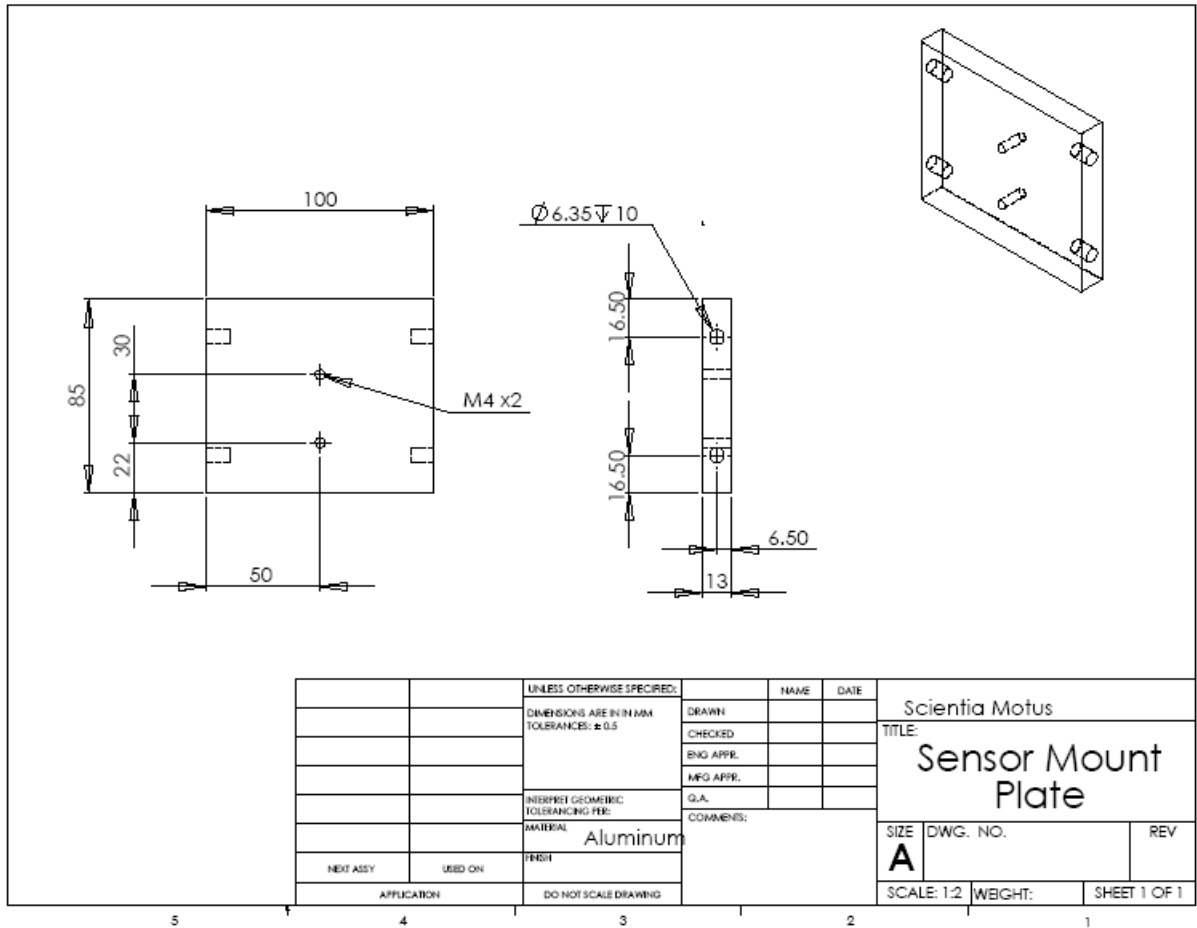
First Iteration Design Models



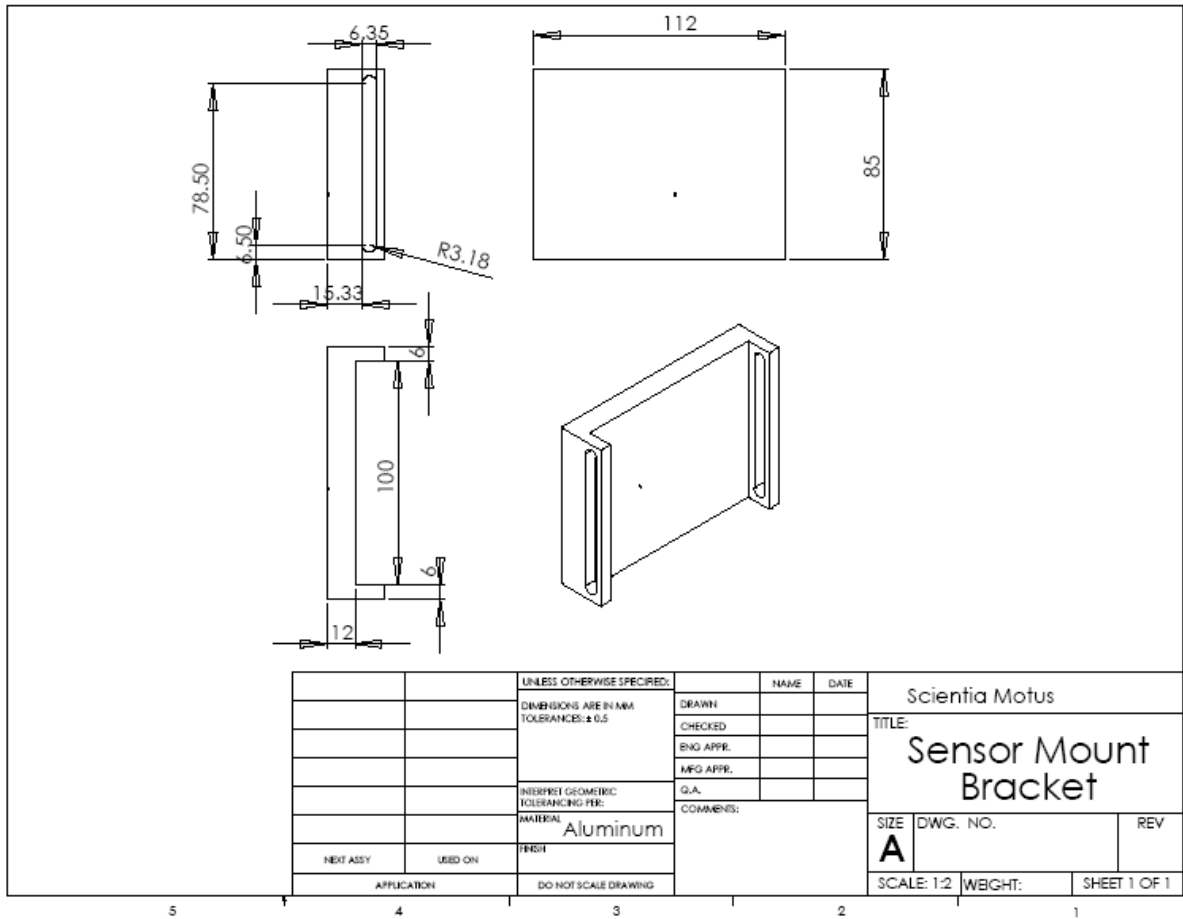
Final Design model



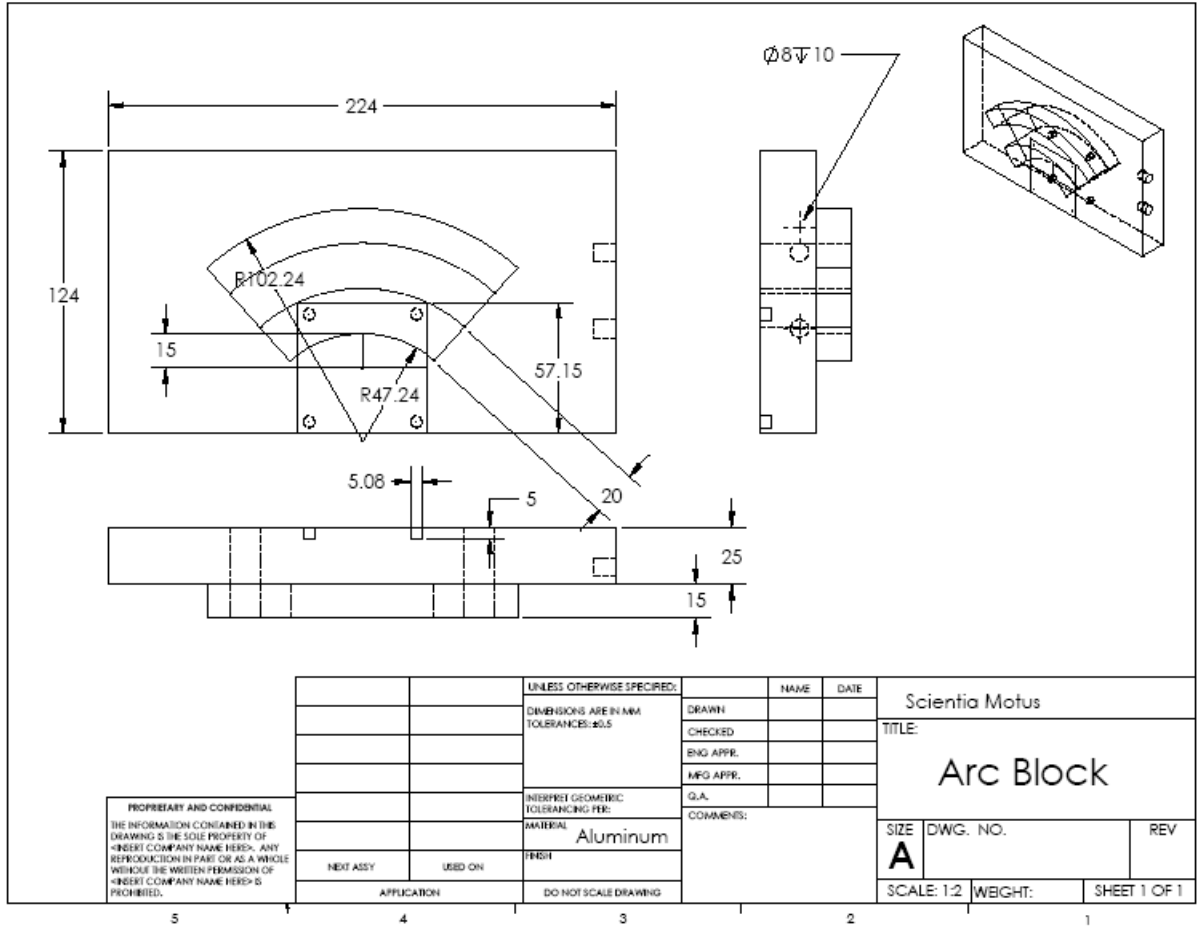
Appendix I.1: Sensor Mount Plate engineering drawing



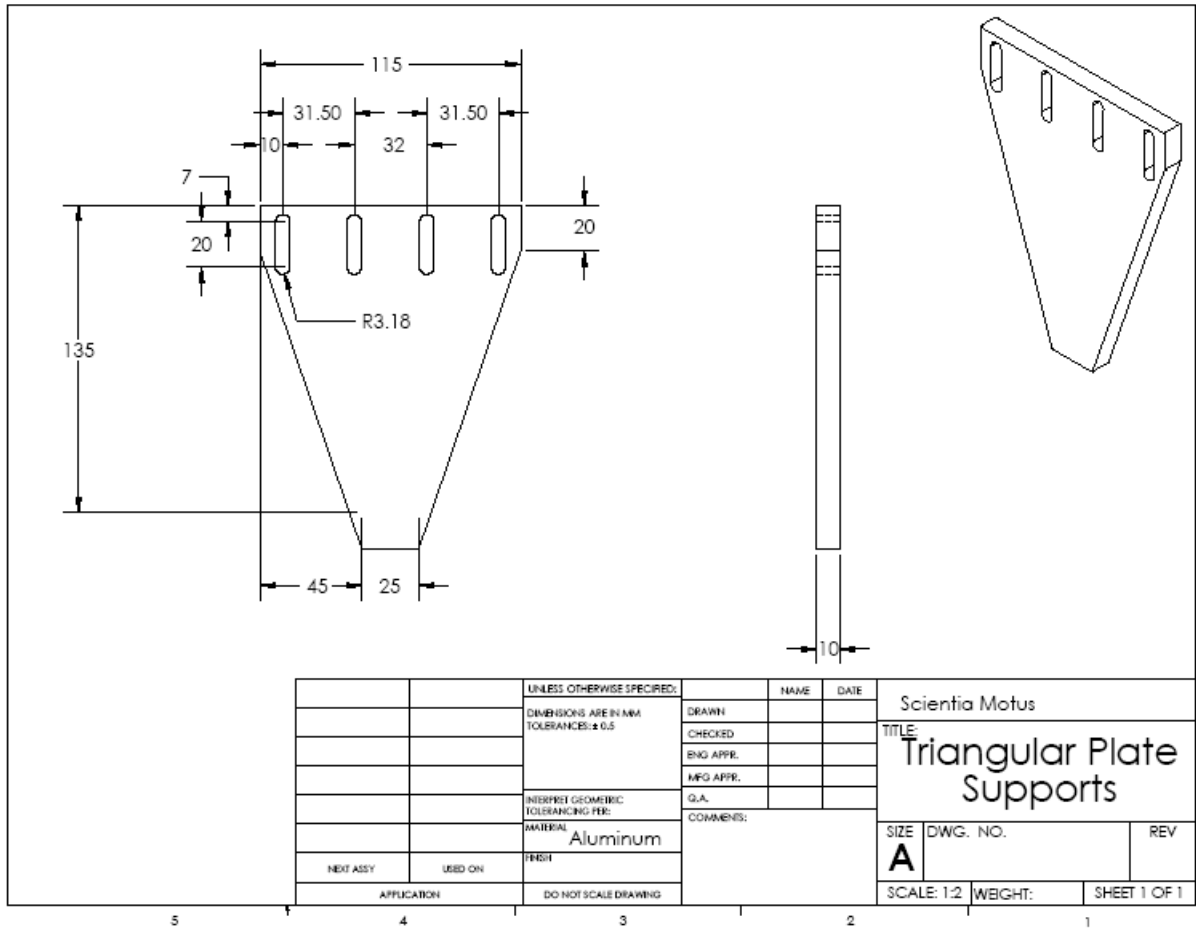
Appendix I.2: Sensor Mount Bracket engineering drawing



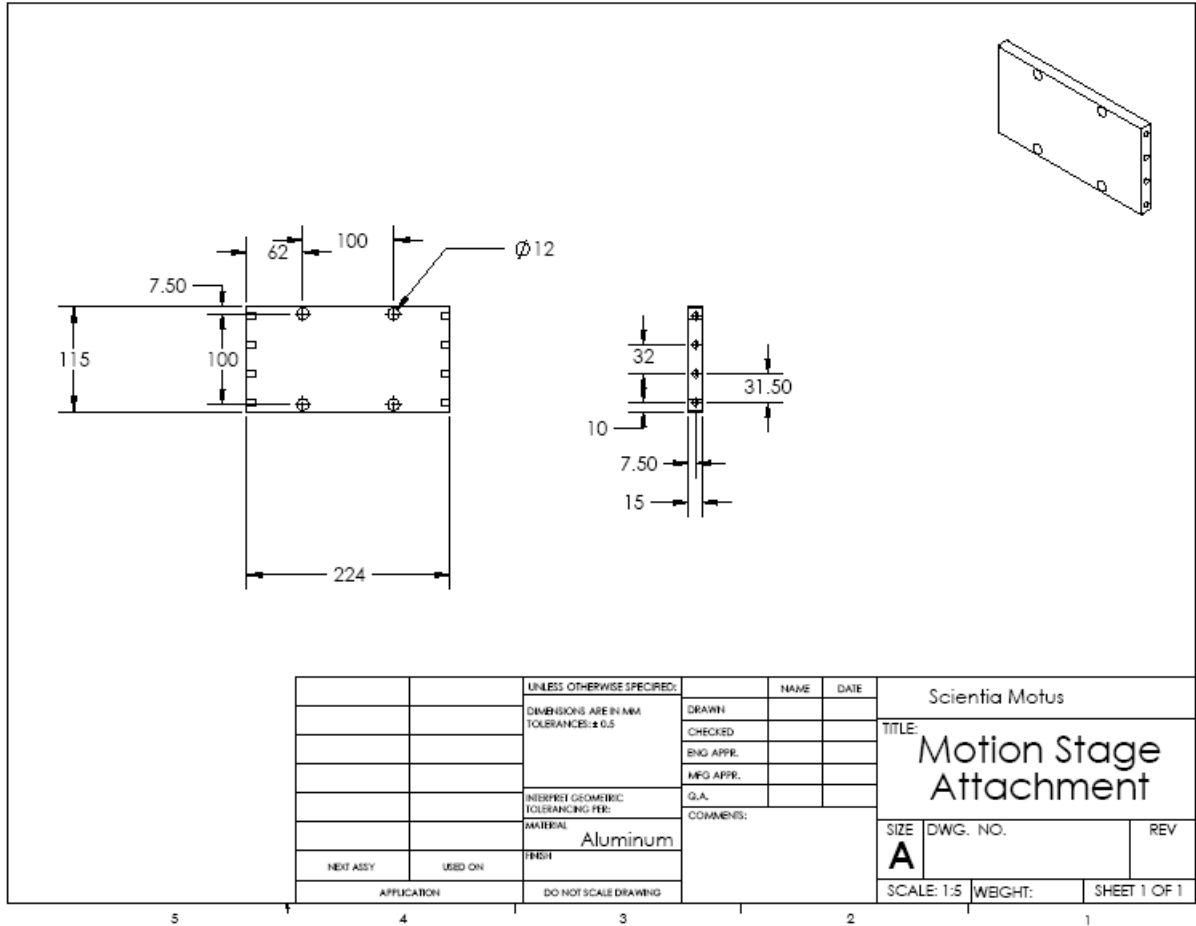
Appendix I.3: Arc Plate engineering drawing



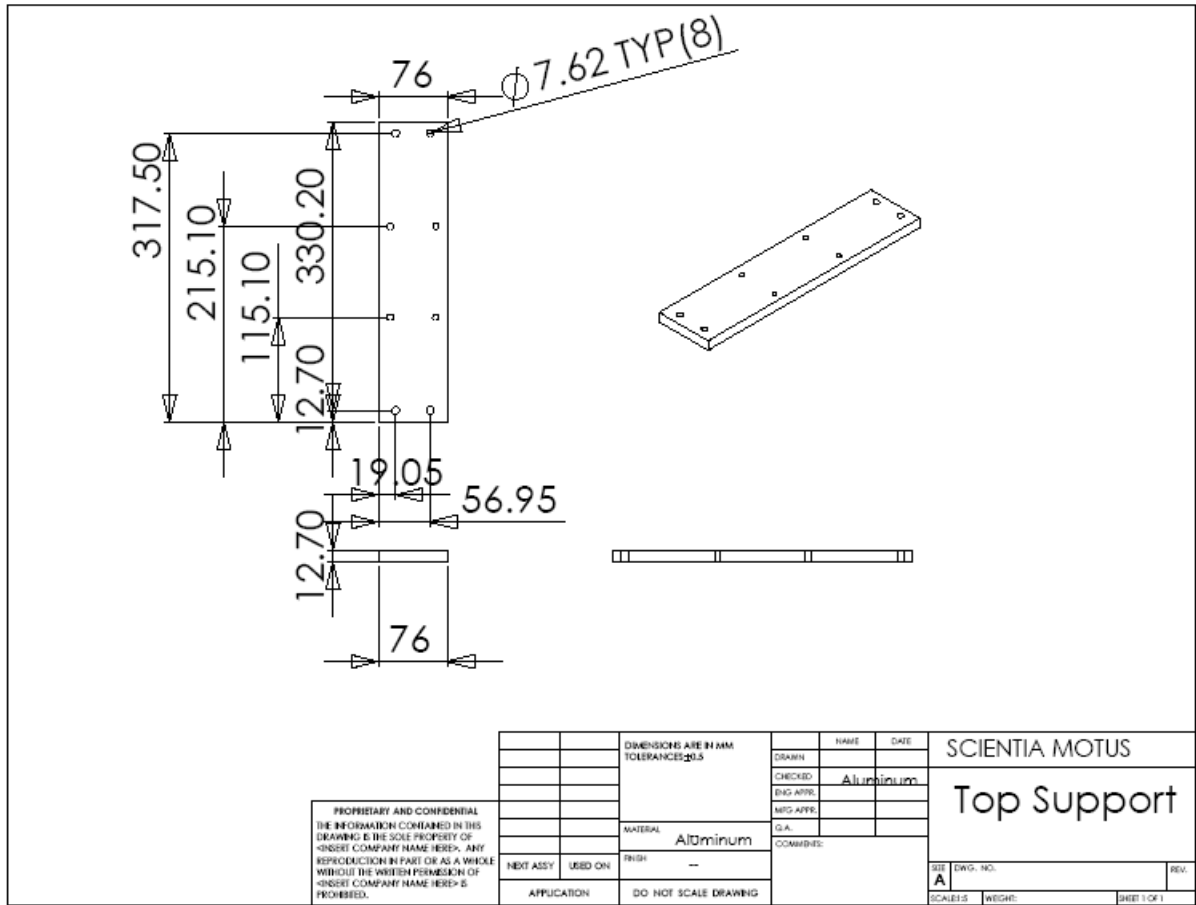
Appendix I.4: Triangular Plate Support engineering drawing



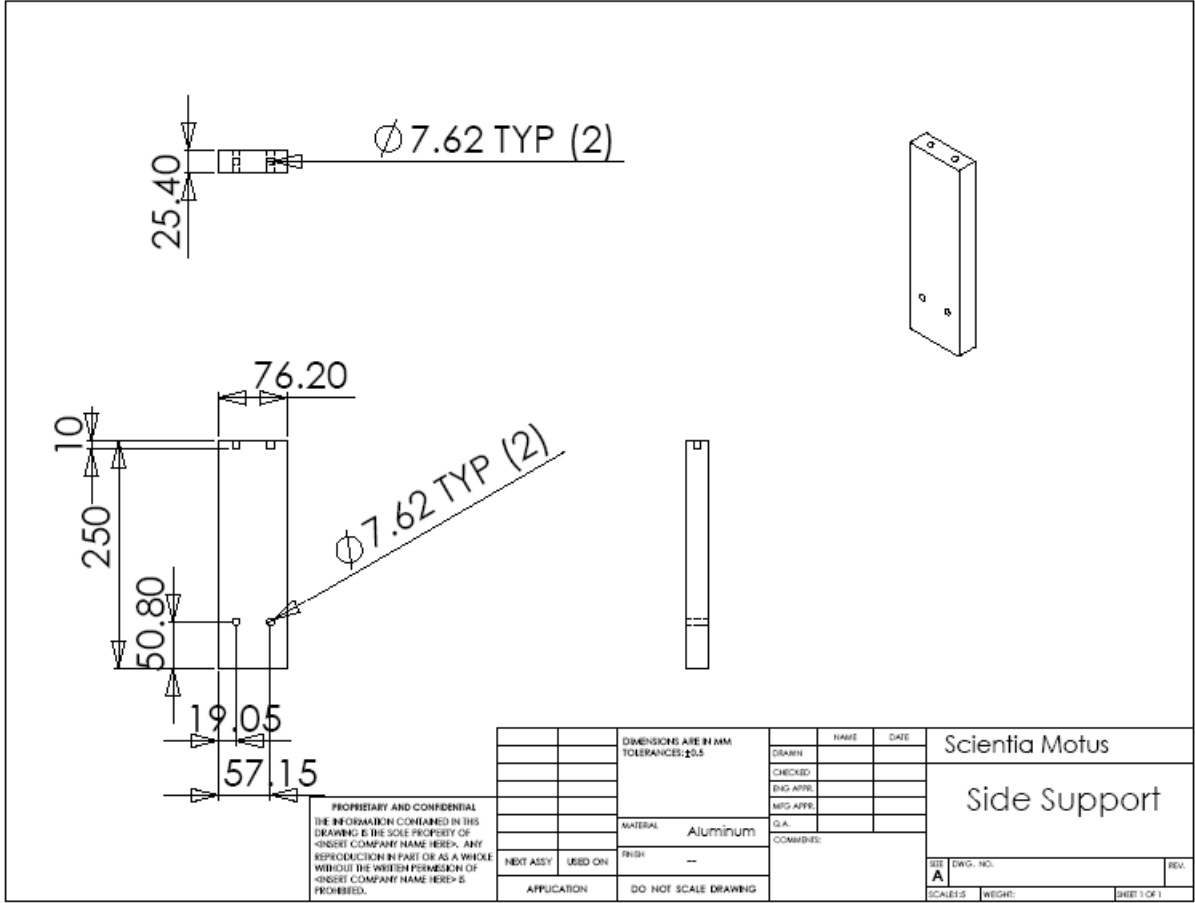
Appendix I.5: Motion Stage Attachment engineering drawing



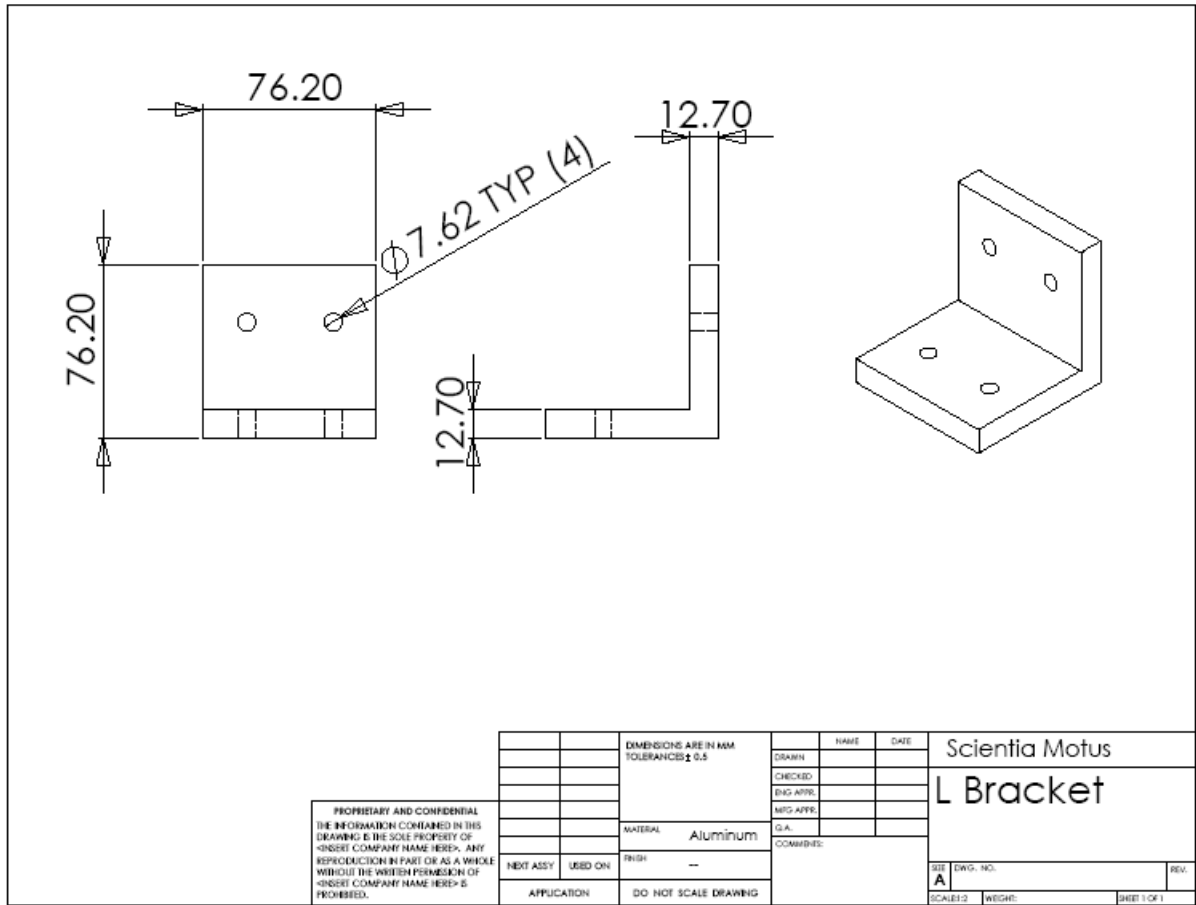
Appendix I.6: Top Support engineering drawing



Appendix I.7: Side Support engineering drawing



Appendix I.8: L-Bracket engineering drawing



Appendix J: Matlab code for vibration analysis

```
clear all
E = 71e9; %Pa
v = 0.345;
a = 0.224; %m
b = 0.124; %m
%h = 0.10; %m

rho = 2700; %kg/m^3

%Note: Side b is clamped

h = .01:.001:.025;

for i = 1:length(h)
    gamma = rho.*h(i);
    lambda =
interp1([.4,2/3,1,1.5,2.5],[3.511,3.502,3.492,3.477,3.456],a./b);
    f(i) = lambda.^2./(a^2)*sqrt(E.*h(i).^3./(12.*gamma.*(1-v^2)));
    r(i) = 20*pi/f(i);
end
figure
plot(h,r,'k')
xlabel('Thickness (m)');
ylabel('Frequency Ratio');

m = 1.5; %kg
g = 9.81; %m/s^2
% Deflection Calculation
for i = 1:length(h)
    I(i) = 1/12*b*h(i)^3;
    d(i) = rho*h(i)*b*g*a^4/(384*E*I(i))+m*g*a^3/(192*E*I(i));
end
figure
plot(h,d,'k');
xlabel('Thickness (m)');
ylabel('Deflection (m)');

clear h;
h = 0.025;
I = 1/12*b*h^3;
P = [1:0.1:6];

for i = 1:length(P)
    d(i) = P(i)*rho*h*b*g*a^4/(384*E*I)+m*g*P(i)*a^3/(192*E*I);
end
figure
plot(P,d,'k');
xlabel('Deceleration (g's)');
ylabel('Deflection (m)');
```


Appendix K: Motion stage specifications

Linear Stages

ATS115 Series

ATS115 Series

Mechanical Bearing, Ball-Screw Stage

- Travels up to 600 mm
- Speeds up to 300 mm/s
- Side seal design with hard-cover
- Low-cost; high performance
- Long-life linear motion guide bearing system



The ATS115 is Aerotech's smallest hard cover, side-sealed stage design. Competitive pricing coupled with Aerotech's reputation for producing high-quality linear motion devices make the ATS115 an attractive stage for medium-performance applications.

Rugged Construction

The hard-cover design provides protection from debris. The robust aluminum cover is hard-coated to provide a scratch resistant surface.

The side seals keep dirt and particulates out of the stage and protect the bearing surfaces from contamination. The vertical orientation of the seals easily deflects debris away from the stage. Competitive top seal designs can collect debris, resulting in the eventual failure and replacement of the sealing mechanism.

NEMA 23 Flange-Mount

The ATS115 has a NEMA 23 flange-mounting interface for attachment of a wide variety of Aerotech and third-party motors. Aerotech can provide brush, brushless, and stepper motors preconfigured and mounted directly to the stage for integration with Aerotech controls. Or the stage can be purchased without the motor for the attachment of third-party motors.

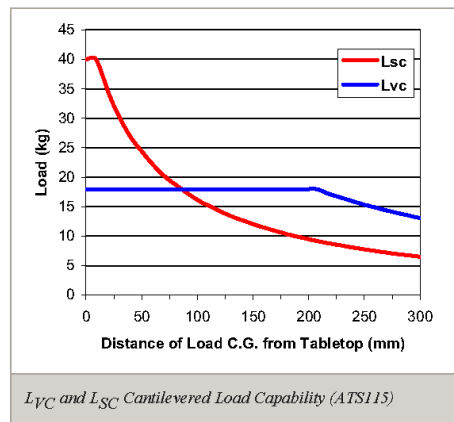
Easily Accessible Mounting

The mounting holes in the ATS115 base are accessible from the outside of the stage for ease of integration. The cover does not have to be removed when mounting the stage to a bread-board or when attaching multiple stages together in an X/Y/Z system. The tabletop is available with

both metric and English hole patterns and can be ordered with brush attachments to clear debris that may collect on the hard cover. Tabletops with hole patterns that allow the direct attachment of Aerotech's ADRS and ACS-LP series low profile direct-drive rotary stages are available.

Configuration Options

Aerotech's BMS series brushless, slotless servomotor with square-wave encoder output provides a net resolution of 0.5 micron. An optional analog output encoder can be coupled with external interpolation electronics to provide higher resolution. A holding brake can be added to the motor for vertical applications. A motor fold-back kit is available for space-constrained applications to reduce the overall stage length.



WORLD HEADQUARTERS: Aerotech, Inc., 101 Zeta Drive, Pittsburgh, PA 15238, USA • 1-412-963-7470 Fax: +1-412-963-7450
 Aerotech Ltd., Jupiter House, Calleva Park, Aldermaston, Berkshire RG7 9NN, UK • +44-118-9409400 Fax: +44-118-9409401
 Aerotech GmbH, Südwestpark 90, 90449 Nürnberg, Germany • +49-911-9679370 Fax: +49-911-96793720

www.aerotech.com

ATS115 Series SPECIFICATIONS

Basic Model		ATS115-50	ATS115-100	ATS115-150	ATS115-200	ATS115-250
Total Travel		50 mm	100 mm	150 mm	200 mm	250 mm
Drive System		Ball Screw/Brushless Servomotor (BMS60-A-D25-E2500H)				
Bus Voltage		Up to 160 VDC				
Continuous Current	A _{pk}	Up to 2.3 A				
	A _{rms}	Up to 1.6 A				
Feedback		Noncontact Rotary Encoder (2500 line)				
Resolution	5 mm/rev lead	0.5 µm with 2500 line Quadrature Encoder				
Maximum Travel Speed ⁶		300 mm/s (12 in/s)				
Maximum Load ²	Horizontal	40.0 kg (88 lb)				
	Vertical	18.2 kg (40 lb)				
	Side	40 kg (88 lb)				
Accuracy		±6 µm	±6 µm	±8 µm	±8 µm	±10 µm
Bidirectional Repeatability		±1 µm				
Nominal Stage Weight	Less Motor	3.7 kg (8.1 lb)	4.1 kg (9.0 lb)	4.6 kg (10.1 lb)	5.0 kg (11.0 lb)	5.5 kg (12.1 lb)
	With Motor	4.8 kg (10.6 lb)	5.2 kg (11.4 lb)	5.7 kg (12.5 lb)	6.1 kg (13.4 lb)	6.6 kg (14.5 lb)
Construction		Black Anodized Aluminum Body with Hardcoated Tabletop				

Notes:

- Excessive duty cycle may impact stage accuracy.
- Payload specifications are for single-axis system and based on ball screw and bearing life of 2500 km (100 million inches) of travel.
- Specifications are for single-axis systems, measured 50 mm above the tabletop. Performance of multi-axis systems is payload and workpoint dependent. Consult factory for multi-axis or non-standard applications.

Basic Model		ATS115-300	ATS115-400	ATS115-500	ATS115-600	
Total Travel		300 mm	400 mm	500 mm	600 mm	
Drive System		Ball Screw/Brushless Servomotor (BMS60-A-D25-E2500H)				
Bus Voltage		Up to 160 VDC				
Continuous Current	A _{pk}	Up to 2.3 A				
	A _{rms}	Up to 1.6 A				
Feedback		Noncontact Rotary Encoder (2500 line)				
Resolution	5 mm/rev lead	0.5 µm with 2500 line Quadrature Encoder				
Maximum Travel Speed ⁶		300 mm/s (12 in/s)		250 mm/s (10 in/s)		
Maximum Load ²	Horizontal	40.0 kg (88 lb)				
	Vertical	18.2 kg (40 lb)				
	Side	40 kg (88 lb)				
Accuracy		±10 µm	±12 µm	±14 µm	±16 µm	
Bidirectional Repeatability		±1 µm				
Nominal Stage Weight	Less Motor	5.9 kg (13.0 lb)	6.8 kg (15.0 lb)	7.6 kg (16.7 lb)	8.5 kg (18.7 lb)	
	With Motor	7.0 kg (15.4 lb)	7.9 kg (17.4 lb)	8.7 kg (19.1 lb)	9.6 kg (21.1 lb)	
Construction		Black Anodized Aluminum Body with Hardcoated Tabletop				

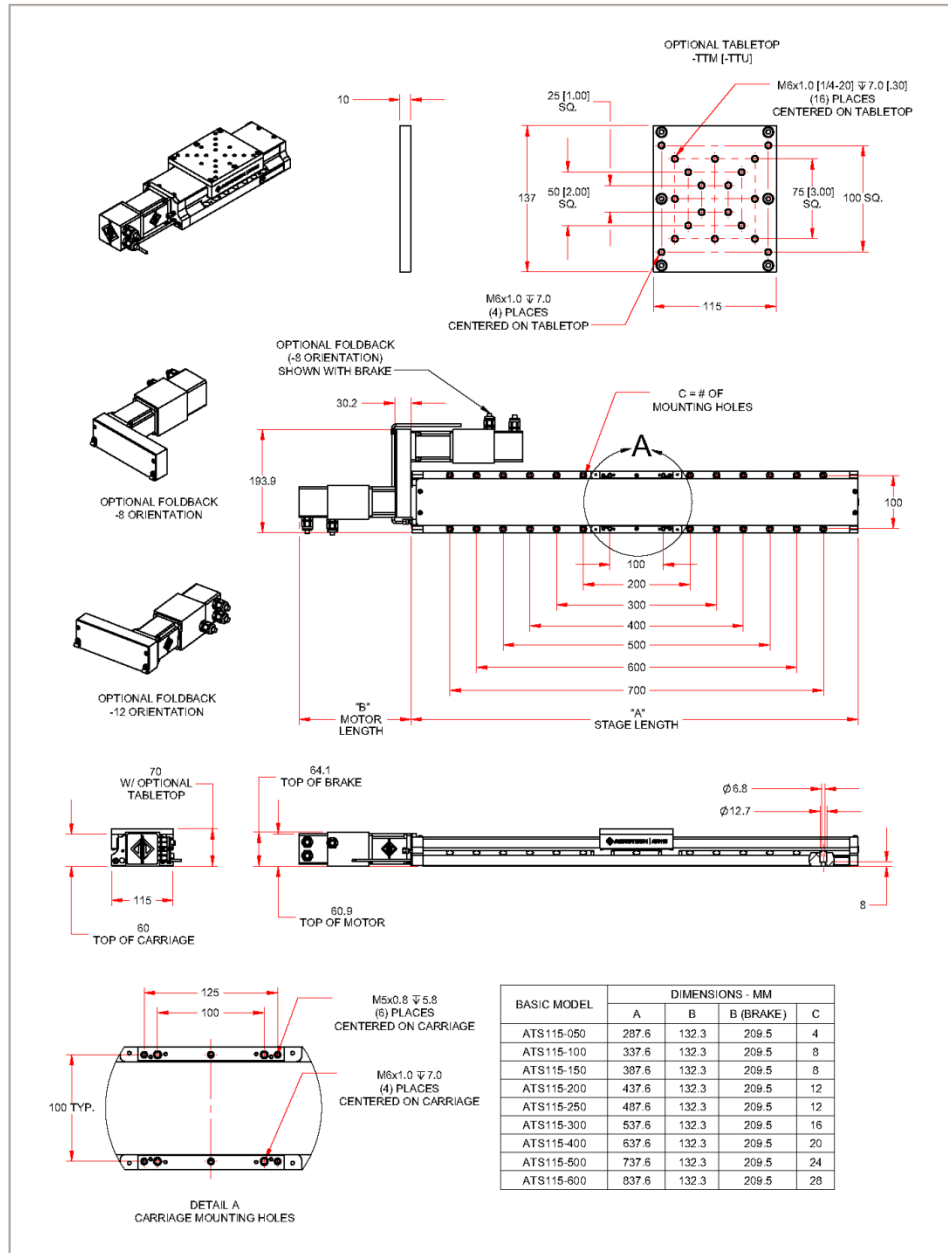
Notes:

- Excessive duty cycle may impact stage accuracy.
- Payload specifications are for single-axis system and based on ball screw and bearing life of 2500 km (100 million inches) of travel.
- Specifications are for single-axis systems, measured 50 mm above the tabletop. Performance of multi-axis systems is payload and workpoint dependent. Consult factory for multi-axis or non-standard applications.

www.aerotech.com

WORLD HEADQUARTERS: Aerotech, Inc., 101 Zeta Drive, Pittsburgh, PA 15238, USA +1-412-963-7470 Fax: +1-412-963-7459
 Aerotech Ltd., Jupiter House, Calleva Park, Aldermaston, Berkshire RG7 8NN, UK +44-118-9409400 Fax: +44-118-9409401
 Aerotech GmbH, Sudwestpark 90, 90449 Nürnberg, Germany +49-911-9679370 Fax: +49-911-96793720

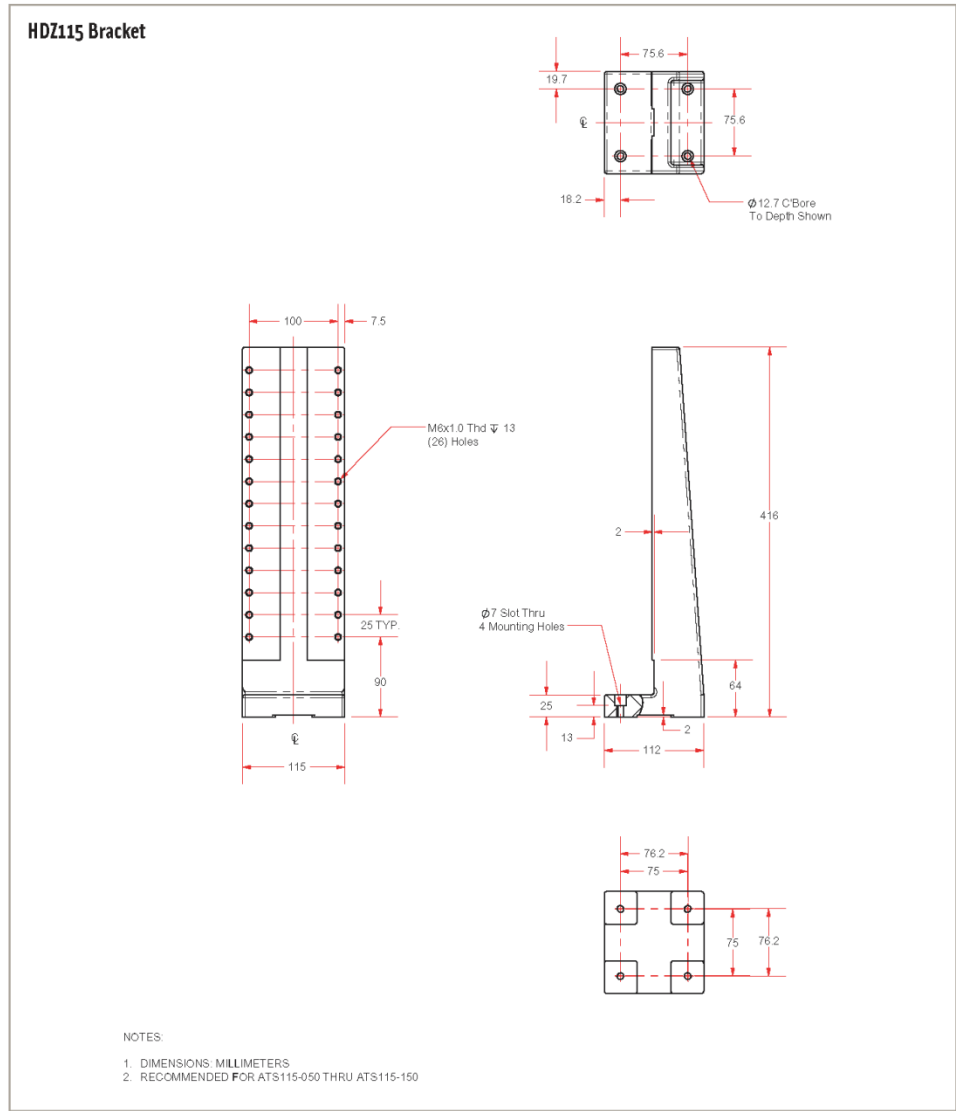
ATS115 Series DIMENSIONS



WORLD HEADQUARTERS: Aerotech, Inc., 101 Zeta Drive, Pittsburgh, PA 15238, USA +1-412-963-7470 Fax: +1-412-963-7459
 Aerotech Ltd., Jupiter House, Calleva Park, Aldermaston, Berkshire RG7 8NN, UK +44-118-9409400 Fax: +44-118-9409401
 Aerotech GmbH, Sudwestpark 90, 90449 Nürnberg, Germany +49-911-9679370 Fax: +49-911-96793720

www.aerotech.com

ATS115 Series – HDZ115 Bracket DIMENSIONS



ATS115 Series ORDERING INFORMATION**Ordering Information**

ATS115	-050	-TTM	-5MM	-NC	-BMS	-0	-FB	-NONE	-PLOTS
Series	Travel (mm)	Tabletop	Ball Screw	Limits	Motor	Cable Exit	Options	Coupling	Testing
ATS115	-050	-TTM	-5MM	-NC	-BMS	-0	-FB025	-NONE	-PLOTS
	-100	-TTU		-NO	-BMS-BRK	-2	-BASE WIPER	-C025	-NO PLOTS
	-150	-NO TT			-NM	-3			
	-200	-TT100				-4			
	-250	-TT150				-5			
	-300	/WIPER				-8			
	-400					-12			
	-500								
	-600								

ATS115 Series Linear Ball-Screw Stage

ATS115-050	50 mm (2 in) travel stage with ball screw and limits
ATS115-100	100 mm (4 in) travel stage with ball screw and limits
ATS115-150	150 mm (6 in) travel stage with ball screw and limits
ATS115-200	200 mm (8 in) travel stage with ball screw and limits
ATS115-250	250 mm (10 in) travel stage with ball screw and limits
ATS115-300	300 mm (12 in) travel stage with ball screw and limits
ATS115-400	400 mm (16 in) travel stage with ball screw and limits
ATS115-500	500 mm (20 in) travel stage with ball screw and limits
ATS115-600	600 mm (24 in) travel stage with ball screw and limits

Tabletop

-TTM	Metric pattern tabletop
-TTU	English pattern tabletop
-NO TT	No tabletop
-TT100	Bolt-hole pattern to attach ADRS100 or ACS-100LP rotary stage with vertical or horizontal axis of rotation
-TT150	Bolt-hole pattern to attach ADRS150 or ACS-150LP rotary stage with vertical or horizontal axis of rotation
/WIPER	Wiper option for English and metric tabletops

Ball Screw

-5MM	5 mm per revolution ball screw
------	--------------------------------

Limits

-NC	Normally-closed limits
-NO	Normally-open limits

Motor

-BMS	Brushless servomotor with 2500 line feedback encoder (BMS60-A-D25-E2500H)
-BMS-BRK	Brushless servomotor with 2500 line feedback encoder and motor-mounted brake (BMS60-A-D25-E2500H-BK1)
-NM	No motor

Motor Orientation

-0	No motor
-2	Bottom cable exit
-3	Left side cable exit
-4	Top cable exit
-5	Right side cable exit
-8	Right side fold-back
-12	Left side fold-back

ATS115 Series ORDERING INFORMATION

Options

-FB025	Motor fold back kit for 0.25" diameter motor shaft
-BASE WIPER	Wiper on base of top axis of X/Y pair to clear hardcover of the bottom axis

Coupling Option

-NONE	No motor coupling supplied
-C025	0.25" diameter motor shaft coupling

Testing

-PLOTS	Accuracy and repeatability plots
-NO PLOTS	No performance plots

Accessories (to be ordered as separate line item)

ALIGNMENT-NPA	Non-precision XY assembly
ALIGNMENT-NPAZ	Non-precision XZ or YZ assembly
ALIGNMENT-PA10	XY assembly; 10 arc sec orthogonal
ALIGNMENT-PA10Z	XZ or YZ assembly with L-bracket; 10 arc second orthogonal
ALIGNMENT-PA5	XY assembly; 5 arc sec orthogonal
ALIGNMENT-PA5Z	XZ or YZ assembly with L-bracket; 5 arc second orthogonal
HDZ115	Right angle L-bracket for ATS115-050, ATS115-100, and ATS115-150 only

Appendix L: Ensemble CP 10 Code and Technical Specifications

ENSEMBLE:

ENABLE X

HOME X

DOMOTION:

MOVEINC X 100 F 150

MOVEABS X 500 F 40

MOVEABS X 600 F 150

LINEAR X -600 F 150

GOTO DOMOTION

%Comments on command algorithm above

%Enable X axis

%Position stage at x=0 mm, absolute position

%Complete following motions in a loop:

%Move stage to x=100 mm relative to last position at a speed of 150 mm/s

%Move stage to x=500 mm, absolute position (relative to home) at a speed of 40 mm/s

%Move stage to x=600 mm, absolute position (relative to home) at a speed of 150 mm/s

%Return stage to home position at a speed of 150 mm/s

%End of loop, return to beginning of loop

Ensemble CP/MP/CL SPECIFICATIONS

CP Electrical Specifications		
Logic Input Voltage	VAC	85 to 240
Bus Input Voltage	VAC	14 to 240
Output Voltage	VDC	20 to 320
Peak Output Current	A_{pk}	10 to 30
Continuous Output Current	A	5 to 15
PWM Switching Frequency	kHz	20
Power Amplifier Bandwidth	kHz	Software Selectable
Minimum Load Inductance	mH	0.1 @ 160 VDC (1 mH @ 320 VDC)
Digital Inputs and Outputs	Standard	4 opto inputs; 2 high-speed opto inputs; 4 opto outputs
	Optional	16 additional opto inputs; 16 additional opto outputs
Analog Inputs and Outputs	Standard	1 (± 10 VDC, 16-bit) input; 1 (± 10 VDC, 16-bit) output
	Optional	1 additional (± 10 VDC, 12-bit) input; 1 additional (± 10 VDC, 16-bit) output
Encoder Inputs		TTL RS-422 standard, and auxiliary encoder input; optional amplified sine encoder input on primary encoder channel; programmable resolution up to 1024 times the analog encoder resolution; 250 kHz amplified sine primary
Operating Temperature	$^{\circ}$ C	0 to 50
Storage Temperature	$^{\circ}$ C	-30 to 85
Weight	kg (lb)	1.6 (3.6)

For Ensemble more detailed controller specifications:

<http://www.aerotech.com/ensemble/drives.cfm>

Ensemble software and manual are available on the CD shipped with the controller.

Appendix M: Si Programmer Code and 3540i Driver Manual Website

Applied Motion Products, Inc.
 Programming Software Version: 2.7.5
 Si Programmer V2.7.5
 Drive: 3540i
 Drive Firmware Version: 2.18
 Steps per revolution: 20000
 Running current: 2.80A
 Idle current: 1.40A (50%)
 Jog speed: 4.000 rev/sec
 Jog accel: 25 rev/s/s
 Quick Decel rate (used for limits, interrupt and stop button): 1000 rev/s/s
 Encoder: 4000 counts/rev (1000 lines).
 Encoder disabled (ignore errors)
 Interrupt action: none
 Condition: input 1 high

- 1 Wait Time 1 seconds
- 2 Feed to Length(ccw) 1,444 steps, V=0.050 rev/sec, A=100 rev/s/s, D=100 rev/s/s
- 3 Wait Time 7 seconds
- 4 Feed to Length(cw) 2,888 steps, V=0.050 rev/sec, A=100 rev/s/s, D=100 rev/s/s
- 5 Wait Time 7 seconds
- 6 Feed to Length(ccw) 2,888 steps, V=0.050 rev/sec, A=100 rev/s/s, D=100 rev/s/s
- 7 Go To Line 3

Technical Specifications

Amplifiers	Dual, MOSFET H-bridge, 3 state, pulse width modulated switching at 20 kHz. 0.2 - 3.5 amps/phase output current, software selectable. 147 watts maximum output power. Automatic idle current reduction (software programmable), reduces current to motor when idle. Minimum motor inductance is 0.8 mH.
Power Supply	Accepts 12 - 42 VDC power supply. 3.5 amps typical max load. 7A maximum power on surge.
Inputs	5 - 24V, optically isolated. 2200 ohms internal resistance. Can be configured for sinking (NPN) or sourcing (PNP) signals.
Outputs	Optically isolated. 24V, 100 mA max.
Microstepping	13 software selectable resolutions. Steps per revolution with 1.8° motor: 2000, 5000, 10000, 12800, 18000, 20000, 21600, 25000, 25400, 25600, 36000, 50000, 50800. Waveform: pure sine.
Motion Update	12800 Hz.
Physical	Constructed on black anodized aluminum chassis/heat sink. 1.5 x 3 x 5 inches overall. 12 oz. 0-70°C ambient temp range. Power LED. See page 17 for detailed drawing .
Connectors	Power, motor: screw terminal block. Wire size: AWG 12 - 28. I/O Signals: screw terminal block. Wire size: AWG 16 - 28.



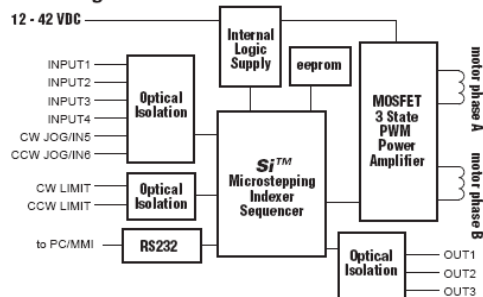
Introduction

Thank you for selecting an Applied Motion Products motor control. We hope our dedication to performance, quality and economy will make your motion control project successful. If there's anything we can do to improve our products or help you use them better, please call or fax. We'd like to hear from you. Our phone number is (800) 525-1609 or you can reach us by fax at (831) 761-6544.

Features

- Powerful, precise and efficient mosfet driver providing up to 3.5 amps per phase and microstepping to 50,800 steps per revolution.
- Accepts 12 - 42 VDC power supply.
- Powerful, flexible, easy to use indexer.
- Connects by a simple cable to your PC for programming (cable included).
- Microsoft Windows-based software for easy set up and programming.
- Eight inputs for interacting with the user and other equipment.
- Three outputs for coordinating external equipment.
- All I/O is optically isolated, 5 - 24 V, sinking or sourcing signals. (Except PC/MMI port which is ±12V RS-232.)
- Sturdy 1.5 x 3 x 5 inch metal chassis.
- Screw terminal connectors for motor, DC power and I/O signals
- Optional man machine interface (MMI) allows operator to enter distances, speeds, loop counts and more.

Block Diagram








For downloads of driver manual and Si Programmer software:

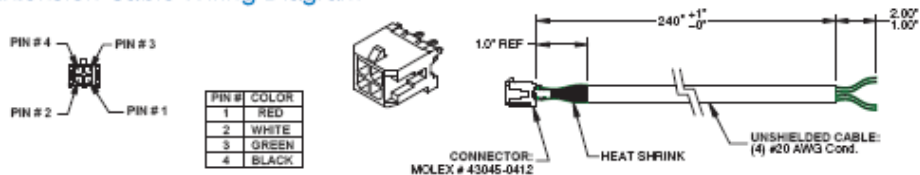
<http://www.applied-motion.com/products/stepper/drives/3540i.php>

Appendix N: Selected Stepper Motor Specifications

SureStep™ Motor Specifications

SureStep™ Series Specifications – High Torque Bipolar Stepping Motors				
Bipolar Stepping Motors				
	STP-MTR-17048	STP-MTR-23055	STP-MTR-23079	STP-MTR-34066
Price	↔	↔	↔	↔
Stepping Motor Face Plate	NEMA 17	NEMA 23	NEMA 23	NEMA 34
Maximum Holding Torque	5.2 lb-in	10.36 lb-in	17.25 lb-in	27.1 lb-in
	83 oz-in	166 oz-in	276 oz-in	434 oz-in
	0.59 Nm	1.17 Nm	1.95 Nm	3.06 Nm
Rotor Inertia	0.00095 lb-in- ²	0.00224 lb-in- ²	0.0042 lb-in- ²	0.0012 lb-in- ²
	0.45 oz-in ²	1.463 oz-in ²	2.596 oz-in ²	7.66 oz-in ²
	0.000068 kg-m ²	0.00027 kg-m ²	0.00047 kg-m ²	0.0014 kg-m ²
Rated Current	2.0 A/phase	2.8 A/phase	2.8 A/phase	2.8 A/phase
Resistance	1.40Ω	0.79Ω	1.10Ω	1.11Ω
Inductance	2.65 mH	2.36 mH	3.62 mH	7.70 mH
Basic Step Angle	1.8° (2-phase motors with connectorized pigtail)			
Weight	0.7 lbs	1.50 lbs	2.2 lbs	3.85 lbs
Shaft Runout	0.002 in			
Shaft Radial Play @ 1 lb load	0.001 in max			
Perpendicularity	0.003 in			
Concentricity	0.002 in			
Operating Temperature Range	-20 °C to 50 °C (motor case temperature should be kept below 100 °C (212 °F))			
Maximum Radial Load	6.0 lb	15.0 lb	15.0 lb	39.0 lb
Maximum Thrust Load	6.0 lb	13.0 lb	13.0 lb	25.0 lb
Agency Approvals	150°C Class B			
Agency Approvals	CE (complies with EN55014-1 (1999) and EN60034-1 (5.11))			
Design Tips	Allow sufficient time to accelerate the load and size the step motor with a 100% torque safety factor. DO NOT disassemble step motors because motor performance will be reduced and the warranty will be voided. DO NOT connect or disconnect the step motor during operation. Mount the motor to a surface with good thermal conductivity, such as steel or aluminum, to allow heat dissipation. Use a flexible coupling with "clamp-on" connections to both the motor shaft and the load shaft to prevent thrust loading on bearings from minor mis-alignment.			
Extension Cable - 20 Foot (motor to drive)	↔	Part Number STP-EXT-020 		

Extension Cable Wiring Diagram



For more detailed stepper motor specifications:

http://web6.automationdirect.com/adc/Technical/Catalog/Motion_Control/Stepper_Systems/Motor_s_-z-_Cables